Accepted Manuscript

Unconventional Knoevenagel-type Indoles: Synthesis and Cell-based Studies for the Identification of Pro-apoptotic Agents

Dr. Andrea Spallarossa, Chiara Caneva, Matteo Caviglia, Silvana Alfei, Stefania Butini, Giuseppe Campiani, Sandra Gemma, Margherita Brindisi, Daniela M. Zisterer, Sandra A. Bright, Clive D. Williams, Emmanuele Crespan, Giovanni Maga, Giuseppina Sanna, Ilenia Delogu, Gabriella Collu, Roberta Loddo

PII: S0223-5234(15)30193-8

DOI: 10.1016/j.ejmech.2015.08.009

Reference: EJMECH 8045

To appear in: *European Journal of Medicinal Chemistry*

Received Date: 25 April 2015

Revised Date: 22 July 2015

Accepted Date: 4 August 2015

Please cite this article as: A. Spallarossa, C. Caneva, M. Caviglia, S. Alfei, S. Butini, G. Campiani, S. Gemma, M. Brindisi, D.M. Zisterer, S.A. Bright, C.D. Williams, E. Crespan, G. Maga, G. Sanna, I. Delogu, G. Collu, R. Loddo, Unconventional Knoevenagel-type Indoles: Synthesis and Cell-based Studies for the Identification of Pro-apoptotic Agents, *European Journal of Medicinal Chemistry* (2015), doi: 10.1016/j.ejmech.2015.08.009.

Graphical Abstract

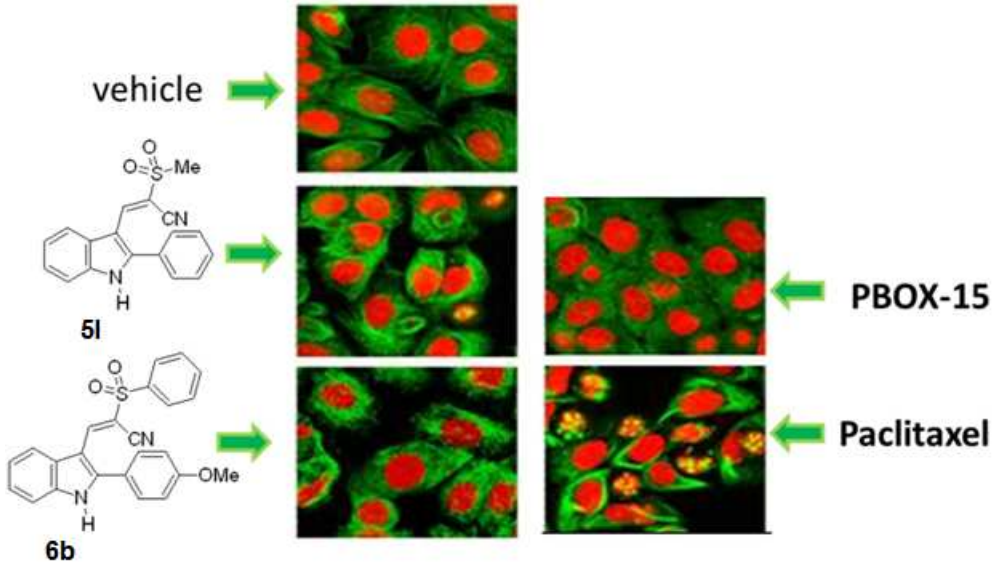

Unconventional Knoevenagel-type Indoles: Synthesis and Cell-based Studies for the Identification of Pro-apoptotic Agents

Andrea Spallarossa,[*,a] Chiara Caneva,[a] Matteo Caviglia,[a] Silvana Alfei,[a] Stefania Butini,[b] Giuseppe Campiani,[b] Sandra Gemma,[b] Margherita Brindisi,[b] Daniela M. Zisterer,[c] Sandra A. Bright,[c] Clive D. Williams,[c] Emmanuele Crespan,[d] Giovanni Maga,[d] Giuseppina Sanna,[e] Ilenia Delogu,[e] Gabriella Collu,[e] Roberta Loddo.[e]

[a]*Dipartimento di Farmacia, Università di Genova, Viale Benedetto XV 3, I-16132 Genova, Italy*

[b]*European Research Centre for Drug Discovery & Development, Dipartimento di Biotecnologie, Chimica e Farmacia, Università di Siena, via Aldo Moro 2, I-53100 Siena, Italy*

[c]*School of Biochemistry and Immunology, Trinity Biomedical Sciences Institute, Trinity College Dublin, 152-160 Pearse Street, Dublin 2, Ireland*

[d]*Institute of Molecular Genetics·IGM-CNR, via Abbiategrasso 207, 27100 Pavia (Italy).*

[e]*Dipartimento di Scienze Biomediche, Sezione di Microbiologia e Virologia, Università di Cagliari, Cittadella Universitaria, s.p. 8, Km 0.700, I-09042 Monserrato (Cagliari), Italy*

[*]*Corresponding author:*

Dr. Andrea Spallarossa
Dipartimento di Farmacia
Sezione di Chimica del Farmaco e del Prodotto Cosmetico
Università degli Studi di Genova
Viale Benedetto XV, 3
16132 - Genova, Italy
phone: +39 010 353 8364;
fax: +39 010 353 8358;
e-mail: andrea.spallarossa@unige.it

Abstract

A new series of indole-based analogues were recently identified as potential anticancer agents. The Knoevenagel-type indoles herein presented were prepared via a one-pot condensation of iminium salts with active methylene reagents and were isolated as single geometric isomers. Biological evaluation in different cell-based assays revealed an antiproliferative activity for some analogues already in the nanomolar range against leukaemia, breast and renal cancer cell lines. To explain these effects, the most promising analogues of the series were engaged in further cell-based studies. Compounds **5e,l,p** and **5a,b** highlighted a pro-apoptotic potential being able to induce apoptosis in HL60, K562 and MCF-7 cell lines in a dose and time-dependent manner. The ability of these compounds to arrest cell cycle at the G2/M phase inspired the immunofluorescence studies which allowed us to identify tubulin as a potential target for compounds **5l** and **6b**.

Keywords

Indoles
Antiproliferative agents
Pro-apoptotic agents
Tubulin immunostaining

1. Introduction

Indole is a privileged scaffold for drug discovery [1,2]. Indole derivatives have been described as useful chemical templates in different therapeutic areas, including the treatment of neurodegenerative diseases [3-5], psychiatric disorders [6] and inflammation [7,8]. Moreover, indole derivatives were found to be endowed with antiviral [9], antioxidant [10], antiplasmodial [11], antiproliferative and antitumor efficacy [12-20]. Recently induction of methuosis, which is one of the most recently acknowledged nonapoptotic cell death phenotype involving the accumulation of cytoplasmic vacuoles derived from macropinosomes, was identified as the mechanism of action of conjugated 3-vinyl indoles [21]. Interestingly, Knoevenagel-type indoles, such as 3-vinyl indoles bearing two electron-withdrawing groups at the terminal exocyclic double bond carbon, showed promising properties in different research areas [22-27].

In previous works, the chemical reactivity of *N*-methyleneiminium chlorides of cyclic (thio)ureas towards active methylene reagents (AMRs) was investigated. By reacting ethylenethiourea and ethyleneurea with benzoyl chloride in DMF, the corresponding iminium salts were isolated and directly condensed with a series of AMRs to obtain the stereoselective synthesis of α,β-unsaturated(thio)ureas [28]. A similar protocol was recently applied for the one-pot stereoselective preparation of Knoevenagel-type indoles [29].

The chemical accessibility to Knoevenagel-type indoles and the above mentioned rich literature background on this heterocyclic scaffold prompted us to evaluate the antiproliferative activity of a series of indole derivatives **2-10** (Chart 1 and Table 2).

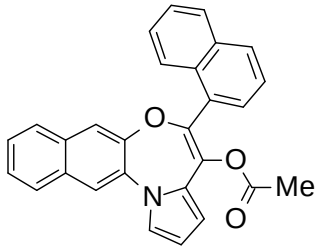

1, PBOX-15

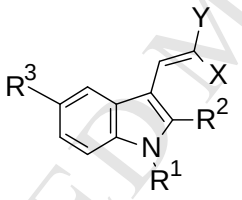

2-10, Title compounds

2a-g, $R^1 = R^2 = R^3 = H$
3a,b, $R^1 = Me$; $R^2 = R^3 = H$
4a-d, $R^2 = Me$; $R^1 = R^3 = H$
5a-ac, $R^2 = Ph$; $R^1 = R^3 = H$
6a,b, $R^2 = 4\text{-MeO-}C_6H_4$; $R^1 = R^3 = H$
7a,b, $R^1 = H$; $R^2 = Ph$; $R^3 = OMe$
8a,b, $R^1 = H$; $R^2 = 4\text{-MeO-}C_6H_4$; $R^3 = OMe$
9a,b, $R^2 = R^3 = H$; $R^1 = CH_2COC_6H_4\text{-}m\text{OMe}$
10a, $R^2 = R^3 = H$; $R^1 = CH_2COC_6H_4\text{-}p\text{C}_6H_5$
X, Y = EWGs as in Table 2 and Scheme 2

Chart 1. General structure of title compounds **2-10** and structure of reference PBOX-15

2. Results and discussion

2.1. Chemistry

As previously described [29], iminium salts **Im11-Im17** were obtained by reacting indoles **11-17** with the DMF-benzoyl chloride complex and directly condensed with the active methylene reagents **I-XXX** (Scheme 1, Table 1) in the presence of triethylamine to afford the desired indole derivatives **2-8** (Table 2). By this two-step one-pot procedure we were able to prepared 48 indole analogues; the series included previously described compounds (namely, **2a-e,g**; **3a,b**; **4a-d**; **5a,b,f,h-m,o,s-u,aa,ab,ac**; **6a,b**; **7a,b**; **8a,b**) [29-31] and 14 unreported derivatives (namely, **2f**; **5c-e,g,n,p-r,v-z**).

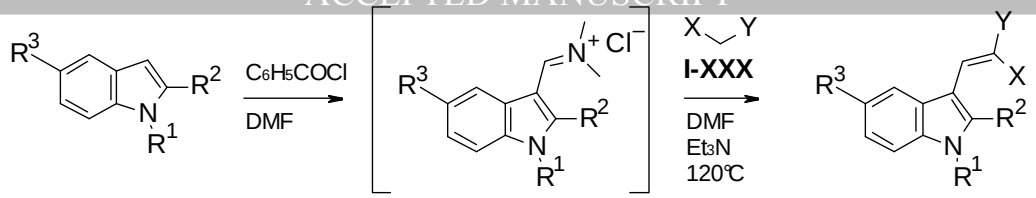

11, $R^1 = R^2 = R^3 = H$
12, $R^1 = Me$; $R^2 = R^3 = H$
13, $R^2 = Me$; $R^1 = R^3 = H$
14, $R^2 = Ph$; $R^1 = R^3 = H$
15, $R^2 = 4\text{-MeO-}C_6H_4$; $R^1 = R^3 = H$
16, $R^1 = H$; $R^2 = Ph$; $R^3 = OMe$
17, $R^1 = H$; $R^2 = 4\text{-MeO-}C_6H_4$; $R^3 = OMe$

Im11-Im17 **2-8**

Scheme 1. Two-step one-pot procedure for the synthesis of antiproliferative indoles **2-8**

Table 1. The active methylene reagents employed in the synthesis.

AMRs	X	Y	AMRs	X	Y
I	CN	CN	**XVI**	COMe	COMe
II	CN	$COC(Me)_3$	**XVII**	COMe	SO_2Me
III	CN	COPh	**XVIII**	COMe	SO_2Ph
IV	CN	$CO\text{-}C_6H_4\text{-}p$Cl	**XIX**	COMe	$SO_2\text{-}C_6H_4\text{-}p$Cl
V	CN	2-thenoyl	**XX**	COPh	COMe
VI	CN	COOEt	**XXI**	COPh	COPh
VII	CN	$COOCH_2CH_2OCH_3$	**XXII**	COPh	COOEt
VIII	CN	$CONH_2$	**XXIII**	COPh	SO_2Ph
IX	CN	$CON[(\text{-}CH_2)_5\text{-}]$	**XXIV**	$CO\text{-}C_6H_4\text{-}p$Cl	COOEt
X	CN	$CO\text{-}NHC_6H_4\text{-}p$Cl	**XXV**	$CO\text{-}C_6H_4\text{-}pNO_2$	COOEt
XI	CN	$PO(OEt)_2$	**XXVI**	2-furoyl	$COCF_3$
XII	CN	$PO(O^iC_3H_7)_2$	**XXVII**	COOMe	SO_2Me
XIII	CN	SO_2Me	**XXVIII**	COOMe	SO_2Ph
XIV	CN	SO_2Ph	**XXIX**	COOEt	COMe
XV	CN	$SO_2\text{-}C_6H_4\text{-}p CH_3$	**XXX**	COOEt	COOEt

The condensation procedure resulted to be stereoselective in terms of *E/Z* isomerism at the exocyclic double bond. In fact, products **2-8** were obtained as single stereoisomers as demonstrated by the measurement of the $^3J_{C,H}$ and the $^3J_{P,H}$ coupling constants between the vinyl proton and the phosphorus (compounds **2b**; **5k**) or the X α-carbon (compounds **2c,g**; **4b,d**; **5c,l,p,q,v,z,aa**) or the X and Y α-carbons (compounds **2f**; **5b,f,h,i,s,u,x,ab**) [29]. The configurations of the remaining compounds have been attributed by comparison with the configurations of the analogues bearing the same X and Y groups. Most of the indole derivatives were isolated as *E*-isomers with the only exception of compounds **5s** and **5ab** that were obtained as *Z*-isomers (Table 2).

Table 2. Yields, *E/Z* ratio and MT-4 cell-based cytotoxicity of Knoevenagel-type indoles **2-8**.

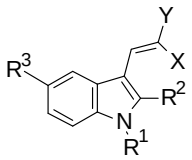

IDs	R^1	R^2	R^3	X	Y	Isomer	Yield	[a]EC_{50} µM
2a	H	H	H	CN	CN	-	72	36±2
2b	H	H	H	CN	$PO(OEt)_2$	*E*	28	80±3
2c	H	H	H	CN	SO_2Me	*E*	73	>100
2d	H	H	H	CN	SO_2Ph	*E*	78	>100
2e	H	H	H	COPh	COOEt	*E*	50	>100
2f	H	H	H	CO-C_6H_4-*p*NO_2	COOEt	*E*	32	100±5
2g	H	H	H	COOMe	SO_2Ph	*E*	53	>100
3a	Me	H	H	CN	SO_2Me	*E*	45	>100
3b	Me	H	H	CN	SO_2Ph	*E*	60	>100
4a	H	Me	H	CN	CN	*E*	77	56±2
4b	H	Me	H	CN	SO_2Me	*E*	40	>100
4c	H	Me	H	CN	SO_2Ph	*E*	45	>100
4d	H	Me	H	COOMe	SO_2Ph	*E*	39	31±1.5
5a	H	Ph	H	CN	CN	-	74	0.4±0.05
5b	H	Ph	H	CN	$COCMe_3$	*E*	51	0.5±0.05
5c	H	Ph	H	CN	COPh	*E*	72	0.5±0.02
5d	H	Ph	H	CN	CO-C_6H_4-*p*Cl	*E*	83	0.4±0.01
5e	H	Ph	H	CN	2-thenoyl	*E*	40	0.4±0.01
5f	H	Ph	H	CN	COOEt	*E*	91	1.7±0.02
5g	H	Ph	H	CN	$COOCH_2CH_2OMe$	*E*	89	1.2±0.05
5h	H	Ph	H	CN	$CONH_2$	*E*	55	6.0±0.4
5i	H	Ph	H	CN	COPip[b]	*E*	60	9.6±0.6
5j	H	Ph	H	CN	CO-NHC_6H_4-*p*Cl	*E*	62	1.7±0.08
5k	H	Ph	H	CN	$PO(OiPr)_2$	*E*	36	11±0.4
5l	H	Ph	H	CN	SO_2Me	*E*	78	0.3±0.06
5m	H	Ph	H	CN	SO_2Ph	*E*	69	0.4±0.03
5n	H	Ph	H	CN	SO_2-C_6H_4-*p*CH_3	*E*	72	0.4±0.02
5o	H	Ph	H	COMe	COMe	-	42	1.5±0.04
5p	H	Ph	H	COMe	SO_2Me	*E*	48	0.5±0.02
5q	H	Ph	H	COMe	SO_2Ph	*E*	4	0.4±0.03
5r	H	Ph	H	COMe	SO_2-C_6H_4-*p*Cl	*E*	12	>100
5s	H	Ph	H	COPh	COMe	*Z*	40	2.0±0.04
5t	H	Ph	H	COPh	COPh	-	14	8.9±0.5
5u	H	Ph	H	COPh	COOEt	*E*	36	7.0±0.9
5v	H	Ph	H	COPh	SO_2Ph	*E*	17	3.0±0.06
5w	H	Ph	H	CO-C_6H_4-*p*Cl	COOEt	*E*	47	9.0±0.5
5x	H	Ph	H	CO-C_6H_4-*p*NO_2	COOEt	*E*	22	1.5±0.08
5y	H	Ph	H	2-furoyl	$COCF_3$	*n.d.*	10	0.8±0.01
5z	H	Ph	H	COOMe	SO_2Me	*E*	43	0.4±0.03
5aa	H	Ph	H	COOMe	SO_2Ph	*E*	42	1.0±0.03
5ab	H	Ph	H	COOEt	COMe	*Z*	45	0.6±0.01
5ac	H	Ph	H	COOEt	COOEt	-	13	2.3±0.07
6a	H	4-MeO-C_6H_4	H	CN	CN	-	70	0.3±0.01
6b	H	4-MeO-C_6H_4	H	CN	SO_2Ph	*E*	62	0.2±0.06
7a	H	Ph	MeO	CN	CN	-	58	1.0±0.05
7b	H	Ph	MeO	CN	SO_2Ph	*E*	78	1.3±0.02
8a	H	4-MeO-C_6H_4	MeO	CN	CN	-	73	0.3±0.01
8b	H	4-MeO-C_6H_4	MeO	CN	SO_2Ph	*E*	53	0.2±0.04
Doxorubicin								0.03±0.001

[a]Compound concentration (µM) required to reduce the viability of mock-infected MT-4 cells by 50%, as determined by the MTT method, under conditions allowing untreated controls to undergo at least three consecutive rounds of multiplication. Data represent mean values (±SD) for three independent determinations.

Moreover, two of the obtained products (derivatives **2d** and **2e**) were *N*-alkylated to afford compounds **9a**,**b** and **10a** via deprotonation of the indole nitrogen with sodium hydride and subsequent reaction of the corresponding salts with different ω-bromoacetophenones (Scheme 2).

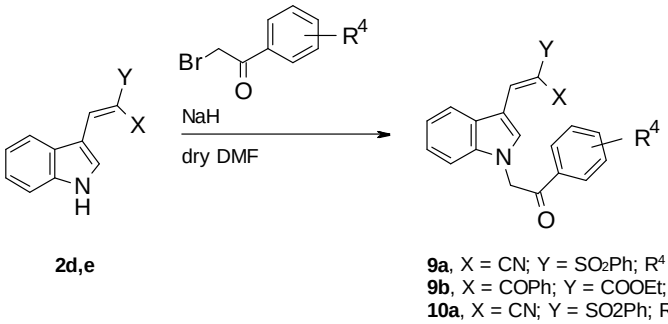

Scheme 2. Synthesis of compounds **9a**,**b** and **10a**

2.2. Biological evaluation

Compounds **2-10** were preliminary tested in MT-4 cell-based assay in order to evaluate their cytotoxic activity (Table 2). The antiproliferative activity was found to be affected by both the nature of the substituent of the indole scaffold and the X and Y groups (Table 2). Thus, all the compounds showing submicromolar EC_{50} values bear at position 2 of the indole nucleus either a phenyl (derivatives **5a-e,g,l-n,p,q,y,z,ab**) or a *p*-anisyl (derivatives **6**, **7** and **8**) group. Conversely, the unsubstituted indole compounds **2** emerged to be poorly active or inactive. Similarly, *N*-alkylation led to inactive compounds (derivatives **3**, **9** and **10**) and also the introduction of a 2-methyl group was found to be detrimental for activity (derivatives **4** vs **5** and **6**). The activity of Knoevenagel-type indoles appears to be influenced also by the nature of the X and Y groups as highlighted by the different potencies of the 2-phenylindole derivatives **5** (Table 2). Thus, when X is a cyano group and Y is a cyano, keto, ester, *N*-phenylamido or sulphonyl substituent we registered a good antiproliferative activity (EC_{50} value range: 0.4-1.7 μM, see derivatives **5a-g,j,l,m,n**); conversely **5h,i,k,** sharing the X cyano group and characterized by an amide or a phosphonic ester as Y substituents were poorly active (EC_{50} value range: 6.0-11.0 μM). The presence of a benzoyl substructure as X substituent seemed to correlate with poor activity (see compounds **5t-v**) even if derivative **5s** emerged to be active at micromolar concentrations. Furthermore the introduction of a *p*-NO_2 group at the benzoyl moiety led to a 5-fold increase in activity (**5u** vs **5x**), while the *p*-Cl substitution caused a slight reduction in potency (**5u** vs **5w**). Finally, derivatives **5y-ac** bearing as X groups a 2-furoyl or an ester substituent showed EC_{50} values in the (sub)micromolar concentration range.

In order to define the safety profile of the most interesting compounds, their cytotoxic activity for tumour cells (haematological and solid human tumour-derived cell lines) was compared to that for non-neoplastic cell lines (Tables 3 and 4). Doxorubicin was used as reference drug. This analysis revealed a cytotoxic potential for compounds **6b** and **8b** against all the human leukaemia-lymphoma-derived cell lines evaluated. Notably, compounds **5g**, **6b** and **8b** showed a good activity against lung squamous, prostate and hepatocellular human carcinoma accompanied by a favourable selectivity index.

Table 3. Cytotoxic activity of selected indole compounds against human leukaemia-lymphoma-derived (CCRF-CEM, WIL-2NS, CCRF-SB) cell lines

	[a]EC_{50} (μM)		
IDs	[b]**CCRF-CEM**	[c]**WIL-2NS**	[d]**CCRF-SB**
5d	1.1±0.1	4.5±0.4	0.6±0.001
5e	1.2±0.2	6.4±0.7	0.6±0.004
5g	1.6±0.1	2.2±0.1	2.2±0.1
5s	8.1±0.3	12±0.9	11±0.8
5t	12±0.5	72±4	12±0.8
5u	8±0.3	12±1	9.6±0.9
5x	1.8±0.2	2.4±0.2	2.2±0.3
5y	1.9±0.09	2.3±0.1	1.8±0.1
5ab	1.4±0.1	2.7±0.1	1.6±0.1
6b	0.3±0.1	0.4±0.008	0.3±0.005
7b	1.5±0.2	2.8±0.2	1.9±0.09
8b	0.3±0.001	0.5±0.003	0.3±0.003
Doxorubicin	0.02±0.001	0.04±0.002	0.01±0.001

[a]Compound concentration (μM) required to reduce cell proliferation by 50%, as determined by the MTT method, under conditions allowing untreated controls to undergo at least three consecutive rounds of multiplication. Data represent mean values (± SD) for three independent determinations. [b]$CD4^+$ human acute T-lymphoblastic leukaemia. [c]Human splenic B-lymphoblastoid cells. [d]Human acute B-lymphoblastic leukaemia.

Table 4. Cytotoxic activity of selected indole compounds against solid tumour-derived (SK-MEL 28, SK-MES-1, DU-145, Hep-G2, MCF-7) and normal control (MRC-5 and CRL 7065) cell lines.

	[a]EC_{50} (μM)						
IDs	[b]**MRC-5**	[c]**CRL-7065**	[d]**SK-MEL28**	[e]**SK-MES 1**	[f]**DU-145**	[g]**Hep-G2**	[h]**MCF-7**
5d	14±1.5	7.4±2.4	15±2.5	19±4	11±2.2	37±14	28±3.5
5e	20±2.1	45±6	28±6	4±0.5	11±0.8	25±1	29±1.2
5g	>100	76±3	9.3±2	5±0.05	4.2±1	85±3	12±0.7
5s	>100	>100	>100	>100	>100	79±2	>100
5t	>100	>100	>100	>100	>100	>100	>100
5u	>100	>100	>100	>100	68±2	31±3	43±5
5x	>100	>100	>100	19±1	11±0.9	28±3	40±2
5y	12	8.1±0.7	33±5	27±1	9.2±0.6	16±3	10±2.6
5ab	31±3	83±2	30±1.5	23±1	11±2	19±2	32±2.5
6b	73±5	>100	>100	43±4	2±0.3	11±2.5	>100
7b	14±2.8	11±0.1	10±0.3	12±1.3	10±0.2	9.6±1.9	12±0.5
8b	22±2	>100	>100	>100	3±1	6.4±0.4	40±3
Doxorubicin	0.3±0.01	0.9±0.02	0.7±0.01	0.1±0.009	0.2±0.03	0.3±0.01	0.3±0.02

[a]Compound concentration (μM) required to reduce cell proliferation by 50%, as determined by the MTT method, under conditions allowing untreated controls to undergo at least three consecutive rounds of multiplication. Data represent mean values (±SD) for three independent determinations. [b]Human normal lung fibroblasts. [c]Human normal foreskin fibroblasts. [d]Human skin melanoma. [e]Human lung squamous carcinoma. [f]Human prostate carcinoma. [g]Human hepatocellular carcinoma. [h]Human breast adenocarcinoma.

Derivatives **2-8** were submitted to the NCI (Bethesda MA-USA) developmental therapeutics program for antiproliferative testing against different human tumour cell lines, organized into 9 disease-oriented panels; the fifteen derivatives reported in Tables 5-7 were selected and screened by NCI. The results are expressed as GI_{50} (measure the growth inhibitory power), TGI (measure of the cytostatic activity) and LC_{50} (measure of the cytocidal effect). Table 5 summarizes the number of cell lines against which each compound was screened, the number of lines against which it

gave a positive (inferior to 100 µM) GI_{50}, TGI or LC_{50} values and the corresponding concentration range. The GI_{50} values of the fifteen molecules are reported in Tables 6 and 7.

Table 5. GI_{50}, TGI and LC_{50} values ranges of selected compounds from NCI's in vitro screening.

	GI_{50} (µM)[a]		TGI (µM)[b]		LC_{50} (µM)[c]	
IDs	***No*** [d]	**Range**	***No*** [d]	**Range**	***No*** [d]	**Range**
4d	*56*	1.1-17.4	*47*	5.2-96.7	*35*	22.2-98.7
5a	*59*	0.246-43.2	*50*	0.698-90.4	*10*	12.1-98.4
5c	*54*	0.370-65.3	*13*	4.1-86.9	*1*	58.2
5m	*60*	0.288-23.6	*52*	4.7-96.3	*12*	7.6-86.7
5p	*59*	0.415-43.8	*21*	5.6-88.1	*3*	17.3-67.7
5s	*59*	0.295-7.2	*56*	2.0-46.6	*39*	4.7-81.4
5v	*31*	3.1-97.1	-	-	-	-
5z	*58*	0.671-19.6	*46*	4.0-98.5	*16*	8.2-69.8
5ac	*60*	0.219-23.9	*60*	12.7-66.0	*37*	33.2-99.1
6a	*60*	0.0173-2.8	*50*	3.2-80.7	*5*	1.9-23.9
6b	*60*	<0.01-19.3	*52*	4.7-96.3	*9*	6.8-90.8
7a	*60*	0.607-44.2	*20*	3.3-57.6	*2*	55.4-75.0
7b	*58*	1.1-37.3	*18*	7.1-85.5	-	-
8a	*47*	0.075-23.0	*21*	5.6-88.1	-	-
8b	*58*	0.276-46.1	*50*	3.2-80.7	*4*	8.5-47.0

[a]Compound concentration that gives 50% growth inhibition. [b]Compound concentration that gives total growth inhibition. [c] Compound concentration that produces 50% lethal (cytocidal) effect. [d] The table shows the number of cell lines on which each compound gave a positive (i.e. lower than 100 µM) GI_{50} or TGI or LC_{50} value and the corresponding concentration ranges.

With the exception of derivatives **4d**, **5v** and **7b**, all the tested compounds showed submicromolar GI_{50} values against specific tumour cell lines. Derivatives **6a,b** and **8a,b** were endowed with a widespread submicromolar activity against the tested tumour panels and proved to be particularly effective against selected cell lines [**6a**: GI_{50} (leukaemia-SR) = 17.3 nM; **6b**: GI_{50} (breast cancer-MDA-MB-468) < 10 nM; **8a**: GI_{50} (renal cancer-A498) = 75 nM].

Table 6. GI_{50} values for compounds **4d** and **5a,c,m,p,q,v,z,ac**.

	Panel / *cell line*	**GI_{50} (μM)[a]**								
		4d	**5a**	**5c**	**5m**	**5p**	**5q**	**5v**	**5z**	**5ac**
Leukaemia	CCRF-CEM	n.d.[b]	2.4	7.3	2.6	4.7	1.4		7.6	2.6
	HL-60 (TB)	n.d.[b]	1.8	n.d.[b]	1.8	2.6	1.7	5.0	3.4	4.4
	K-562		**0.478**		**0.348**	**0.679**	**0.442**	6.5	n.t.[c]	3.6
	MOLT-4	1.9	43.2	n.d.[b]	2.2	4.4	1.6	n.d.[b]	4.7	3.9
	RPMI-8226	3.2	**0.582**	2.4	**0.714**	3.0	2.2	7.6	6.2	**0.219**
	SR	1.1		n.d.[b]	17.3	n.t.[c]	n.tc	9.9	8.1	2.1
Non-Small Cell Lung Cancer	A549/ATCC	4.9	4.6	7.6	3.7	7.3	7.2	35.0	5.3	6.4
	EKVX	5.0	5.8	10.0	6.2	6.4	3.3	4.6	8.9	12.4
	HOP-62	7.7	11.3	16.3	9.3	12.1	1.2		10.7	5.5
	HOP-92	4.1	7.7	4.5	10.3	3.8	5.9	5.0	6.6	8.8
	NCI-H226	4.3	4.1	6.8	4.1	27.1	1.9		5.0	11.4
	NCI-H23	4.8	4.7	16.0	4.7	4.0	1.6	9.6	8.0	2.9
	NCI-H322M	8.8	11.4	3.8	9.2	9.6	6.1		7.4	12.7
	NCI-H460	3.0	2.1	4.5	2.7	2.8	1.1	5.9	3.5	3.8
	NCI-H522	3.2	9.6	4.0	4.6	3.6	1.3	91.8	3.1	3.4
Colon Cancer	COLO 205	7.5	1.8	5.0	1.4	3.0	1.7	7.8	4.4	4.9
	HCC-2998	4.9	10.4	14.5	10.9	8.0	1.4		8.8	10.1
	HCT-116	3.8	2.3	5.3	2.0	2.9	**0.754**	4.9	4.2	4.3
	HCT-15	3.1	**0.971**	3.5	1.1	2.0	**0.836**	n.d.[b]	2.4	4.1
	HT29	5.2	**0.526**	3.4	**0.595**	1.6	**0.589**		3.6	4.6
	KM12	2.4	**0.684**	2.0	**0.652**	2.1	1.0	5.1	1.5	3.5
	SW-620	5.2	**0.539**	3.0	**0.570**	2.1	**0.778**	n.d.[b]	2.9	5.6
CNS Cancer	SF-268	3.3	13.4	5.7	4.5	4.2	3.4		4.3	6.8
	SF-295	3.1	1.6	3.0	2.4	3.9	2.4	3.5	3.1	7.6
	SF-539	3.4	2.1	6.0	2.5	1.9	1.3		3.1	14.5
	SNB-19	7.6	5.7	16.8	8.3	3.4	6.1		8.7	23.9
	SNB-75	3.1	2.0	3.2	1.7	1.5	1.7	10.1	2.3	7.0
	U251	3.4	1.2	4.7	2.6	2.9	1.2	8.6	3.6	4.9
Melanoma	LOX IMVI	2.0	3.3	7.4	4.6	3.4	1.4	74.7	5.1	5.6
	MALME-3M	7.3	26.0	12.3	8.4	4.8	2.1		12.2	8.9
	M14	4.4	1.9	4.8	3.8	1.6	**0.521**	15.6	3.3	4.2
	MDA-MB-435	2.9	**0.246**	**0.370**	**0.288**	**0.415**	**0.295**	3.9	**0.671**	3.4
	SK-MEL-2	10.6	27.6	35.2	12.7	8.6	1.4		11.8	4.7
	SK-MEL-28	5.8	5.1	12.0	8.3	3.3	2.0		6.0	7.7
	SK-MEL-5	n.t.[c]	1.1	n.t.[c]	1.82	1.9	**0.832**	9.0	n.t [c]	3.8
	UACC-257	7.0	28.1	10.9	18.2	43.8	2.2		11.2	7.5
	UACC-62	2.8	2.6	3.6	2.6	3.2	1.0	9.0	3.3	4.6
Ovarian Cancer	IGROV1	1.5	**0.757**	2.5	3.3	8.3	1.5		1.7	5.7
	OVCAR-3	2.7	1.8	2.4	1.4	2.3	1.6		1.9	4.2
	OVCAR-4	5.7	5.2	65.3	5.5	3.8	3.7	6.6	6.2	10.5
	OVCAR-5	17.4	19.7		13.9	16.1	2.0		19.6	18.5
	OVCAR-8	3.9	6.0	2.2	6.0	5.2	2.5		6.3	4.1
	NCI/ADR-RES	4.2	**0.826**	3.1	1.1	2.1	**0.520**		3.3	2.9
	SK-OV-3	9.3	6.0	15.2	6.8	4.4	2.9	7.6	12.1	13.6
Renal Cancer	786-0	8.2	8.6	16.5	9.2	3.5	1.6		7.5	12.9
	A498	5.5	3.0	15.3	11.0	3.9	2.0	n.d.[b]	6.6	16.9
	ACHN	5.5	7.3	7.2	7.0	5.8	1.8	6.7	9.2	4.4
	CAKI-1	3.3	6.1	2.5	5.5	5.6	2.4	3.1	1.8	10.3
	RXF 393	3.6	3.3	9.6	3.6	2.6	1.3	97.1	7.2	3.7
	SN12C	2.6	6.8	5.7	5.2	6.9	1.9		3.1	5.1
	TK-10	8.1	5.3	11.1	5.6	13.5	3.8		7.7	13.6
	UO-31	4.4	11.1	30.5	6.7	5.8	1.6		5.5	4.0
Prostate Cancer	PC-3	5.6	3.0	3.5	3.4	4.5	2.5	5.0	4.2	3.3
	DU-145	2.9	3.3	5.2	2.9	3.5	3.0		2.5	9.7
Breast Cancer	MCF7	2.8	1.1	4.0	2.2	2.7	**0.945**	5.0	2.9	4.5
	MDA-MB-231	2.7	1.8	13.2	3.8	5.5	1.7		2.4	5.8
	HS 578T	2.9	2.3	6.3	23.6	1.6	5.0	39.5	3.5	3.8
	BT-549	5.4	9.4	3.0	11.6	2.4	1.9		4.3	5.3
	T-47D	3.2	4.6	5.3	3.8	2.3	1.4	3.4	2.8	2.7
	MDA-MB-468	6.3	1.0	5.6	1.9	1.8	1.7	4.2	5.4	3.1

[a]Compound concentration that gives 50% growth inhibition (Only the values < 100 μM are reported). [b]Not determined. [c]Not tested. GI_{50} values lower than 1.0 μM are reported in bold.

Table 7. GI_{50} values for compounds **6a,b, 7a,b** and **8a,b.**

	Panel / *cell line*	**GI_{50} (μM)[a]**					
		6a	**6b**	**7a**	**7b**	**8a**	**8b**
Leukaemia	CCRF-CEM	**0.352**	1.3	3.4	6.5		1.3
	HL-60 (TB)	**0.271**	**0.294**	2.5	2.4	**0.363**	**0.899**
	K-562	**0.343**	**0.535**	2.1	1.4	**0.345**	**0.508**
	MOLT-4	**0.578**	**0.871**	3.7	4.7	**0.369**	**0.765**
	RPMI-8226	**0.490**	2.1	2.6	n.t.[c]	5.1	1.3
	SR	**0.0173**	**0.350**	**0.865**	2.2	**0.152**	**0.305**
Non-Small Cell Lung Cancer	A549/ATCC	**0.700**	**0.803**	7.0	6.0	3.8	2.8
	EKVX	**0.656**	1.3	4.1	6.9	n.d.[b]	3.3
	HOP-62	1.2	1.0	5.3	8.3	3.3	3.1
	HOP-92	1.2	2.3	2.4	6.1	23.0	**0.698**
	NCI-H226	1.1	2.8	3.5	9.4	1.5	3.7
	NCI-H23	**0.600**	**0.932**	4.1	8.0	2.0	**0.946**
	NCI-H322M	**0.490**	1.5	7.4	30.1	**0.380**	4.3
	NCI-H460	**0.359**	**0.404**	3.6	4.6	**0.472**	**0.687**
	NCI-H522	**0.798**	3.0	4.6	4.0		1.7
Colon Cancer	COLO 205	**0.223**	**0.254**	2.1	7.4	**0.291**	0.396
	HCC-2998	**0.751**	1.2	6.1	18.7	n.d.[b]	2.0
	HCT-116	**0.411**	**0.399**	4.4	3.7	**0.487**	0.539
	HCT-15	**0.593**	**0.554**	3.2	4.0	**0.778**	0.632
	HT29	**0.354**	**0.314**	3.1	3.5	**0.407**	0.435
	KM12	**0.374**	**0.374**	3.5	3.0	**0.590**	0.654
	SW-620	**0.440**	**0.506**	3.6	4.0	**0.579**	0.540
CNS Cancer	SF-268	**0.709**	1.1	8.3	13.3	1.7	1.6
	SF-295	**0.336**	**0.500**	4.2	2.8	**0.306**	**0.760**
	SF-539	**0.263**	**0.299**	2.9	5.5	**0.774**	**0.510**
	SNB-19	1.8	**0.863**	6.0	13.5	13.7	3.2
	SNB-75	**0.418**	**0.379**	2.8	5.9	**0.593**	**0.612**
	U251	**0.483**	**0.473**	3.5	4.6	**0.635**	**0.563**
Melanoma	LOX IMVI	1.8	1.3	4.9	7.4		1.2
	MALME-3M	**0.874**	1.2	4.4	19.4		3.2
	M14	**0.295**	**0.383**	2.3	3.7	**0.308**	**0.500**
	MDA-MB-435	**0.128**	**0.203**	**0.607**	1.1	**0.122**	**0.276**
	SK-MEL-2	**0.763**	18.1	5.9	3.7	5.9	9.0
	SK-MEL-28	1.2	1.8	4.4	6.1	1.7	**0.787**
	SK-MEL-5	**0.350**	0.344	2.9	3.1	**0.324**	**0.319**
	UACC-257	**0.424**	10.7	30.0	4.9		46.1
	UACC-62	**0.357**	0.597	2.5	3.8	**0.357**	**0.660**
Ovarian Cancer	IGROV1	1.4	19.3	8.4	4.8	5.8	10.6
	OVCAR-3	**0.265**	**0.244**	3.1	5.0	**0.424**	**0.359**
	OVCAR-4	**0.798**	**0.578**	5.4	8.3		2.1
	OVCAR-5	1.8	1.9	44.2	37.3		4.6
	OVCAR-8	1.2	1.3	7.7	7.8		3.1
	NCI/ADR-RES	**0.343**	**0.428**	2.8	3.8	**0.403**	**0.494**
	SK-OV-3	**0.445**	**0.528**	4.8	7.1	**0.892**	**0.901**
Renal Cancer	786-0	**0.720**	1.2	6.6	6.1	14.3	2.1
	A498	**0.458**	1.1	2.0	9.3	**0.075**	n.t.[c]
	ACHN	2.3	1.9	7.4	12.9		1.8
	CAKI-1	**0.679**	**0.997**	4.1	4.5	**0.392**	4.2
	RXF 393	**0.518**	1.0	9.8	n.t.[c]	5.5	
	SN12C	1.2	1.5	4.7	7.8	15.9	2.3
	TK-10	**0.925**	4.8	5.1	17.5		5.0
	UO-31	2.8	4.7	6.4	4.0		3.1
Prostate Cancer	PC-3	**0.547**	**0.557**	5.4	8.3	**0.342**	**0.534**
	DU-145	**0.484**	**0.450**	6.5	10.1	**0.917**	**0.875**
Breast Cancer	MCF7	**0.347**	**0.398**	2.2	3.9	**0.385**	**0.851**
	MDA-MB-231/ATCC	**0.562**	**0.649**	3.8	7.5	1.3	1.4
	HS 578T	**0.241**	**0.682**	2.4	7.6	**0.513**	**0.538**
	BT-549	**0.769**	1.6	2.2	11.6		4.8
	T-47D	**0.481**	**0.533**	2.3	5.2	2.6	**0.905**
	MDA-MB-468	**0.418**	**<0.01**	2.1	4.2	**0.503**	1.3

[a]Compound concentration that gives 50% growth inhibition (Only the values < 100 μM are reported). [b]Not determined. [c]Not tested. GI_{50} values lower than 1.0 μM are reported in bold.

With the aim of identifying the mechanism behind the Knoevenagel-type indoles antiproliferative activity and considering the recent literature on the pro-apoptotic properties of indole derivatives [32], the most promising compounds (**5e,l,p** and **5a,b**) were selected for further cellular studies concerning their antimitotic and pro-apoptotic efficacy. Time-dependent G2/M cell cycle arrest and time-dependent apoptosis induction were evaluated on various cancer cell lines. MCF-7, a breast carcinoma cell line, K562, a chronic myeloid leukaemia cell line and HL-60, a promyelocytic leukaemia cell line, were thus used as representative solid and haematological malignancies to evaluate the antitumor properties of these novel compounds. The obtained results are shown in Figures 1 and 2 while Figure 3 describes the immunofluorescence studies performed on MCF-7 cells.

A.

	Panel / *cell line*	GI_{50} (μM)[a]				
		5e	**5l**	**5p**	**6a**	**6b**
Leukaemia	HL-60	2.11	1.32	2.57	1.08	0.66
	K562	>10	>10	7.71	4.78	5.28
Breast Cancer	MCF-7	>10	>10	>10	>10	5.6

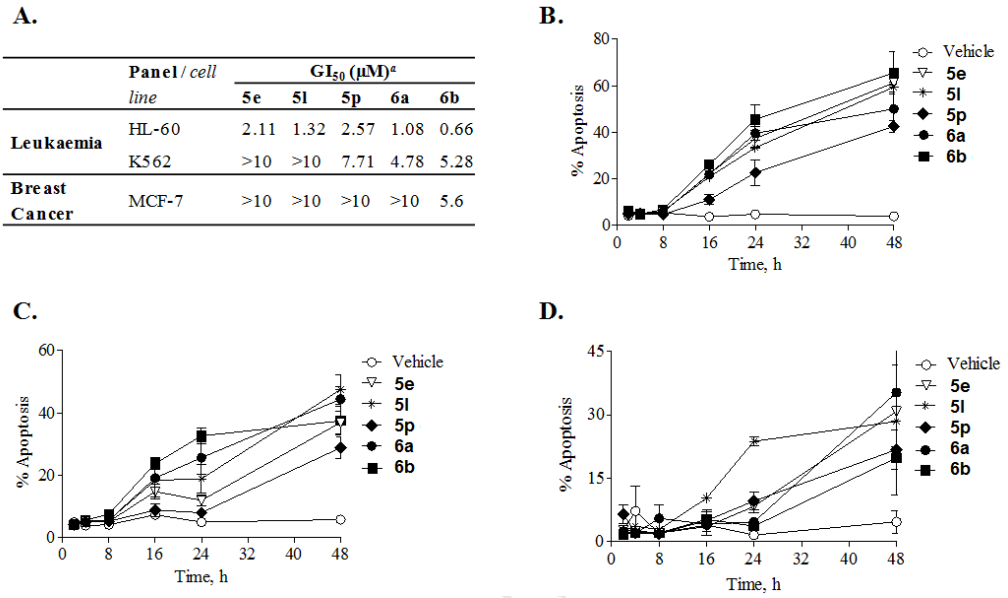

Figure 1. Compounds **5e,l,p** and **6a,b** potently reduce cell viability and induce apoptosis in HL-60, K562 and MCF-7 cell lines. **A.** Cellular viability; [a]Compound concentration that gives 50% growth inhibition. Cells were analyzed for apoptotic cell death **B.** HL-60 cells, **C.** K562 cells and **D.** MCF-7 cells. Values represent the mean ± S.E.M. of three independent experiments performed in triplicate.

Results showed that the five compounds tested were able to dose-dependently and significantly reduce cell viability in all three cell lines used following a 48 h treatment (Figure 1A). Further analysis showed the compounds to actively induce apoptosis in these cells in a time dependent manner (Figure 1B-D). Our results highlighted **5e** and **6b** as the most potent compounds in HL-60 cells, inducing 61.3 ± 4.2 and 65.5 ± 9.1% apoptosis, while **5l** and **6a** were most potent in K562 cells inducing 47.5 ± 4.8 and 44.4 ± 4.0% apoptosis, respectively. For MCF-7 cells, **5l** and **5e** induced 28.4 ± 6.0 and 34.1 ± 7.9% apoptosis.

These results prompted us to study cell cycle progression for the most potent pro-apoptotic agents identified. Accordingly, compounds **5l** and **6b** were chosen for further testing. Cell cycle analysis of cells treated with these two compounds showed apoptosis to be preceded by a G2/M arrest (Figure 2). **5l** induced a G2/M arrest of 39.7 ± 5.0, 46.8 ± 0.9 and 41.3 ± 3.5% in HL-60, K562 and MCF-7 cells after 18 h (HL-60, MCF-7) or 24 h (K562), respectively. Similarly, **6b** induced a G2/M arrest of 47.3 ± 3.0, 42.4 ± 7.6 and 40.4 ± 7.0% in the same cell lines.

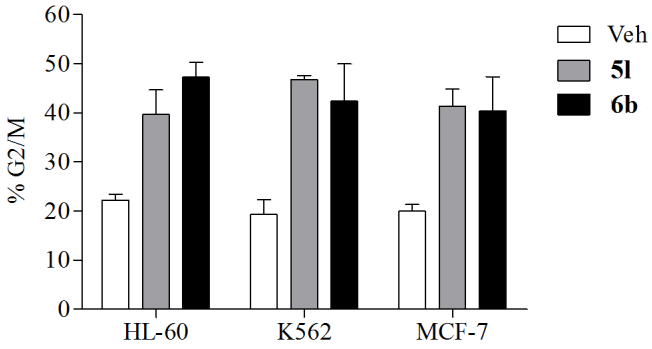

Figure 2. Apoptosis is preceded by a G2/M arrest following treatment with **5l** and **6b**. Values represent the mean ± S.E.M. of three independent experiments.

In the majority of cell proliferation and apoptosis assays performed, compound **6b** demonstrated the highest potency in terms of apoptosis and G2/M arrest, while **5e** and **5p** were somehow the less effective. Overall, the data so far acquired confirmed a pro-apoptotic character of the five indoles tested.

As microtubule targeting agents (MTAs) are associated with eliciting a G2/M arrest [33], MCF-7 cells were stained for tubulin and DNA and subjected to immunofluorescence. Cells treated with paclitaxel, a tubulin polymeriser and PBOX-15, a tubulin depolymeriser [34-36] were used as positive controls for highlighting the effect of MTAs on tubulin. In comparison to these MTAs, the tested analogues (**5l** and **6b**) had, in analogy with PBOX-15, a partial depolymerising effect on tubulin suggesting that the molecular target of the **5l** and **6b** compounds might be tubulin (Figure 3).

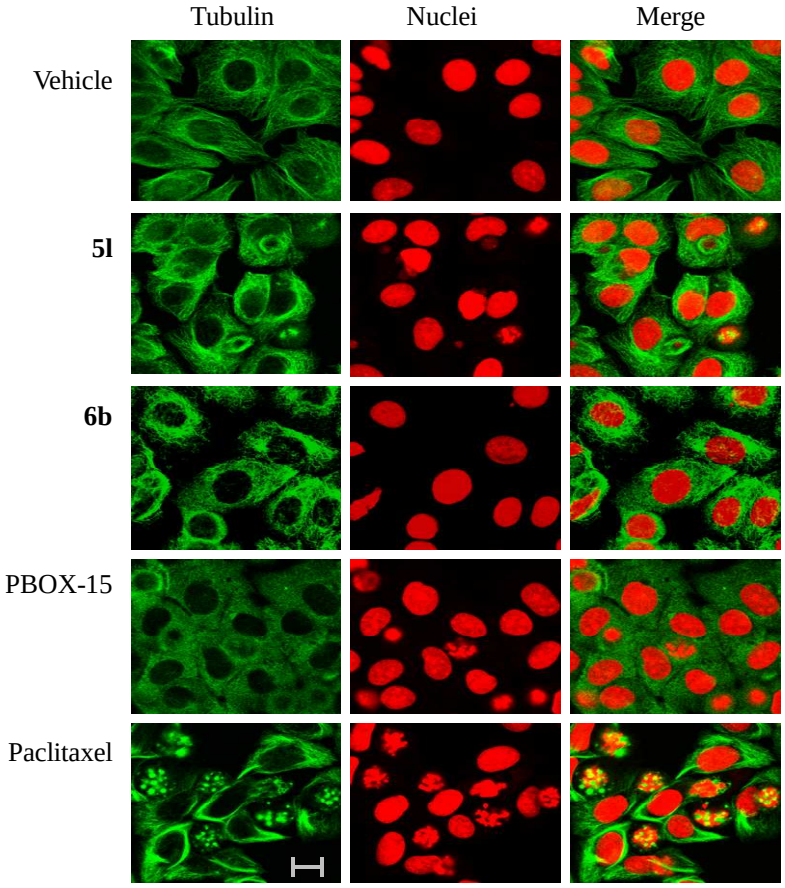

Figure 3. Effect of **5l** and **6b** on tubulin. DNA is colored red and microtubules in green. Bar represents 20 µm. Results are representative of three independent experiments

As a further analysis we also explored the possibility that **5l** could behave as a DNA intercalating agent. To this purpose we incubated saturating amounts of the inhibitor in the presence of double stranded plasmid DNA. Our experiments showed that **5l** does not intercalate DNA since the electrophoretic mobility properties of the plasmid in the presence of **5l** are not different from those of the plasmid alone (see figure S1 of the Supplementary Information).

3. Conclusions

The synthesized indole derivatives showed an overall good antiproliferative activity, which was specifically dependent on the presence of aryl substituents at position 2. Some of the compounds resulted selective for tumor cells, ensuring a good level of safety for normal cells. Moreover, activity data generated by NCI further confirmed the anti-proliferative potential of different indole compounds, in particular **6a,b** and **8a,b** are able to inhibit proliferation at submicromolar concentrations in most of the cancer cell lines tested. Further studies on selected compounds demonstrated their pro-apoptotic efficacy and tubulin was identified as their potential biological target.

4. Experimental section

4.1. Chemistry

All reactions were carried out in dried glassware. The commercially available building blocks were purchased from Alfa Aesar and Aldrich Chemical (Milan, Italy) and were used without further purification. 2-(4-methoxyphenyl)indole **15**, 5-methoxy-2-phenyl-1H-indole **16**, 5-methoxy-2-(4-methoxyphenyl)-1H-indole **17** were prepared according literature procedures [37].

Solvents were reagent grade. DMF was dried on molecular sieves (5Å 1/16" inch pellets). Organic solutions were dried over anhydrous sodium sulfate and evaporated using a rotatory evaporator operating at reduced pressure of about 10-20 Torr. Thin layer chromatography system for routine monitoring the course of reactions and confirming the purity of analytical samples employed aluminium-backed silica gel plates (Merck DC-Alufolien Kieselgel 60 F254); chloroform and methanol were used as developing solvents and detection of spots was made by UV light and/or by iodine vapours. Melting points were determined on a Fisher-Johns apparatus and are uncorrected. IR spectra were recorded on a Perkin Elmer 398 spectrometer. ^{1}H NMR spectra were collected on a BRUKER DPX-300 (300 MHz) or on a Varian Gemini 200 (200 MHz) instrument. ^{13}C NMR spectra were acquired on a BRUKER DPX-300 at 75.5 MHz. TMS was used as internal reference and DMSO-d_6 or $CDCl_3$ were used as solvents. ^{1}H NMR spectra were assigned with the help of homo-decoupling, COSY and NOE-difference experiments. Coupling constant values were given in Hertz. Fully decoupled ^{13}C NMR spectra are reported. For the determination of $^{3}J_{CH}$, fully coupled ^{13}C NMR spectra were acquired in the gated-decoupled mode with at least 0.5 Hz/pt digital resolution. Some selective proton-decoupling experiments were also needed. Chemical shifts were reported in δ (parts per million) units relative to the internal standard tetramethylsilane, and the splitting patterns were described as follows: s (singlet), d (doublet), t (triplet) and m (multiplet). Elemental analyses were performed by an EA1110 Analyser, Fison Instruments (Milan) and were within ±0.4% of theoretical values. UV analysis was carried out by a Thermo Scientific Evolution 300 spectrophotometer.

4.1.1. General one-pot procedure for the preparation of compounds 2-8.

To a stirred solution of the suitable indole **11-17** (10 mmol) in dry DMF (5 mL), benzoyl chloride (1.41 g, 10 mmol) was added in a single portion. After stirring at rt for 1 h, the reaction mixture was allowed to stand at 0 °C for 18-48 h. Then, a solution of the suitable active methylene reagent (11 mmol) and triethylamine (1.21 g, 12 mmol) in dry DMF (8 mL) pre-warmed at 80 °C, were added in a single portion. The reaction mixture was stirred for 45 min at 90 °C (for **5b** and **5u**: 1.5 h at 105 °C; for **5v**: 1.5 h at 120 °C). After cooling to rt, $Et_3N{\cdot}HCl$ precipitated and the resulting suspension was treated with water (50 mL). Then, work-ups 1-4 were carried out, as follows:

Work-up 1 (for **2a,c-g, 3b, 4a,b, 5a-h,j,l-p,r,s,u,x,z, 6a,b, 7a,b, 8a,b**): the precipitate obtained was filtered off, dried and crystallized from the suitable solvent or solvent mixture.

Work-up 2 (for **4d**, **5i,w,y**): the precipitate was filtered off and dissolved in CH_2Cl_2. The organic layer was washed with water (3 × 20 mL), dried over anhydrous Na_2SO_4 and filtered through a pad of Florisil. After evaporation of the solvent, the crude product was purified by crystallization from ethanol.

Work-up 3 (for **4c**, **5k,q,t**): the precipitate was filtered off, air dried, purified by chromatography (eluents: petroleum ether/ethyl acetate) and then crystallized from the suitable solvent or solvent mixture.

Work-up 4 (for **2b, 3a, 5v,aa-ac**): the reaction mixture was extracted with ethyl acetate (**2b**, **3a**, **5ac**) or CH_2Cl_2 (**5v,aa,ab**) (3×35 mL). The combined organic extracts were washed with water (5×30 mL), dried over anhydrous Na_2SO_4 and filtered through a pad of Florisil. After evaporation of the filtrate, the crude products **3a** and **5v,ac** were crystallized from the proper solvent(s). Conversely, the crude products of **2b** and **5z,aa** were purified by chromatography (eluent: petroleum ether/ethyl acetate) and then crystallized from the proper solvent mix.

*4.1.1.1. 1H-(Indol-3-ylmethylene)malononitrile (**2a**)* [29].

*4.1.1.2. Diethyl (E)-1-cyano-2-(1H-indol-3-yl)vinylphosphonate (**2b**)* [29].

*4.1.1.3. (2E)-3-(1H-Indol-3-yl)-2-(methylsulfonyl)acrylonitrile (**2c**)* [29].

*4.1.1.4. (2E)-3-(1H-Indol-3-yl)-2-(phenylsulfonyl)acrylonitrile (**2d**)* [29].

*4.1.1.5. Ethyl (2E)-2-benzoyl-3-(1H-indol-3-yl)acrylate (**2e**)* [29].

*4.1.1.6. Ethyl (2E)-3-(1H-indol-3-yl)-2-(4-nitrobenzoyl)acrylate (**2f**)*. Yellow solid; Yield 32%; mp: 161-162°C; IR (KBr, υ_{max} cm^{-1}): 3228 (NH), 1698 (COOEt), 1675 (COAr), 1603 (C=C), 1523 (NO_2), 1345 (NO_2), 1249 (COOEt); ^{1}H NMR (300 MHz, DMSO-d_6): δ 1.07 (t, *J* = 7.0 Hz, 3H, CH_3), 4.12 (q, *J* = 7.0 Hz, 2H, CH_2), 7.14-7.18 (m, 2H, Ar-H), 7.39-7.42 (m, 2H, Ar-H), 7.71-7.75 (m, 1H, Ar-H), 8.12 (d, *J* = 8.4 Hz, 2H, Ar-H), 8.25 (s, 1H, CH=C), 8.29 (d, *J* = 8.4 Hz, 2H, Ar-H), 11.87 (br s, 1H, NH); ^{13}C NMR (75.5 MHz, DMSO-d_6): δ 13.95, 60.61, 108.90, 112.43, 118.18, 121.11, 122.30, 122.83, 124.23, 124.23, 126.81, 129.75, 129.94, 129.94, 135.58, 136.02, 140.79, 150.25, 164.70, 195.16; $^3J_{C,H}$ = 10.2 Hz (CO); 7.5 Hz (COO); Anal. Calcd for $C_{20}H_{16}N_2O_5$: C, 65.93; H, 4.43; N, 7.69; Found: C, 65.84; H, 4.34; N, 7.64.

*4.1.1.7. Methyl (2E)-3-(1H-indol-3-yl)-2-(phenylsulfonyl)acrylate (**2g**)* [29].

*4.1.1.8. (2E)-3-(1-Methyl-1H-indol-3-yl)-2-(methylsulfonyl)acrylonitrile (**3a**)* [29].

*4.1.1.9. (2E)-3-(1-methyl-1H-indol-3-yl)-2-(phenylsulfonyl)acrylonitrile (**3b**)* [29].

*4.1.1.10. [(2-Methyl-1H-indol-3-yl)methylene]malononitrile (**4a**)* [29].

*4.1.1.11. (2E)-3-(2-Methyl-1H-indol-3-yl)-2-(methylsulfonyl)acrylonitrile (**4b**)* [29].

*4.1.1.12. (2E)-3-(2-Methyl-1H-indol-3-yl)-2-(phenylsulfonyl)acrylonitrile (**4c**)* [29].

*4.1.1.13. Methyl (2E)-3-(2-methyl-1H-indol-3-yl)-2-(phenylsulfonyl)acrylate (**4d**)* [29].

*4.1.1.14. [(2-Phenyl-1H-indol-3-y)lmethylene]malononitrile (**5a**)* [29].

*4.1.1.15. (2E)-2-(2,2-Dimethylpropanoyl)-3-(2-phenyl-1H-indol-3-yl)acrylonitrile (**5b**)* [29].

*4.1.1.16. (2E)-2-Benzoyl-3-(2-phenyl-1H-indol-3-y)acrylonitrile (**5c**)*. Yellow solid; Yield: 72%; mp: 254-256 °C; IR (KBr, υ_{max} cm^{-1}): 3323 (NH), 2209 (CN), 1622 (CO), 1549 (C=C); ^{1}H NMR (300 MHz, DMSO-d_6): δ 7.23-7.40 (m, 2H, Ar-H), 7.48-7.60 (m, 9H, Ar-H), 7.73-7.78 (m, 2H, Ar-H), 8.08 (s, 1H, CH=C), 8.22-8.31 (m, 1H, indole H-4), 12.97 (br s, 1H, NH); ^{13}C NMR (75.5 MHz, DMSO-d_6): δ 103.25, 108.42, 112.65, 118.92, 121.78, 122.92, 123.95, 124.71, 128.37, 128.37, 128.44, 128.44, 128.89, 128.89, 129.53, 130.01, 130.05, 130.05, 131.91, 137.13, 137.27, 149.32,

151,18, 190.89; $^{3}J_{C,H}$ = 13.5 Hz (CN); Anal. Calcd for $C_{24}H_{16}N_2O$: C, 82.74; H, 4.63; N, 8.04; Found: C, 83.02; H, 4.94; N, 8.04.

*4.1.1.17. (E)-2-(4-Chlorobenzoyl)-3-(2-phenyl-1H-indol-3-yl)prop-2-enenitrile (**5d**).* Yellow solid; Yield: 83%; mp: 232-234 °C; IR (KBr, υ_{max} cm^{-1}): 3219 (NH), 2210 (CN), 1632 (CO), 1558 (C=C); ^{1}H NMR (200 MHz, DMSO-d_6): δ 7.15-7.65 (m, 10H, Ar-H), 7.73-7.81 (m, 2H, Ar-H), 8.07 (s, 1H, CH=C), 8.28-8.33 (m, 1H, indole H-4), 13.01 (br s, 1H, NH); ^{13}C NMR (50.3 MHz, DMSO-d_6): δ 97.25, 102.41, 108.24, 112.37, 118.55, 121.56, 122.61, 123.73, 124.53, 128.17, 128.59, 129.14, 129.77, 130.03, 135.65, 136.39, 136.95, 149.38, 150.99, 189.47; Anal. Calcd for $C_{24}H_{15}ClN_2O$: C, 75.29; H, 3.95; N, 7.32; Found: C, 75.29; H, 4.18; N, 7.25.

*4.1.1.18. (2E)-3-(2-Phenyl-1H-indol-3-yl)-2-(thien-2-ylcarbonyl)acrylonitrile (**5e**).* Orange solid; Yield: 40%; mp: 206-207 °C; IR (KBr, υ_{max} cm^{-1}): 3232 (NH), 2206 (CN), 1587 (CO), 1561 (C=C); ^{1}H NMR (200 MHz, DMSO-d_6): δ 7.27-7.42 (m, 3H, Ar-H), 7.58-7.66 (m, 6H, Ar-H), 8.06-8.29 (m, 3H, Ar-H), 8.40 (s, 1H, CH=C), 13.02 (br s, 1H, NH); ^{13}C NMR (50.3 MHz, DMSO-d_6): δ 100.83, 108.46, 112.34, 119.08, 121.48, 122.61, 123.66, 124.40, 128.28, 128.67, 129.38, 129.79, 130.38, 135.02, 136.89, 141.68, 149.16, 150.51, 178.99; Anal. Calcd for $C_{22}H_{14}N_2OS$: C, 74.55; H, 3.98; N, 7.90; S, 9.05; Found: C, 74.64; H, 4.34; N, 7.90; S, 8.88.

*4.1.1.19. Ethyl (2E)-2-cyano-3-(2-phenyl-1H-indol-3-yl)acrylate (**5f**)* [29].

*4.1.1.20. 2-Methoxyethyl (2E)-2-cyano-3-(2-phenyl-1H-indol-3-yl)acrylate (**5g**).* Yellow solid; Yield: 89%; mp: 198-200 °C; IR (KBr, υ_{max} cm^{-1}): 3445 (NH), 2218 (CN), 1716 (CO), 1577 (C=C); ^{1}H NMR (200 MHz, DMSO-d_6): δ 3.28 (s, 3H, CH_3), 3.58-3.63 (m, 2H, CH_2), 4.32-4.37 (m, 2H, CH_2), 7.30-7.39 (m, 2H, Ar-H), 7.56-7.64 (m, 6H, Ar-H), 8.21-8.25 (m, 1H, indole H-4), 8.30 (s, 1H, CH=C), 12.94 (br s, 1H, NH); ^{13}C NMR (50.3 MHz, DMSO-d_6): δ 57.82, 64.31, 69.30, 93.77, 107.57, 112.28, 117.31, 121.38, 122.20, 123.53, 124.44, 128.64, 129.38, 129.74, 136.78, 148.45, 149.47, 163.43; Anal. Calcd for $C_{21}H_{18}N_2O_3$: C, 72.82; H, 5.24; N, 8.09; Found: C, 72.95; H, 5.54; N, 8.03.

*4.1.1.21. (2E)-2-Cyano-3-(2-phenyl-1H-indol-3-yl)acrylamide (**5h**)* [29].

*4.1.1.22. (2E)-3-(2-Phenyl-1H-indol-3-yl)-2-(piperidin-1-ylcarbonyl)acrylonitrile (**5i**)* [29].

*4.1.1.23. (E)-N-(4-Chlorophenyl)-2-cyano-3-(2-phenyl-1H-indol-3-yl)prop-2-enamide (**5j**)* [29].

*4.1.1.24. Diisopropyl (E)-1-cyano-2-(2-phenyl-1H-indol-3-yl)vinylphosphonate (**5k**)* [29].

*4.1.1.25. (2E)-2-(Methylsulfonyl)-3-(2-phenyl-1H-indol-3-yl)acrylonitrile (**5l**)* [29].

*4.1.1.26. (2E)-3-(2-Phenyl-1H-indol-3-yl)-2-(phenylsulfonyl)acrylonitrile (**5m**)* [29].

*4.1.1.27. (E)-3-(2-Phenyl-1H-indol-3-yl)-2-(p-tolylsulfonyl)prop-2-enenitrile (**5n**).* Orange solid; Yield: 72%; mp: 234-235 °C; IR (KBr, υ_{max} cm^{-1}): 3262 (NH), 2209 (CN), 1566 (C=C), 1327 (SO_2), 1150 (SO_2); ^{1}H NMR (200 MHz, DMSO-d_6): δ 2.44 (s, 3H, CH_3), 7.29-7.37 (m, 2H, Ar-H), 7.51-7.71 (m, 8H, Ar-H), 7.82-7.86 (m, 2H, Ar-H), 8.05 (s,

1H, CH=C), 8.11-8.16 (m, 1H, indole H-4), 13.09 (br s, 1H, NH); ^{13}C NMR (50.3 MHz, DMSO-d_6): δ 20.74, 104.10, 106.48, 112.58, 115.28, 121.65, 121.93, 123.91, 124.32, 127.03, 128.78, 128.95, 129.82, 130.04, 130.11, 136.17, 136.89, 144.67, 146.14, 149.95; Anal. Calcd for $C_{24}H_{18}N_2O_2S$: C, 72.34; H, 4.55; N, 7.03; S, 8.05; Found: C, 72.39; H, 4.68; N, 7.02; S, 7.84.

*4.1.1.28. 3-[(2-Phenyl-1H-indol-3-yl)methylene]pentane-2,4-dione (**5o**)* [29].

*4.1.1.29. (3E)-3-(Methylsulfonyl)-4-(2-phenyl-1H-indol-3-yl)but-3-en-2-one (**5p**)*. Orange solid; Yield: 48%; mp: 229-230 °C; IR (KBr, υ_{max} cm^{-1}): 3248 (NH), 1666 (CO), 1579 (C=C), 1346 (SO_2), 1131 (SO_2); ^{1}H NMR (300 MHz, DMSO-d_6): δ 2.17 (s, 3H, CH_3), 3.25 (s, 3H, CH_3), 7.12-7.32 (m, 4H, Ar-H), 7.51-7.63 (m, 5H, Ar-H), 8.01 (s, 1H, CH=C), 12.58 (br s, 1H, NH); ^{13}C NMR (75.5 MHz, DMSO-d_6): δ 30.85, 44.21, 105.70, 112.63, 118.96, 121.55, 123.31, 126.18, 129.01, 129.01, 129.49, 129.49, 129.59, 130.13, 135.19, 136.77, 139.24, 144.12, 198.87; $^3J_{C,H}$ = 9.9 Hz (CO); Anal. Calcd for $C_{19}H_{17}NO_3S$: C, 67.24; H, 5.05; N, 4.13; S, 9.45; Found: C, 67.34; H, 5.24; N, 3.77; S, 9.10.

*4.1.1.30. (3E)-4-(2-Phenyl-1H-indol-3-yl)-3-(phenylsulfonyl)but-3-en-2-one (**5q**)*. Yellow solid; Yield: 4%; mp: 172-173 °C; IR (KBr, υ_{max} cm^{-1}): 3257 (NH), 1672 (CO), 1568 (C=C), 1347 (SO_2), 1137 (SO_2); ^{1}H NMR (300 MHz, DMSO-d_6): δ 2.13 (s, 3H, CH_3), 7.07-7.18 (m, 2H, Ar-H), 7.24-7.29 (m, 1H, Ar-H), 7.53-7.74 (m, 9H, Ar-H), 7.89-7.92 (m, 2H, Ar-H), 8.23 (s, 1H, CH=C), 12.61 (br s, 1H, NH); ^{13}C NMR (75.5 MHz, DMSO-d_6): δ 30.86, 106.19, 112.66, 118.98, 121.64, 123.35, 125.99, 127.46, 127.46, 129.02, 129.02, 129.22, 129.22, 129.59, 129.59, 129.67, 130.10, 133.19, 134.71, 136.83, 139.97, 141.49, 144.74, 197.38; $^3J_{C,H}$ = 9.6 Hz (CO); Anal. Calcd for $C_{24}H_{19}NO_3S$: C, 71.80; H, 4.77; N, 3.49; S, 7.99; Found: C, 71.76; H, 4.48; N, 3.49; S, 7.63.

*4.1.1.31. (E)-3-(4-Chlorophenyl)sulfonyl-4-(2-phenyl-1H-indol-3-yl)but-3-en-2-one (**5r**)*. Yellow solid; Yield: 12%; mp: 173-174 °C; IR (KBr, υ_{max} cm^{-1}): 3261 (NH), 1666 (CO), 1576 (C=C), 1346 (SO_2), 1133 (SO_2); ^{1}H NMR (200 MHz, DMSO-d_6): δ 2.14 (s, 3H, CH_3), 7.09-7.32 (m, 3H, Ar-H), 7.53-7.72 (m, 8H, Ar-H), 7.71-7.94 (m, 2H, Ar-H), 8.25 (s, 1H, CH=C), 12.69 (br s, 1H, NH); ^{13}C NMR (50.3 MHz, DMSO-d_6): δ 30.53, 105.85, 112.39, 118.60, 121.44, 123.12, 125.65, 128.71, 129.04, 129.18, 129.33, 129.44, 129.68, 133.65, 136.50, 137.89, 140.10, 140.23, 144.74, 197.15; Anal. Calcd for $C_{24}H_{18}ClNO_3S$: C, 66.13; H, 4.16; N, 3.21; S, 7.36; Found: C, 66.06; H, 4.23; N, 3.18; S, 7.52.

*4.1.1.32. (2Z)-1-Phenyl-2-[(2-phenyl-1H-indol-3-yl)methylene]butane-1,3-dione (**5s**)* [29].

*4.1.1.33. 1,3-Diphenyl-2-[(2-phenyl-1H-indol-3-yl)methylene]propane-1,3-dione (**5t**)* [30]. Yellow solid; Yield: 14%; mp: 223-224 °C; IR (KBr, υ_{max} cm^{-1}): 3228 (NH), 1661 (CO), 1563 (C=C); ^{1}H NMR (200 MHz, DMSO-d_6): δ 6.88-6.96 (m, 1H, Ar-H), 7.10-7.24 (m, 2H, Ar-H), 7.38-7.50 (m, 12H, Ar-H), 7.76-7.78 (m, 3H, Ar-H), 7.92-7.96 (m, 2H, Ar-H and CH=C), 12.32 (br s, 1H, NH); ^{13}C NMR (50.3 MHz, DMSO-d_6): δ 107.75, 111.72, 120.29, 120.37, 122.50, 124.91, 128.11, 128.28, 128.42, 128.48, 128.81, 129.09, 130.12, 131.52, 132.94, 133.25, 136.33, 137.06, 137.79, 141.11, 143.82, 194.88, 196.63; Anal. Calcd for $C_{30}H_{21}NO_2$: C, 84.29; H, 4.95; N, 3.28; Found: C, 84.01; H, 5.02; N, 3.20.

*4.1.1.34. Ethyl (2E)-2-benzoyl-3-(2-phenyl-1H-indol-3-yl)acrylate (**5u**)* [29].

*4.1.1.35. (2E)-1-Phenyl-3-(2-phenyl-1H-indol-3-yl)-2-(phenylsulfonyl)prop-2-en-1-one (**5v**).* Yellow solid; Yield: 17%; mp: 212-214 °C; IR (KBr, υ_{max} cm^{-1}): 3325 (NH), 1655 (CO), 1575 (C=C), 1360 (SO_2), 1138 (SO_2); ^{1}H NMR (300 MHz, $CDCl_3$): δ 6.95-7.27 (m, 6H, Ar-H), 7.38-7.71 (m, 11H, Ar-H), 7.98-8.01 (m, 2H, Ar-H), 8.53 (s, 1H, CH=C), 8.59 (br s, 1H, NH); ^{13}C NMR (75.5 MHz, DMSO-d_6): δ 106.37, 112.11, 119.55, 120.95, 123.00, 125.55, 127.64, 127.64, 128.39, 128.39, 128.88, 128.88, 129.04, 129.04, 129.22, 129.22, 129.58, 129.58, 130.10, 131.51, 133.25, 133.76, 136.43, 136.43, 136.94, 139.45, 141.44, 144.47, 192.89; $^3J_{C,H}$ = 9.8 Hz (CO); Anal. Calcd for $C_{29}H_{21}NO_3S$: C, 75.14; H, 4.57; N, 3.02; S, 6.92; Found: C, 74.82; H, 4.98; N, 2.93; S, 6.60.

*4.1.1.36. Ethyl (E)-2-(4-chlorobenzoyl)-3-(2-phenyl-1H-indol-3-yl)prop-2-enoate (**5w**).* Yellow solid; Yield: 47%; mp: 154-156 °C; IR (KBr, υ_{max} cm^{-1}): 3299 (NH), 1659 (CO), 1569 (C=C); ^{1}H NMR (200 MHz, DMSO-d_6): δ 1.07 (s, 3H, CH_3), 4.01-4.21 (m, 2H, CH_2), 6.87-6.95 (m, 1H, Ar-H), 7.05-7.17 (m, 2H, Ar-H), 7.37-7.70 (m, 8H, Ar-H), 7.85-7.90 (m, 2H, Ar-H), 8.08 (s, 1H, CH=C), 12.32 (br s, 1H, NH); ^{13}C NMR (50.3 MHz, DMSO-d_6): δ 13.59, 60.20, 107.09, 111.76, 120.09, 120.29, 122.44, 123.81, 124.76, 128.49, 128.56, 128.92, 129.33, 130.20, 130.27, 135.82, 136.21, 136.55, 137.90, 138.64, 143.91, 165.25, 194.11; Anal. Calcd for $C_{26}H_{20}ClNO_3$: C, 72.64; H, 4.69; N, 3.26; Found: C, 72.43; H, 4.62; N, 3.27.

*4.1.1.37. Ethyl (2E)-2-(4-nitrobenzoyl)-3-(2-phenyl-1H-indol-3-yl)acrylate (**5x**).* Red solid; Yield: 22%; mp: 175-177 °C; IR (KBr, υ_{max} cm^{-1}): 3298 (NH), 1678 (COOEt), 1656 (COAr), 1570 (C=C), 1523 (NO_2), 1346 (NO_2), 1238 and 1221 (COOEt);^{1}H NMR (300 MHz, DMSO-d_6): δ 0.99 (t, J = 7.0 Hz, 3H, CH_3), 4.07 (q, J = 7.0 Hz, 2H, CH_2), 6.93-7.17 (m, 3H, Ar-H) 7.39 (d, J = 6.0 Hz. 1H, Ar-H), 7.53-7.59 (m, 5H, Ar-H), 7.97-8.03 (m, 3H, 2 Ar-H + CH=C), 8.24 (d, J = 8.6 Hz, 2H, Ar-H), 12.40 (br s, 1H, NH); Anal. Calcd for $C_{26}H_{20}N_2O_5$: C, 70.90; H, 4.58; N, 6.36; Found: C, 70.86; H, 4.91; N, 5.96.

*4.1.1.38. (2E)-4,4,4-Trifluoro-1-(2-furyl)-2-[(2-phenyl-1H-indol-3-yl)methylene]butane-1,3-dione (**5y**).* Yellow Solid; Yield: 10%; mp: 192-194°C; IR (KBr, υ_{max} cm^{-1}): 3370 (NH), 1671 ($COCF_3$), 1633 cm^{-1} (CO), 1556 (C=C); ^{1}H NMR (200 MHz, DMSO-d_6): δ 6.54-6.57 (m, 1H, furan H-4), 7.03-7.72 (m, 10H, Ar-H), 7.95 (s, 1H, furan H-5) 8.13 (s, 1H, CH=C), 12.87 (br s, 1H, NH); ^{13}C NMR (50.3 MHz, DMSO-d_6): δ 40.95, 58.07, 110.50, 112.46, 115.45, 118.70, 122.12, 122.90, 126.98, 128.57, 128.92, 129.58, 130.72, 130.74, 132.58, 139.48, 147.17, 149.70, 150.55, 180.65, 180.80; Anal. Calcd for $C_{23}H_{14}F_3NO_3$: C, 67.48; H, 3.45; N, 3.42; Found: C, 67.18; H, 3.78; N, 3.49.

*4.1.1.39. Methyl (2E)-2-(methylsulfonyl)-3-(2-phenyl-1H-indol-3-yl)acrylate (**5z**).* Yellow solid; Yield: 43%; mp: 201-202 °C; IR (KBr, υ_{max} cm^{-1}): 3247 (NH), 1693 (CO), 1578 (C=C), 1348 (SO_2), 1291 and 1248 (COOMe), 1138 (SO_2); ^{1}H NMR (300 MHz, DMSO-d_6): δ 3.29 (s, 3H, CH_3), 3.62 (s, 3H, CH_3) 7.18-7.23 (m, 3H, Ar-H), 7.48-7.58 (m, 6H, Ar-H), 7.95 (s, 1H, CH=C), 12.50 (br s, 1H, NH); ^{13}C NMR (75.5 MHz, DMSO-d_6): δ 43.58, 52.25, 106.09, 112.47, 119.61, 121.36, 123.15, 125.62, 126.58, 128.99, 128.99, 129.45,129.45, 129.57, 130.18, 136.73, 140.53, 145.04, 164.47; $^3J_{C,H}$ = 11.0 Hz (CO); Anal. Calcd for $C_{19}H_{17}NO_4S$: C, 64.21; H, 4.82; N, 3.94; S, 9.02; Found: C, 64.15; H, 4.89; N, 3.89; S, 8.80.

*4.1.1.40. Methyl (2E)-3-(2-phenyl-1H-indol-3-yl)-2-(phenylsulfonyl)acrylate (**5aa**)* [29].

*4.1.1.41. Ethyl (2Z)-2-acetyl-3-(2-phenyl-1H-indol-3-yl)acrylate (**5ab**)* [29].

*4.1.1.42. Diethyl [(2-phenyl-1H-indol-3-yl)methylene]malonate (**5ac**)* [31]. Yellow solid; Yield: 13%; mp: 148-150 °C; IR (KBr, υ_{max} cm^{-1}): 3262 (NH), 2980 (CH_2CH_3), 1722 (COOEt), 1599 (C=C), 1262 and 1242 (COOEt); ^{1}H NMR (300 MHz, DMSO-d_6): δ 1.09 (t, *J* = 7.0 Hz, 3H, CH_3), 1.23 (t, *J* = 7.0 Hz, 3H, CH_3), 4.09-4.24 (m, 4H, $2CH_2$), 7.12-7.27 (m, 3H, Ar-H), 7.39-7.64 (m, 6H, Ar-H), 7.84 (s, 1H, CH=C), 12.32 (br s, 1H, NH); ^{13}C NMR (75.5 MHz, DMSO-d_6): δ 13.63, 14.05, 60.67, 60.72, 107.29, 112.17, 119.64, 120.43, 122.87, 125.65, 128.90, 129.17, 129.36, 130.70, 136.54, 138.40, 143.33, 164.85, 166.60; Anal. Calcd for $C_{22}H_{21}NO_4$: C, 72.71; H, 5.82; N, 3.85; Found: C, 72.79; H, 6.18; N, 3.90.

*4.1.1.43. {[2-(4-Methoxyphenyl)-1H-indol-3-yl]methylene}malononitrile (**6a**)* [29].

*4.1.1.44. (2E)-3-[2-(4-Methoxyphenyl)-1H-indol-3-yl]-2-(phenylsulfonyl)acrylonitrile (**6b**)* [29].

*4.1.1.45. [(5-Methoxy-2-phenyl-1H-indol-3-yl)methylene]malononitrile (**7a**)* [29].

*4.1.1.46. (2E)-3-[(5-Methoxy-2-phenyl-1H-indol-3-yl)-2-(phenylsulfonyl)acrylonitrile (**7b**)* [29].

*4.1.1.47. {[5-Methoxy-2-(4-methoxyphenyl)-1H-indol-3-yl]methylene}malononitrile (**8a**)* [29].

*4.1.1.48. (2E)-3-[5-Methoxy-2-(4-methoxyphenyl)-1H-indol-3-yl]-2-(phenylsulfonyl)acrylonitrile (**8b**)* [29].

4.1.2. General procedure for the preparation of *N*-alkylindoles 9 and 10.

A solution of **2d** (0.771, 2.5 mmol) or **2e** (0.798 g, 2.5 mmol) in dry DMF (5 mL) was added dropwise to a stirred suspension of sodium hydride (60% dispersion in mineral oil, 0.110 g, 2.75 mmol) in dry DMF (5 mL) at 0°C. After stirring at 0°C for 10 min and at rt for 20 min, the reaction mixture was cooled again to 0°C and a solution of the suitable ω-bromoacetophenone (2.5 mL) in dry DMF (2 mL) was added dropwise. After stirring at rt for 18 h, a saturated aqueous NH_4Cl solution (15 mL) was added. For **9a** and **9b**, the mixture was extracted with CH_2Cl_2 (3×20 mL); the combined extracts were washed with water (5×20 mL) and dried over anhydrous Na_2SO_4; after evaporation of the solvent, the crude product was purified by crystallization from ethanol. For **10a**, the precipitate obtained was filtered off, dried and crystallized from ethyl acetate.

*4.1.2.1. (2E)-3-{1-[2-(3-Methoxyphenyl)-2-oxoethyl]-1H-indol-3-yl}-2-(phenylsulfonyl)acrylonitrile (**9a**).* Yellow solid; Yield: 34%; mp: 212-213 °C; IR (KBr, υ_{max} cm^{-1}): 2206 (CN), 1688 (CO), 1571 (C=C), 1324 (SO_2), 1152 (SO_2); ^{1}H NMR (200 MHz, $CDCl_3$): δ 3.85 (s, 3H, OCH_3), 6.21 (s, 2H, CH_2), 7.33-7.37 (m, 3H, Ar-H), 7.55-7.85 (m, 7H, Ar-H), 8.03-8.08 (m, 3H, Ar-H), 8.63 (s, 1H, CH=C); ^{13}C NMR (50.3 MHz, DMSO-d_6): δ 53.28, 55.10, 102.73, 108.33, 111.44, 112.47, 114.80, 118.68, 119.63, 120.28, 122.42, 123.63, 126.57, 127.09, 129.55, 129.72, 133.87, 135.35, 136.83, 137.11, 139.22, 144.07, 159.11, 192.41; Anal. Calcd for $C_{26}H_{20}N_2O_4S$: C, 68.41; H, 4.42; N, 6.14; S, 7.02; Found: C, 68.20; H, 4.65; N, 6.20; S, 6.89.

*4.1.2.2. Ethyl (2E)-2-Benzoyl-3-{1-[2-(3-methoxyphenyl)-2-oxoethyl]-1H-indol-3-yl}acrylate (**9b**).* Yellow solid; Yield: 22%; mp: 123-125 °C; IR (KBr, υ_{max} cm^{-1}): 1700 (COOEt), 1692 (COAr), 1669 (COPh), 1582 (C=C); ^{1}H NMR (300 MHz, $CDCl_3$): δ 1.10 (t, *J* = 7.1 Hz, 3H, CH_3), 3.83 (s, 3H, OCH_3), 4.16 (q, *J* = 7.1 Hz, 2H, CH_2), 5.92 (s, 2H, NCH_2), 7.19-7.66 (m, 11H, Ar-H), 7.81-7.92 (m, 3H, Ar-H), 8.21 (s, 1H, CH=C); ^{13}C NMR (75.5 MHz, DMSO-d_6): δ 13.97,

52.95, 55.40, 60.45, 108.63, 110.96, 112.73, 118.16, 119.82, 120.50, 121.16, 122.75, 123.99, 127.38, 128.66, 128.87, 129.95, 133.00, 133.36, 133.76, 135.80, 136.12, 159.41, 164.95, 193.33, 196.05; Anal. Calcd for $C_{29}H_{25}NO_5$: C, 75.50; H, 5.39; N, 3.00; Found: C, 75.41; H, 5.71; N, 3.11.

*4.1.2.3. (2E)-3-{1-[2-(1,1'-Biphenyl-4-yl)-2-oxoethyl]-1H-indol-3-yl}-2-(phenylsulfonyl)acrylonitrile (**10a**).* Yellow solid; Yield: 32%; mp: 222-223 °C; IR (KBr, υ_{max} cm^{-1}): 2212 (CN), 1701 (CO), 1574 (C=C), 1350 (SO_2), 1156 (SO_2); ^{1}H NMR (300 MHz, $CDCl_3$): δ 6.24 (s, 2H, CH_2), 7.31-7.82 and 7.92-8.18 (m, 19H, Ar-H), 8.62 (s, 1H, CH=C); ^{13}C NMR (75.5 MHz, DMSO-d_6): δ 53.55, 60.23, 103.01, 108.69, 111.84, 114.13, 115.16, 119.05, 122.79, 124.00, 126.93, 126.97, 127.03, 127.43, 128.57, 128.94, 129.12, 129.91, 133.19, 134.23, 137.52, 138.68, 139.60, 145.34, 192.45; Anal. Calcd for $C_{31}H_{22}N_2O_3S$: C, 74.08; H, 4.41; N, 5.57; S, 6.38; Found: C, 74.17; H, 4.62; N, 5.56; S, 6.01.

4.2. Biological studies

4.2.1 Cytotoxicity assays (MTT method).

Compounds were dissolved in DMSO at 100 mM and then diluted in culture medium. Cell lines were purchased from American Type Culture Collection (ATCC). Haematological tumour-derived cells were grown in RPMI-1640 medium supplemented with 10% fetal calf serum (FCS), 100 units/mL penicillin G and 100 µg/mL streptomycin. Solid tumour-derived cells were grown in their specific media supplemented with 10% FCS and antibiotics. Cell cultures were incubated at 37 °C in a humidified 5% CO_2 atmosphere. The absence of mycoplasma contamination was checked periodically by the Hoechst staining method. Exponentially growing cells derived from human haematological tumours [$CD4^+$ human T-cells containing an integrated HTLV-1 genome (MT-4)] were seeded at an initial density of $1x10^5$ cells/mL in 96 well plates in RPMI-1640 medium supplemented with 10% FCS, 100 units/mL penicillin G and 100 µg/mL streptomycin. Cell cultures were then incubated at 37 °C in a humidified 5% CO_2 atmosphere in the absence or presence of serial dilutions of test compounds. Cell viability was determined after 96 hrs at 37 °C by the by the 3-(4,5-dimethylthiazol-2-yl)-2,5-diphenyl-tetrazolium bromide (MTT) method [37]. The compound concentrations resulting in 50% cell growth inhibition in comparison with untreated controls and expressed as EC_{50} values were determined by linear regression analysis. The most cytotoxic derivatives were also evaluated against a panel of cell lines derived from human haematological [$CD4^+$ acute T-lymphoblastic leukaemia (CCRF-CEM); splenic B-lymphoblastoid cells (WIL-2NS) and acute B-lymphoblastic (CCRF-SB) and human solid tumours [skin melanoma (SKMEL-28); lung squamous carcinoma (SK-MES-1); prostate carcinoma (DU-145); hepatocellular carcinoma (Hep-G2) and breast adenocarcinoma (MCF-7)] and against normal tissues [lung fibroblasts (MRC-5) and foreskin fibroblasts (CRL-7065)]. Cell viability was determined after 96 hrs at 37 °C by the MTT method.

4.2.2. Evaluation of anticancer activity at NCI

The NCI high-flux anticancer drug screen [39-41] utilized a panel of 60 human tumor cell lines in culture derived from nine cancer types (lung, colon, CNS, ovarian, renal, prostate and breast cancer, leukemia and melanoma). The compound were tested at 10-fold dilutions of five concentrations ranging from 10^{-4} to 10^{-8} M. According to the NCI protocol, cell lines were exposed to test agents in 96-well plates for the last 48 of a 72 h incubation and a sulforhodamine B (SRB) protein assay was used to estimate cell viability or growth. For each compound, the drug concentration required to produce 50% (GI_{50}) and total (TGI) growth inhibition, and 50% cytocidal effect (LC_{50}) were

obtained for up to 60 cell lines. Values were calculated for each of these parameters if the level activity was reached; if the effect was not reached or was exceeded, the value is expressed as greater or lesser than the maximum or minimum concentration tested.

4.2.3. Evaluation of antiproliferative activity in HL-60, K562 and MCF-7 cells (Alamar blue method).

Antiproliferative of HL-60, K562 and MCF-7 was determined [cells from European Cell Culture Collection (Salisbury, UK). grown in RPMI 1640 (HL-60, K562) or DMEM (MCF-7) containing 10% foetal calf serum (FCS), 100 UI/mL penicillin G and 100 µg/mL streptomycin]. Briefly, 200 µL of $4x10^4$ (HL-60, K562) or $2x10^4$ (MCF-7) cells were added to each well of flat-bottomed microtiter trays and serial dilutions of test compounds. After a 3 day incubation at 3 7°C the number of viable cells was determined by the Alamar blue method. Alamar blue (20 µL) was added to each well and plates were incubated at 37°C in the dark for 3 h. Plates were then read on a fluorescent plate reader (SpectraMax Gemini, Molecular Devices) with excitement and emission wavelengths of 544 nm and 590 nm respectively. The compound concentrations resulting in 50% cell growth inhibition in comparison with untreated controls and expressed as IC_{50} values were determined by linear regression analysis.

4.2.4. Flow cytometry.

Following treatment with the desired compound/s, cells were harvested by centrifugation and resuspended in 100µL ice-cold phosphate buffered saline (PBS) and fixed in ice-cold 70% ethanol (1 mL) at 4°C. Samples were then centrifuged at 800xg for 10 mins and resuspended in 200 µL PBS containing 10µg/mL RNase A and 100 µg/mL propidium iodide. Samples were incubated for 30 min at 37 °C in the dark. Following sample preparation, cell cycle analysis was performed at 488 nm using a Becton Dickinson fluorescent activated cell sorting analysis (FACS) Calibur flow cytometer (Becton Dickinson, California, U.S). The Macintosh-based application CellQuest was then used to analyze the data of 10,000 gated cells once cell debris had been excluded. The data was stored as frequency histograms.

4.2.5. Immunofluorescence.

MCF-7 cells were grown and treated on chamber well slides. Cells were then fixed in 100% ice-cold methanol, washed in PBS-T (0.1% (v/v) Triton X-100 in PBS) and blocked for 30 min in 5% (w/v) BSA in PBS-T. Cells were then incubated with a mouse anti-tubulin antibody for 1 h, washed 3 times with PBS-T and incubated for a further 1 h in the secondary antibody Alexa 488. Cells were again washed 3 times in PBS-T, after which the DNA was stained with 0.2 µg/mL propidium iodide in blocking buffer for 2 min. Slides were mounted with phenylene diamine (2 µL/mL) in 50:50 PBS/glycerol. Projected images from a z-series of images were captured using the OLYMPUS 1X81 microscope coupled with Olympus Fluoview Ver 1.5 software. All images were collected on the same day using identical parameters.

4.2.6. Electrophoretic mobility assay.

The compound to be tested was dissolved in MetOH and incubated with a commercial double strand plasmid DNA vector (pQE-30, Qiagen) for 10 min at 37 °C. Gel loading buffer (0.04% bromophenol blue, 0.04% xylene cyanol, 10% sucrose) was added and the samples were run onto a 0.7% Agarose gel to separate the closed circular (CC) and supercolied (SC) forms. The gel was stained with EtBr to visualize the corresponding DNA bands.

Acknowledgments

This work was financially supported by the University of Genova (PRA 2013) and MIUR (Ministero dell'Istruzione, dell'Università e della Ricerca, PRIN # 20105YY2HL_004). The authors thank Mr. O. Gagliardo for the microanalyses, Mr. F. Tuberoni, Dr. M. Anzaldi and Dr. R. Raggio for the IR and NMR spectra. University of Genova is gratefully acknowledged for financially supporting C.C.

References and notes

[1] F.R. De Sá Alves, E.J. Barreiro, C.A. Fraga, From nature to drug discovery: the indole scaffold as a 'privileged structure', Mini Rev. Med. Chem. 9 (2009) 782-793.

[2] S. Lal, T. J. Snape, 2-Arylindoles: a privileged molecular scaffold with potent, broad-ranging pharmacological activity, Curr. Med. Chem. 19 (2012) 4828-4837.

[3] M.J. Thompson, V. Borsenberger, J.C. Louth, K.E. Judd, B. Chen, Design, synthesis, and structure−activity relationship of indole-3-glyoxylamide libraries possessing highly potent activity in a cell line model of prion disease, J. Med. Chem. 52 (2009) 7503-7511.

[4] B. López-Iglesias, C. Pérez, J.A. Morales-García, S. Alonso-Gil, A. Pérez-Castillo, A. Romero, M.G. López, M. Villarroya, S. Conde, M.I. Rodríguez-Franco, New melatonin-N,N-dibenzyl(N-methyl)amine hybrids: potent neurogenic agents with antioxidant, cholinergic, and neuroprotective properties as innovative drugs for Alzheimer's disease, J. Med. Chem. 57 (2014) 3773-3785.

[5] L.C. Klein Jr., C.S. Passos, A.P. Moraes, V.G. Wakui, E.L. Konrath, A. Nurisso, P.A. Carrupt, C.M. de Oliveira, L. Kato, A.T. Henriques, Indole alkaloids and semisynthetic indole derivatives as multifunctional scaffolds aiming the inhibition of enzymes related to neurodegenerative diseases--a focus on Psychotria L. Genus, Curr. Top Med. Chem. 14 (2014) 1056-1075.

[6] R. Chakrabarty, J. Rao, A. Anand, A.D. Roy, R. Roy, G. Shankar, P.R. Dua, A.K. Saxena, Rational design, synthesis and evaluation of (6a*R**,11b*S**)-1-(4-fluorophenyl)-4-{7-[4-(4-fluorophenyl)-4-oxobutyl]1,2,3,4,6,6a,7,11b,12,12a(RS)-decahydropyrazino[2′,1′:6,1]pyrido[3,4-*b*]indol-2-yl}-butan-1-one as a potential neuroleptic agent, Bioorg. Med. Chem. 15 (2007) 7361-7367.

[7] M. Amir, K. Somakala, S. Ali, p38 MAP kinase inhibitors as anti inflammatory agents, Mini Rev. Med. Chem. 13 (2013) 2082-2096.

[8] A.S. Guerra, D.J. Malta, L.P. Laranjeira, M.B. Maia, N.C. Colaço, M. do C. de Lima, S.L. Galdino, I. da R. Pitta, T. Gonçalves-Silva, Anti-inflammatory and antinociceptive activities of indole-imidazolidine derivatives, Int. Immunopharmacol. 11 (2011) 1816-1822.

[9] M.-Z. Zhang, Q. Chen, G.-F. Yang, A review on recent developments of indole-containing antiviral agents, Eur. J. Med. Chem. 89 (2015) 421-441.

[10] C. Karaaslan, H. Kadri, T. Coban, S. Suzen, A.D. Westwell, Synthesis and antioxidant properties of substituted 2-phenyl-1*H*-indoles, Bioorg. Med. Chem. Lett. 23 (2013) 2671-2674.

[11] C. Passemar, M. Saléry, P.N. Soh, M.-D. Linas, A. Ahond, C. Poupat, F. Benoit-Vical, Indole and aminoimidazole moieties appear as key structural units in antiplasmodial molecules, Phytomedicine 18 (2011) 1118-1125.

[12] Shaveta, P. Singh, Structural optimization of indole based compounds for highly promising anti-cancer activities: Structure activity relationship studies and identification of lead molecules, Eur. J. Med. Chem. 74 (2014) 440-450.

[13] S.-H. Zhuang, Y.-C. Lin, L.-C. Chou, M.-H. Hsu, H.-Y. Lin, C.-H. Huang, J.-C. Lien, S.-C. Kuo, L.-J. Huang, Synthesis and anticancer activity of 2,4-disubstituted furo[3,2-b]indole derivatives, Eur. J. Med. Chem. 66 (2013) 466-479.

[14] A.E. Shchekotikhin, V.A. Glazunova, L.G. Dezhenkova, Y.N. Luzikov, V.N. Buyanov, H.M. Treshalina, N.A. Lesnaya, V.I. Romanenko, D.N. Kaluzhny, J. Balzarini, K. Agama, Y. Pommier, A.A. Shtil, M.N.

Preobrazhenskaya, Synthesis and evaluation of new antitumor 3-aminomethyl-4,11-dihydroxynaphtho[2,3-f]indole-5,10-diones, Eur. J. Med. Chem. 86 (2014) 797-805.

[15] J.-P. Liou, N. Mahindroo, C.-W. Chang, F.-M. Guo, S.W.-H. Lee, U.-K. Tan, T.-K. Yeh, C.-C. Kuo, Y.-W. Chang, P.-H. Lu, Y.-S. Tung, K.-T. Lin, J.-Y. Chang, H.-P. Hsieh, Structure-activity relationship studies of 3-aroylindoles as potent antimitotic agents, ChemMedChem. 1 (2006) 1106-1118.

[16] G. La Regina, M.C. Edler, A. Brancale, S. Kandil, A. Coluccia, F. Piscitelli, E. Hamel, G. De Martino, R. Matesanz, J.F. Díaz, A.I. Scovassi, E. Prosperi, A. Lavecchia, E. Novellino, M. Artico, R. Silvestri, Arylthioindole inhibitors of tubulin polymerization. 3. Biological evaluation, structure-activity relationships and molecular modeling studies, J. Med. Chem. 50 (2007) 2865-2874.

[17] S.N. Baytas, N. Inceler, A. Yilmaz, A. Olgac, S. Menevse, E. Banoglu, E. Hamel, R. Bortolozzi, G. Viola, Synthesis, biological evaluation and molecular docking studies of trans-indole-3-acrylamide derivatives, a new class of tubulin polymerization inhibitors, Bioorg. Med. Chem. 22 (2014) 3096-3104.

[18] M.-J. Lai, H.-L. Huang, S.-L. Pan, Y.-M. Liu, C.-Y. Peng, H.-Y. Lee, T.-K. Yeh, P.-H. Huang, C.-M. Teng, C.-S. Chen, H.-Y. Chuang, J.-P. Liou, Synthesis and biological evaluation of 1-Arylsulfonyl-5-(*N*-hydroxyacrylamide)indoles as potent histone deacetylase inhibitors with antitumor activity in vivo, J. Med. Chem. 55 (2012) 3777-3791.

[19] A. Brancale, R. Silvestri, Indole, a core nucleus for potent inhibitors of tubulin polymerization, Med. Res. Rev. 27 (2006) 209-238.

[20] S.A. Patil, R. Patil, D.D. Miller, Indole molecules as inhibitors of tubulin polymerization: potential new anticancer agents, Future Med. Chem. 16 (2012) 2085-2115.

[21] W.A. Maltese, J.H. Overmeyer, Methuosis: nonapoptotic cell death associated with vacuolization of macropinosome and endosome compartments, Am. J. Pathol. 184 (2014) 1630-1642.

[22] Y. Lv, Y. Guo, J. Xu, S. Shao, Simple indole-based colorimetric sensors with electron-withdrawing chromophores: Tuning selectivity in anion sensing, J. Fluorine Chem. 132 (2011) 973-977 and references therein.

[23] A. Gazit, H. App, G. McMahon, J. Chen, A. Levitzki, F.D. Bohmer, Tyrphostins. 5. Potent inhibitors of Platelet-Derived Growth Factor Receptor tyrosine kinase: structure−activity relationships in quinoxalines, quinolines, and indole tyrphostins, J. Med. Chem. 39 (1996), 2170-2177.

[24] (a) M. Matsuoka, M. Takao, T. Kitao, T. Fujiwara, K. Nakatsu, Cyanovinylheteroaromatics for organic nonlinear optics, Mol. Cryst. Liq. Cryst. Inc. Nonlinear Opt. 182 (1990) 71-79; (b) L. Zhengdong, W. Kechen, S. Genbo, H. Youping, Nonlinear optical properties of some derivatives of stilbene and vinyl cyanide, Opt. Mater. 20 (2002) 295-299.

[25] T.A., Hill, C.P. Gordon, A.B. McGeachie, B. Venn-Brown, L.R. Odell, N. Chau, A. Quan, A. Mariana, J.A. Sakoff, M. Chircop, P.J. Robinson, A. McCluskey, Inhibition of Dynamin Mediated Endocytosis by the *Dynoles*—Synthesis and Functional Activity of a Family of Indoles, J. Med. Chem. 52 (2009) 3762–3773.

[26] M. Pojarová, D. Kaufmann, R. Gastpar, T. Nishino, P. Reszka, P.J. Bednarski, E. von Angerer, [(2-Phenylindol-3-yl)methylene]propanedinitriles inhibit the growth of breast cancer cells by cell cycle arrest in G_2/M phase and apoptosis, Bioorg. Med. Chem. 15 (2007) 7368-7379.

[27] (a) B. Hansen, T. Hansen, S. Tullin, M. Colding-Jorgensen, Chemical uncouplers for the treatment of obesity, US Pat. Appl. (2004) US20040138301 A1. (b) L.B. Christiansen, T.K. Hansen, P.H. Olesen, T.M. Tagmose, Indole derivatives for use as chemical uncoupler, Int. Pat. Appl. (2005) WO2005051908 A1.

[28] A. Ranise, S. Cesarini, A. Spallarossa, F. Sancassan, F. Bondavalli, O. Bruno, S. Schenone, G. Menozzi, P. Fossa, L. Mosti, Unprecedented one-pot stereoselective synthesis of Knoevenagel-type derivatives via in situ condensation of *N*-Methyleniminium Salts of Ethylenethiourea and Ethyleneurea with active methylene reagents, Synthesis 16 (2007) 2495-2502.

[29] A. Ranise, F. Lucchesini, M. Caviglia, S. Alfei, A. Spallarossa, C. Caneva, Unconventional stereoselective one-pot synthesis of Knoevenagel-type indoles via in situ condensation of iminium salts with active methylene reagents, Tetrahedron 69 (2013) 10858-10868.

[30] J. Liu, X. Wang, H. Guo, X. Shi, X. Ren, G. Huang, A novel NH_4OAc and $CuBr(PPh_3)_3$-induced intermolecular Pummerer-type reaction between free (NH)-indoles and dimethylsulfoxide: facile synthesis of 3-methylthiomethyl substituted indoles, Tetrahedron 68 (2012) 1560-1565.

[31] C.H. Oh, H.S. Park, N. Park, S.Y. Kim, L. Piao, Scandium-Catalyzed Intramolecular Friedel-Crafts reactions of 2-[(2-Alkyl-1*H*-indol-3-yl)methylene]malonates, Synlett 25 (2014) 579-585.

[32] Z. Shiokawa, K. Hashimoto, B. Saito, Y. Oguro, H. Sumi, M. Yabuki, M. Yoshimatsu, Y. Kosugi, Y. Debori, N. Morishita, D.R. Dougan, G.P. Snell, S. Yoshida, T. Ishikawa, Design, synthesis, and biological activities of novel hexahydropyrazino[1,2-*a*]indole derivatives as potent inhibitors of apoptosis (IAP) proteins antagonists with improved membrane permeability across MDR1 expressing cells, Bioorg. Med. Chem. 21 (2013) 7938-7954.

[33] E. Pasquier, M. Kavallaris, Microtubules: a dynamic target in cancer therapy, IUBMB Life 60 (2008) 165-170.

[34] Greene, L. M.; Campiani, G.; Lawler, M.; Williams, D. C.; Zisterer, D. M.; BubR1 is required for a sustained mitotic spindle checkpoint arrest in human cancer cells treated with tubulin-targeting pyrrolo-1,5-benzoxazepines. Mol. Pharmacol. 73 (2008) 419-430

[35] J.M. Mulligan, L.M. Greene, S. Cloonan, M.M. Mc Gee, V. Onnis, G. Campiani, C. Fattorusso, M. Lawler, D.C. Williams, D.M. Zisterer, Identification of tubulin as the molecular target of proapoptotic pyrrolo-1,5-benzoxazepines, Mol. Pharmacol. 70 (2006) 60-70

[36] McElligott, A. M.; Maginn, E. N.; Greene, L. M.; McGuckin, S.; Hayat, A.; Browne, P. V.; Butini, S.; Campiani, G.; Catherwood, M. A.; Vandenberghe, E.; Williams, D. C.; Zisterer, D. M.; Lawler, M.; The novel tubulin-targeting agent pyrrolo-1,5-benzoxazepine-15 induces apoptosis in poor prognostic subgroups of chronic lymphocytic leukemia. Cancer Res. 69 (2009) 8366-8375.

[37] S, Mahboobi, E. Eichhorn, M. Winkler, A. Sellmer, U. Möllmann, Antibacterial activity of a novel series of 3-bromo-4-(1*H*-3-indolyl)-2,5-dihydro-1*H*-2,5-pyrroledione derivatives - An extended structure–activity relationship study, Eur. J. Med. Chem. 43 (2008) 633-656.

[38] R. Pauwels, J. Balzarini, M. Baba, R. Snoeck, D. Schols, P. Herdewijn, J. Desmyter, E. De Clercq, Rapid and automated tetrazolium-based colorimetric assay for the detection of anti-HIV compounds, J. Virol. Methods 20 (1988) 309-321.

[39] A. Monks, D. Scudiero, P. Skehan, R. Shoemaker, K. Paull, D. Vistica, C. Hose, J. Langley, P. Cronise, A. Vaigro-Wolff, M. Gray-Goodrich, H. Campbell, J. Mayo, M. Boyd, Feasibility of a High-Flux anticancer drug screen using a diverse panel of cultured human tumor cell lines, J. Natl. Cancer Inst. 83 (1991) 757-766.

[40] M.R. Grever, S.A. Shepartz, B.A. Chabner, The National Cancer Institute: cancer drug discovery and development program, Semin. Oncol. 19 (1992) 622-638.

[41] J.N. Weinstein, T.G. Myers, P.M. O'Connor, S.H. Friend, A. J. Fornace Jr., K.W. Kohn, T. Fojo, S.E. Bates, L.V. Rubinstein, N.L. Anderson, J.K. Buolamwini, W.W. van Osdol, A.P. Monks, D.A. Scudiero, E.A.

Sausville, D.W. Zaharevitz, B. Bunow, V.N. Viswanadhan, G.S. Johnson, R.E. Wittes, K.D. Paull, An Information-Intensive Approach to the Molecular Pharmacology of Cancer, Science 275 (1997) 343-349.

Highlights

- Synthesis of Knoevenagel-type indoles via one-pot procedure
- Selected compounds showed antiproliferative activities in cell-based assays
- Some derivatives caused apoptosis and partially depolymerised tubulin

Supplementary data

Unconventional Knoevenagel-type Indoles: Synthesis and Cell-based Studies for the Identification of Pro-apoptotic Agents

Andrea Spallarossa,[*,a] Chiara Caneva,[a] Matteo Caviglia,[a] Silvana Alfei,[a] Stefania Butini,[b] Giuseppe Campiani,[b] Sandra Gemma,[b] Margherita Brindisi,[b] Daniela M. Zisterer,[c] Sandra A. Bright,[c] Clive D. Williams,[c] Emmanuele Crespan,[d] Giovanni Maga,[d] Giuseppina Sanna,[e] Ilenia Delogu,[e] Gabriella Collu,[e] Roberta Loddo.[e]

[a]*Dipartimento di Farmacia, Università di Genova, Viale Benedetto XV 3, I-16132 Genova, Italy*

[b]*European Research Centre for Drug Discovery & Development, Dipartimento di Biotecnologie, Chimica e Farmacia, Università di Siena, via Aldo Moro 2, I-53100 Siena, Italy*

[c]*School of Biochemistry and Immunology, Trinity Biomedical Sciences Institute, Trinity College Dublin, 152-160 Pearse Street, Dublin 2, Ireland*

[d]*Institute of Molecular Genetics IGM-CNR, via Abbiategrasso 207, 27100 Pavia (Italy).*

[e]*Dipartimento di Scienze Biomediche, Sezione di Microbiologia e Virologia, Università di Cagliari, Cittadella Universitaria, s.p. 8, Km 0.700, I-09042 Monserrato (Cagliari), Italy*

[*]*Corresponding author:*
Dr. Andrea Spallarossa
Dipartimento di Farmacia
Sezione di Chimica del Farmaco e del Prodotto Cosmetico
Università degli Studi di Genova
Viale Benedetto XV, 3
16132 - Genova, Italy
phone: +39 010 353 8364;
fax: +39 010 353 8358;
e-mail: andrea.spallarossa@unige.it

Table of Contents

^{1}H NMR (300 MHz, DMSO) of compound 2f.

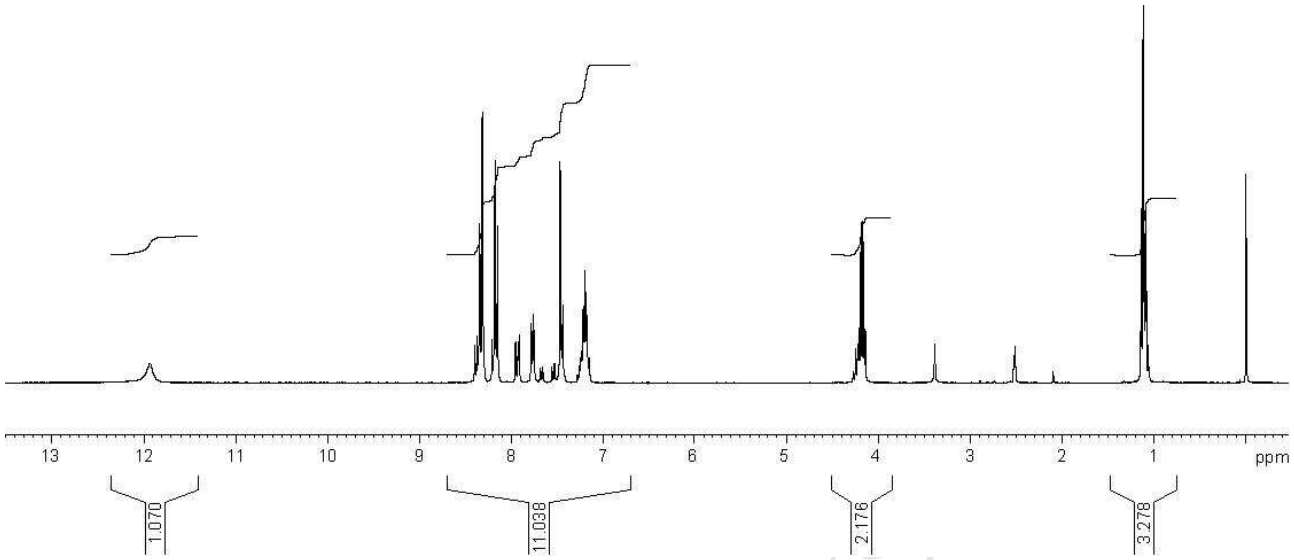

^{1}H NMR (300 MHz, DMSO) of compound 5c.

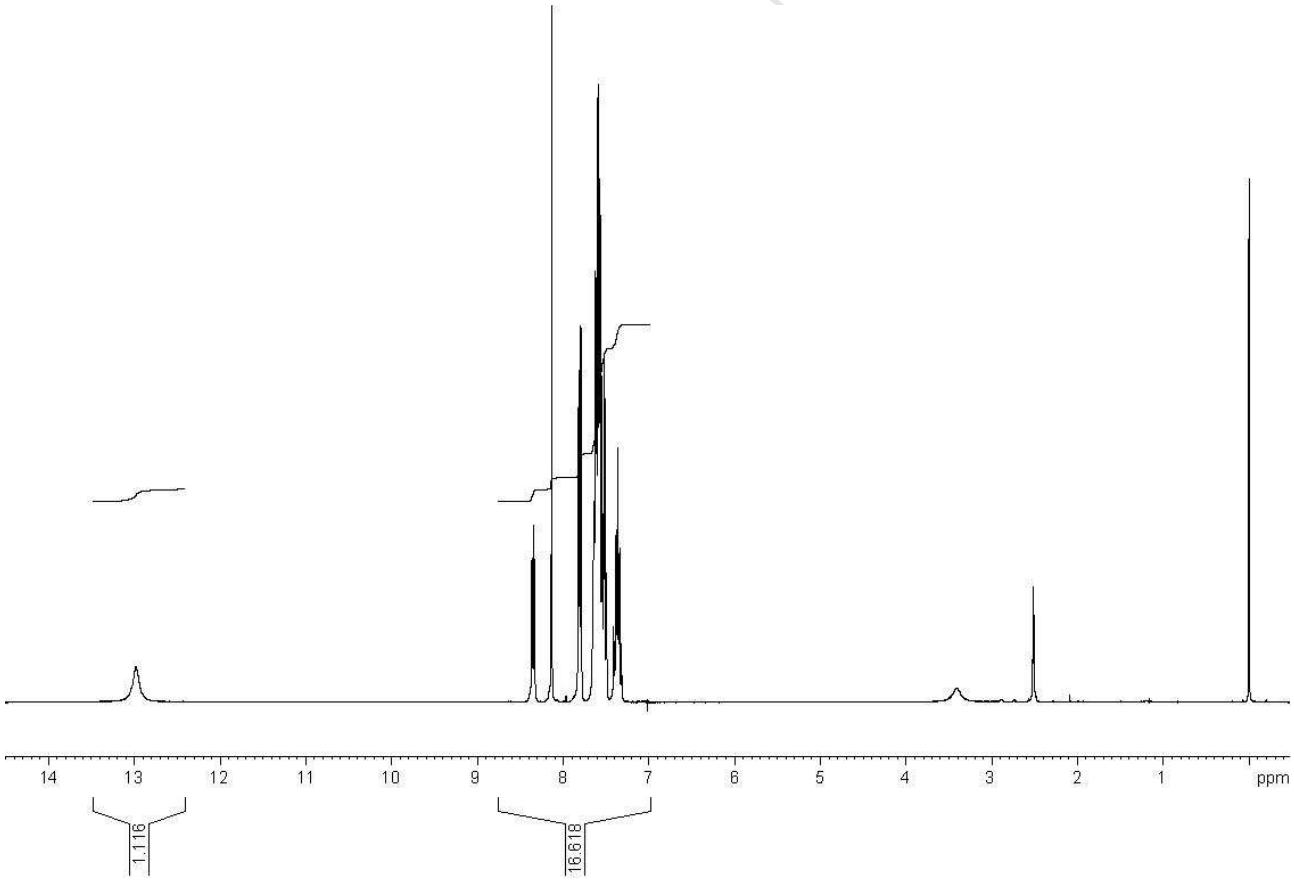

^{1}H NMR (200 MHz, DMSO) of compound 5d.

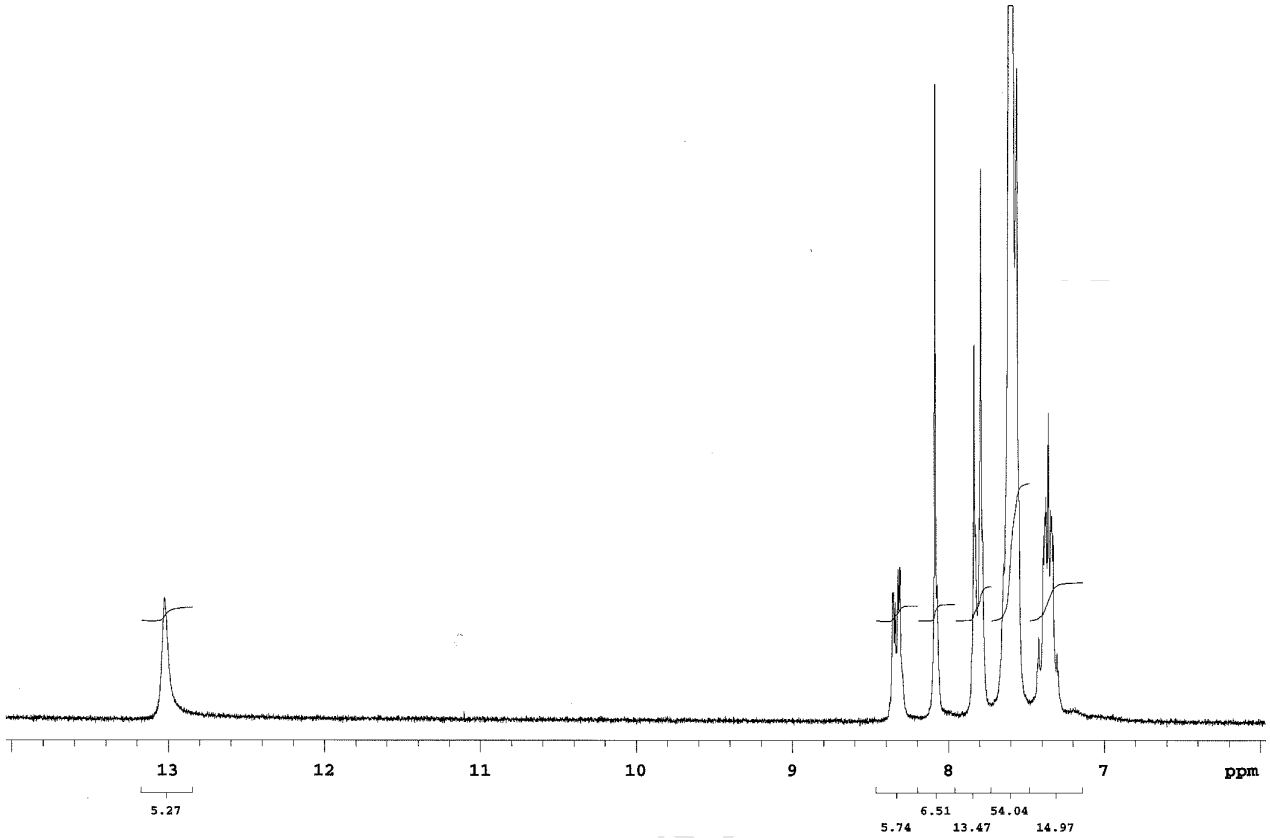

^{1}H NMR (200 MHz, DMSO) of compound 5e.

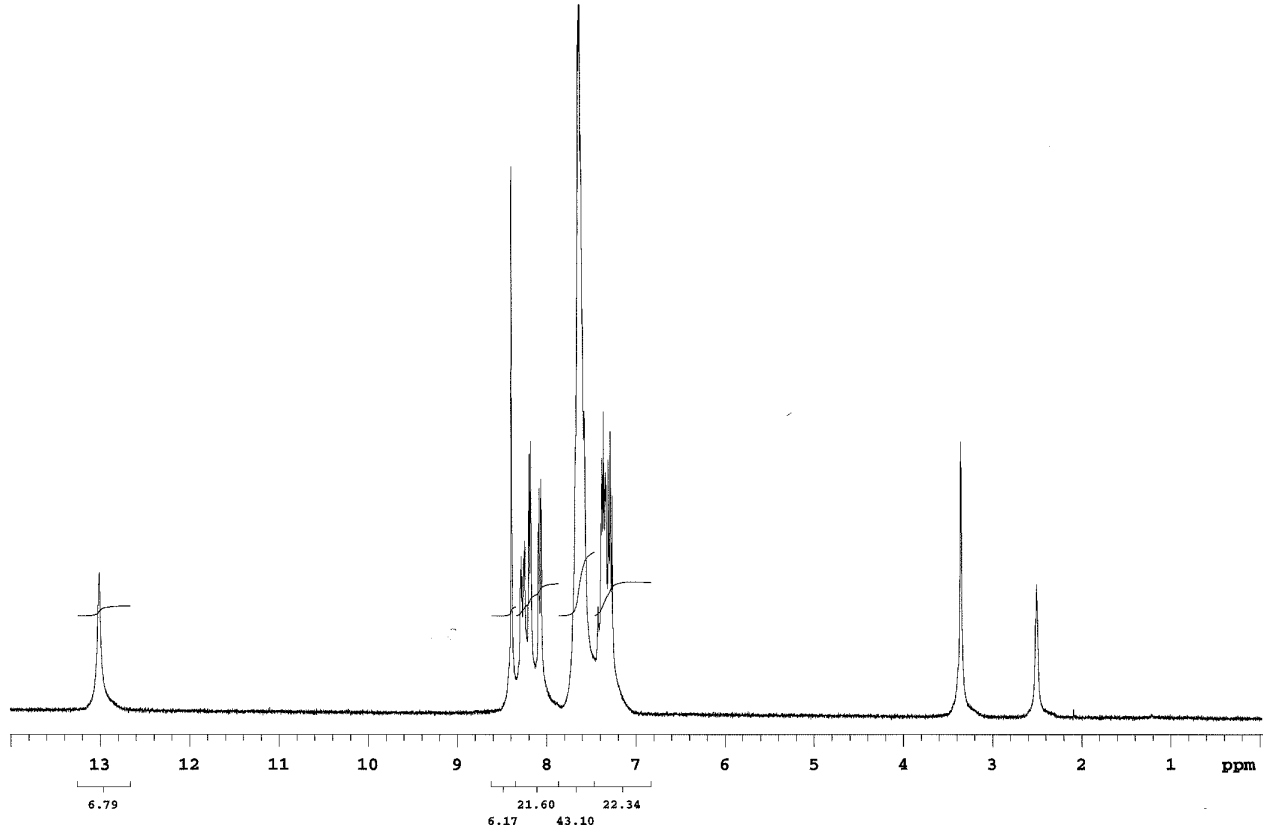

^{1}H NMR (200 MHz, DMSO) of compound 5g.

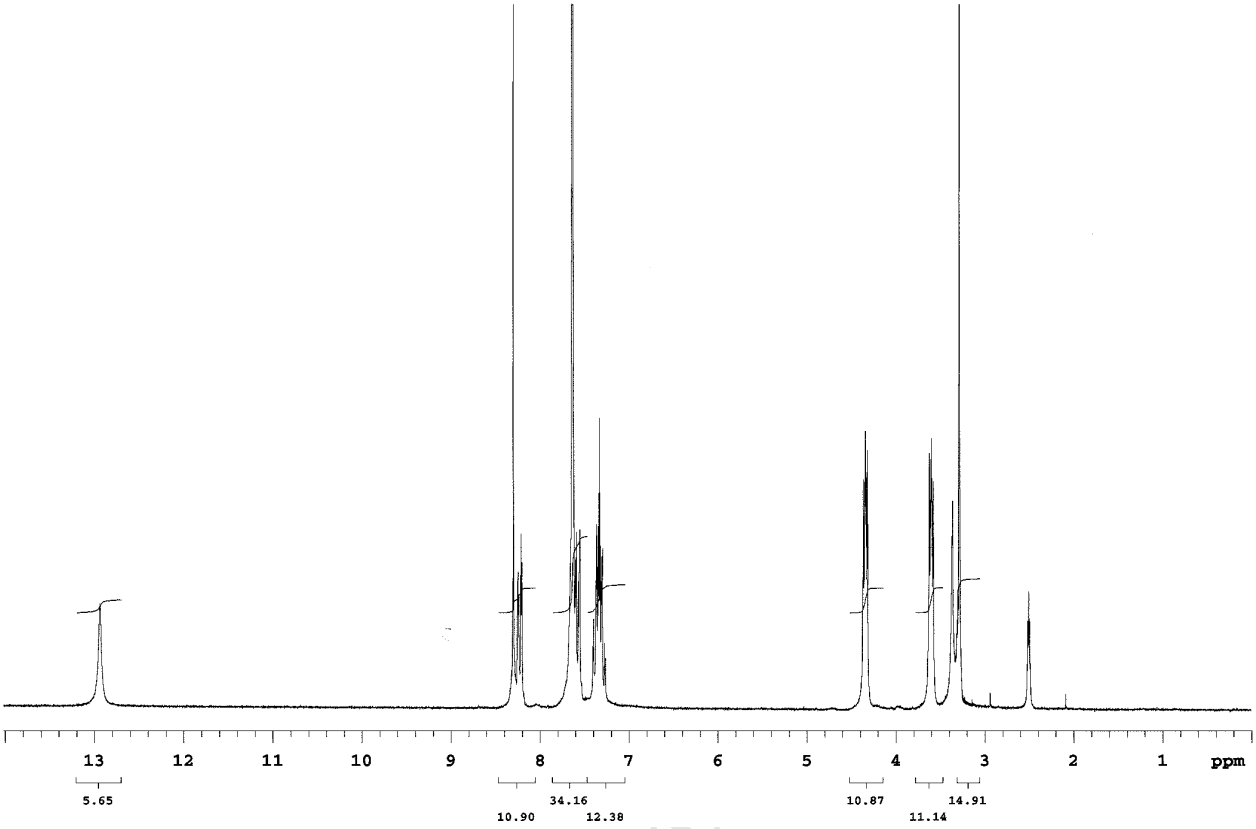

^{1}H NMR (200 MHz, DMSO) of compound 5n.

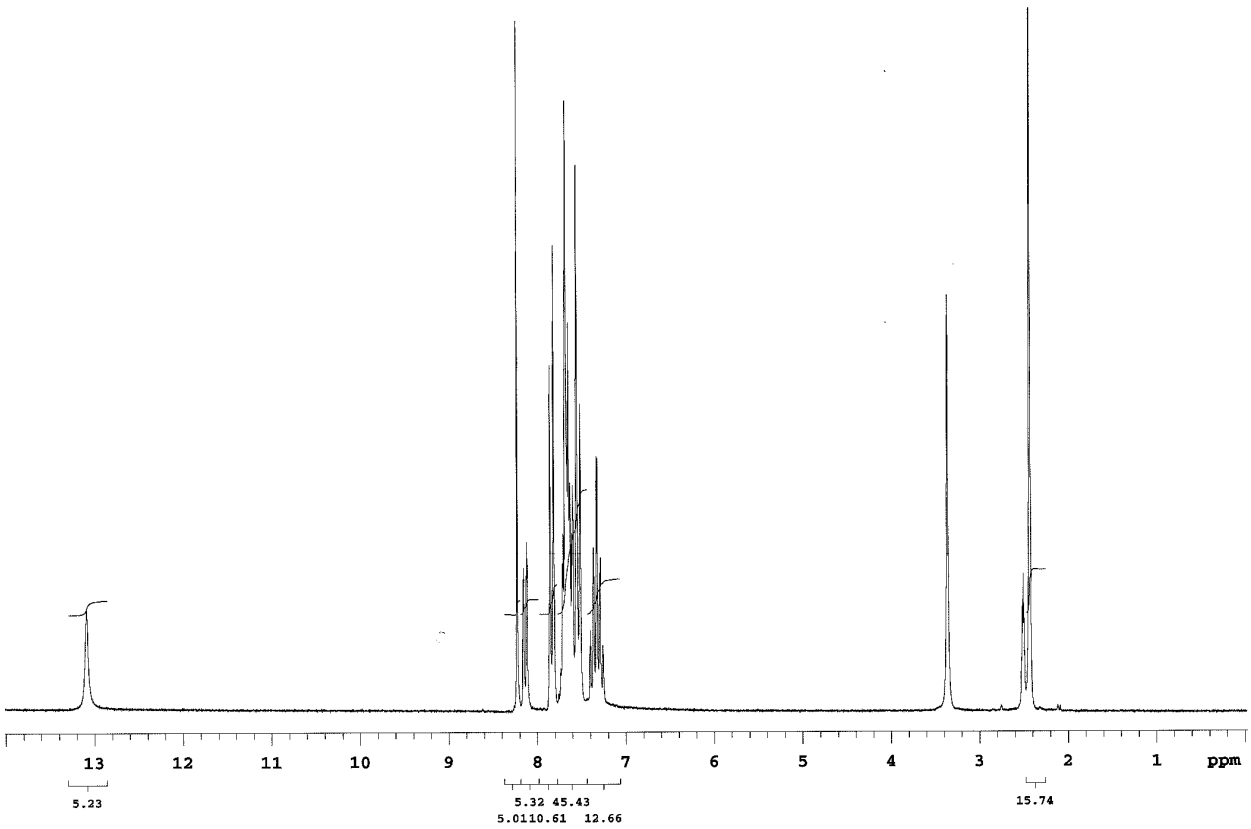

^{1}H NMR (300 MHz, DMSO) of compound 5p.

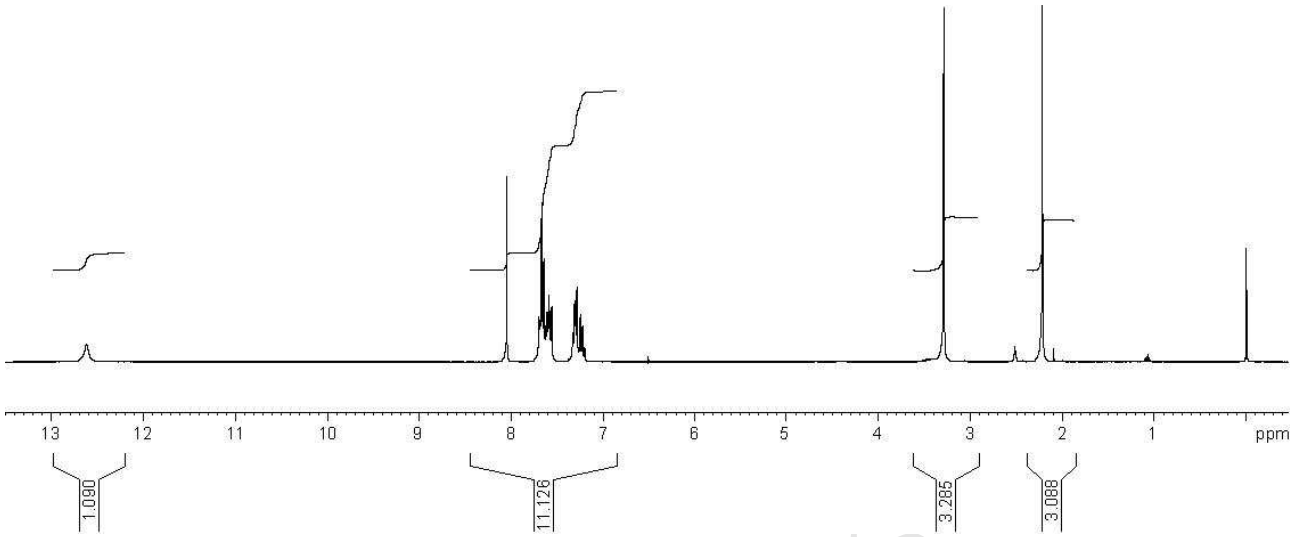

^{1}H NMR (300 MHz, DMSO) of compound 5q.

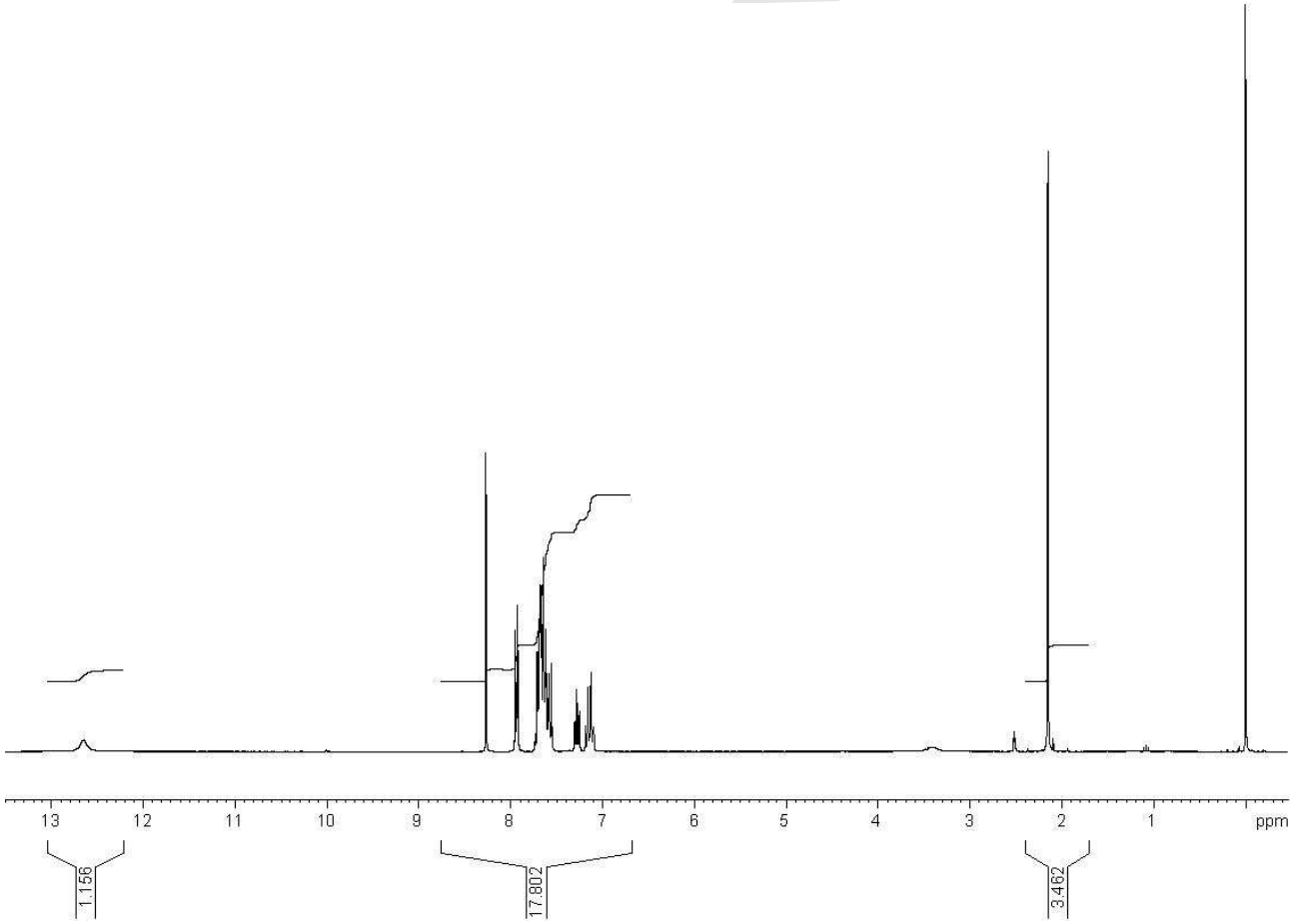

^{1}H NMR (200 MHz, DMSO) of compound 5r.

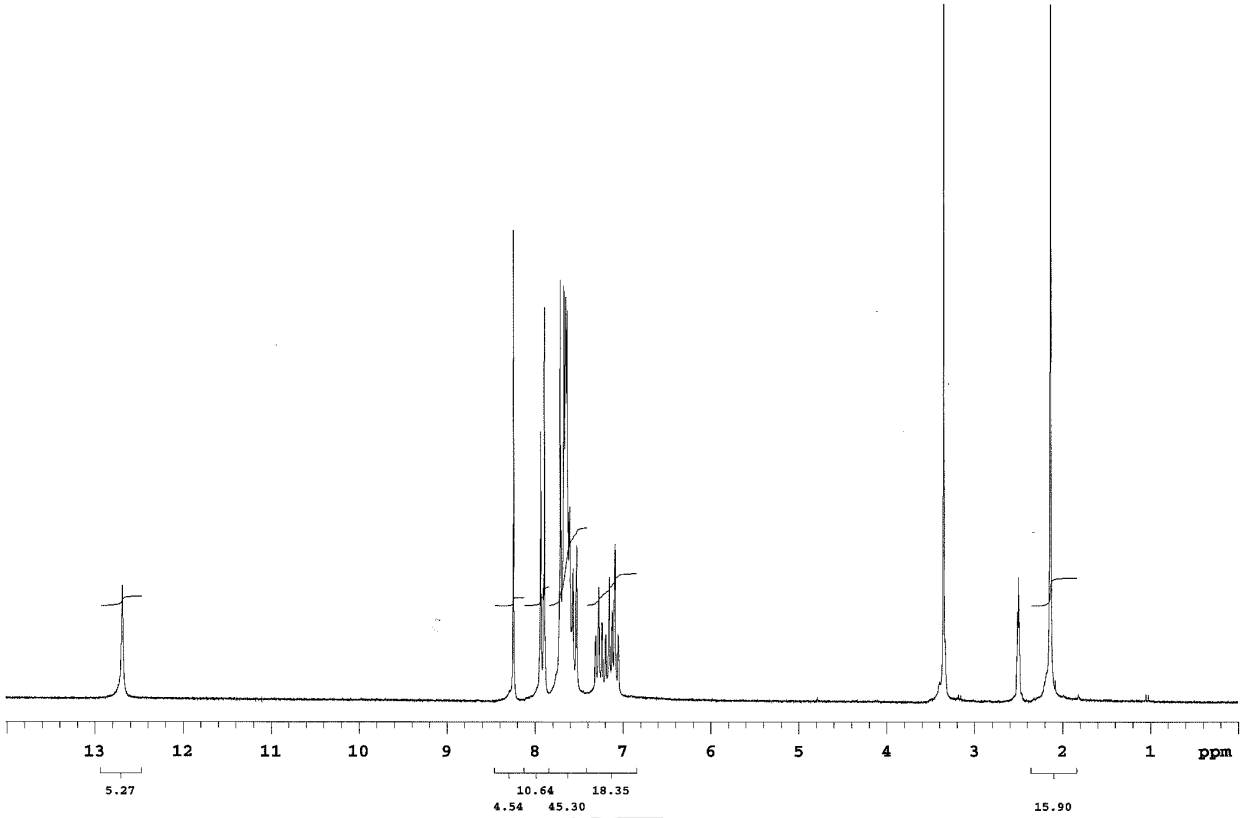

^{1}H NMR (200 MHz, DMSO) of compound 5t.

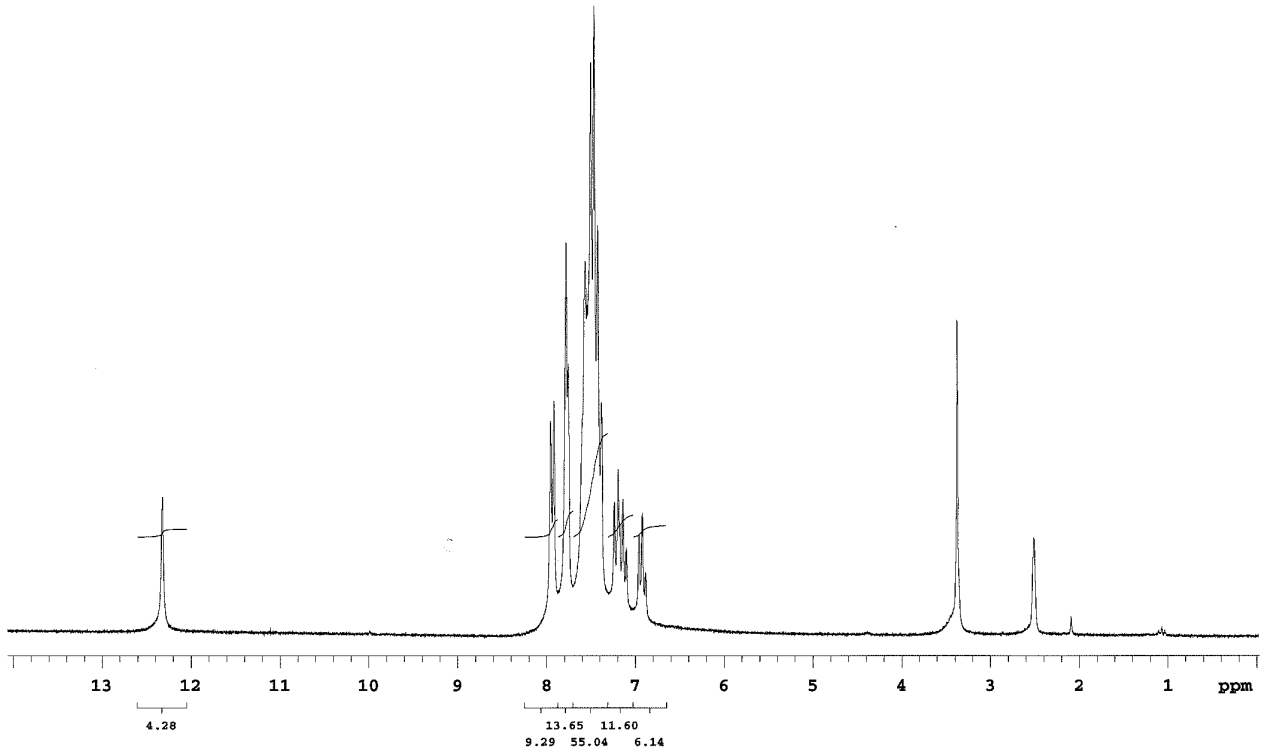

^{1}H NMR (300 MHz, DMSO) of compound 5v.

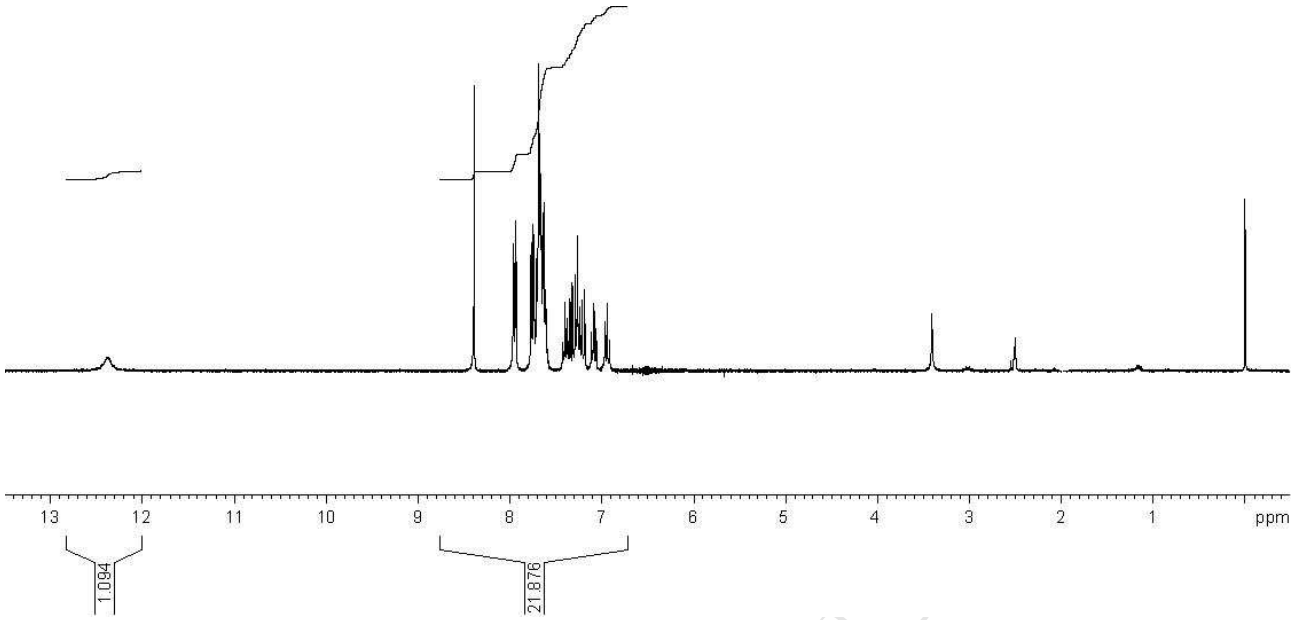

^{1}H NMR (200 MHz, DMSO) of compound 5w.

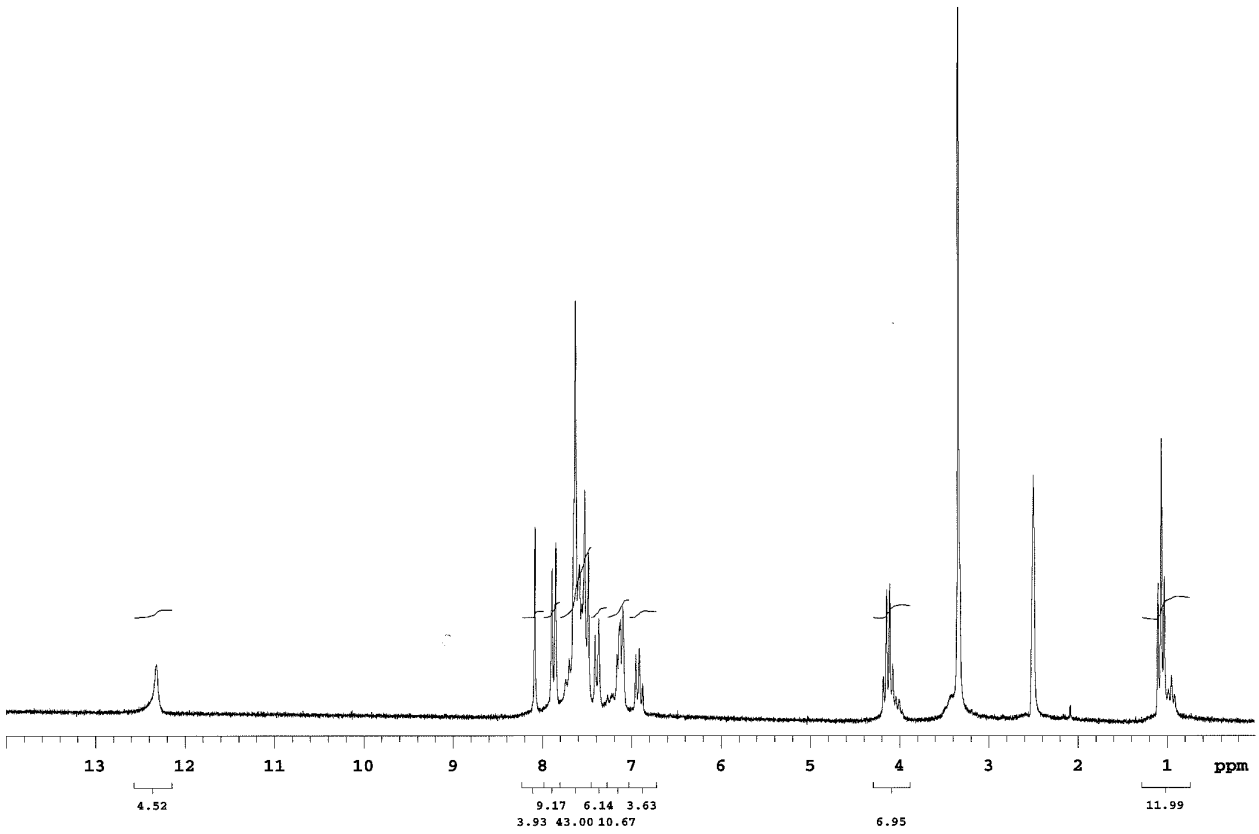

^{1}H NMR (300 MHz, DMSO) of compound 5x.

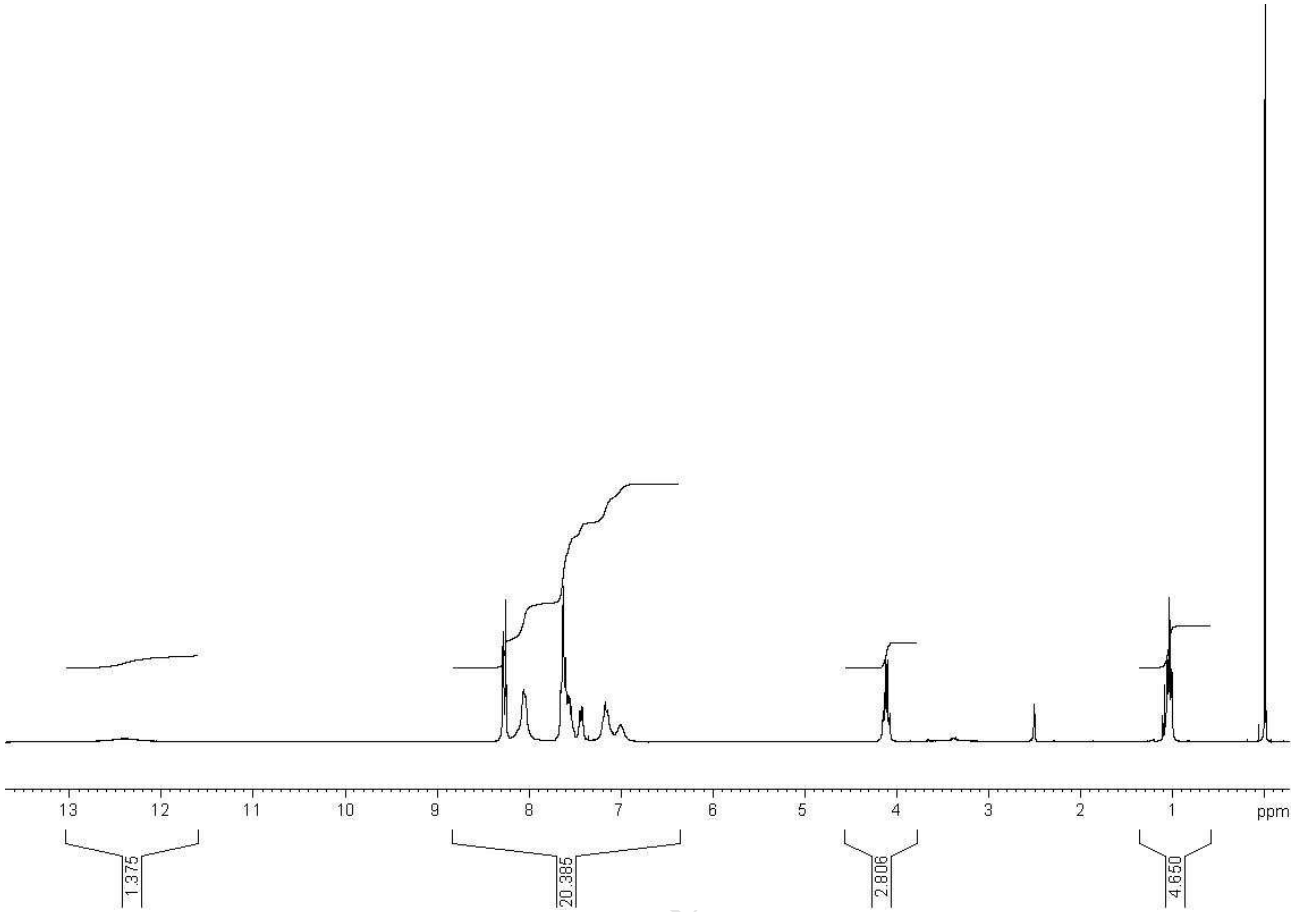

^{1}H NMR (200 MHz, DMSO) of compound 5y.

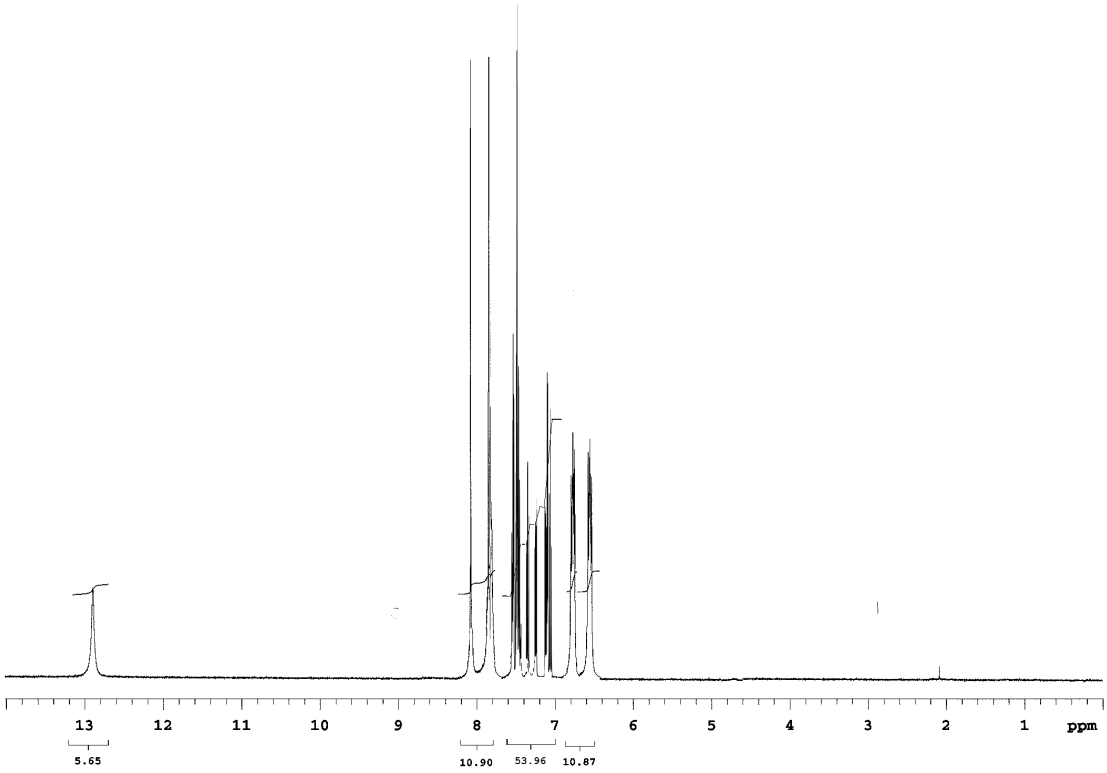

^{1}H NMR (300 MHz, DMSO) of compound 5z.

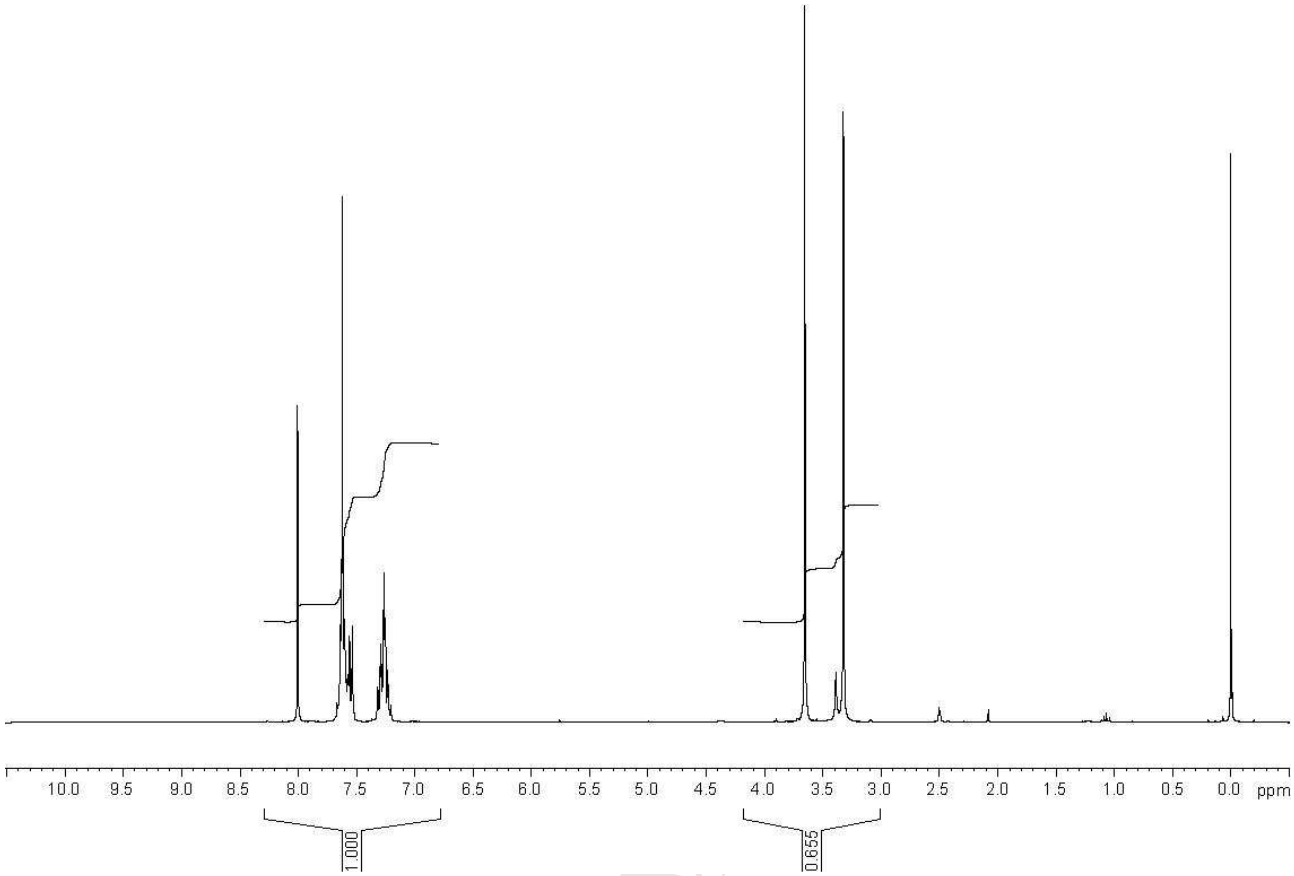

^{1}H NMR (300 MHz, DMSO) of compound 5ac.

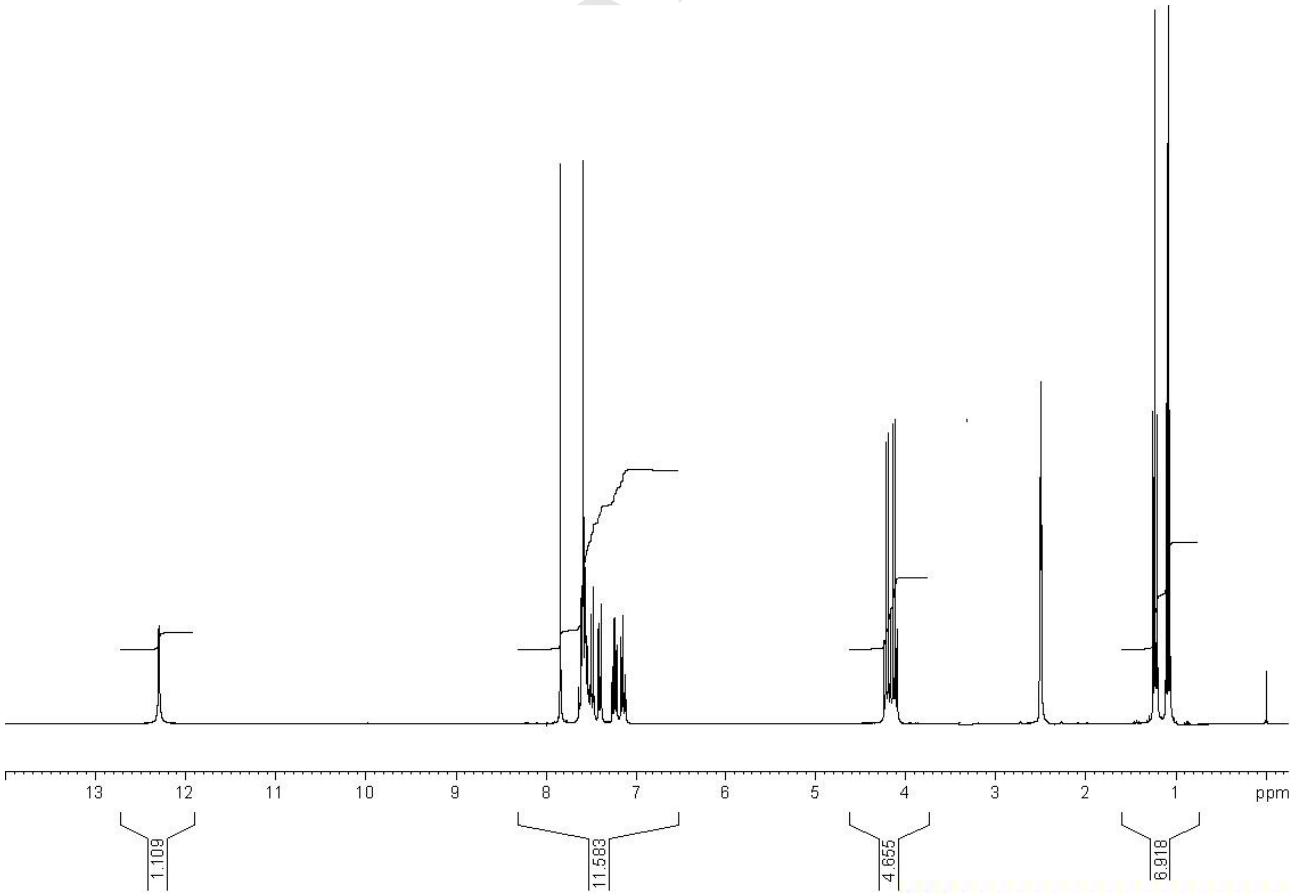

^{1}H NMR (200 MHz, DMSO) of compound 9a.

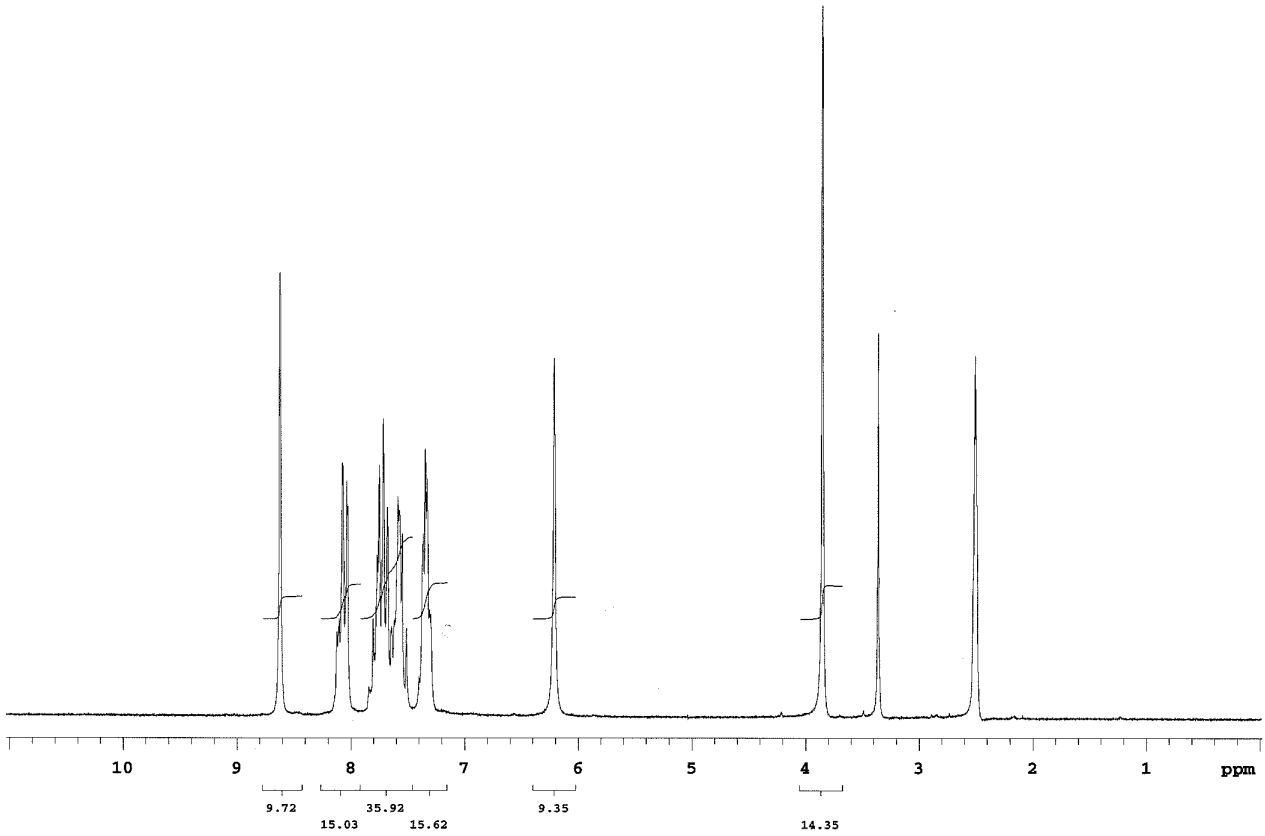

^{1}H NMR (300 MHz, DMSO) of compound 9b.

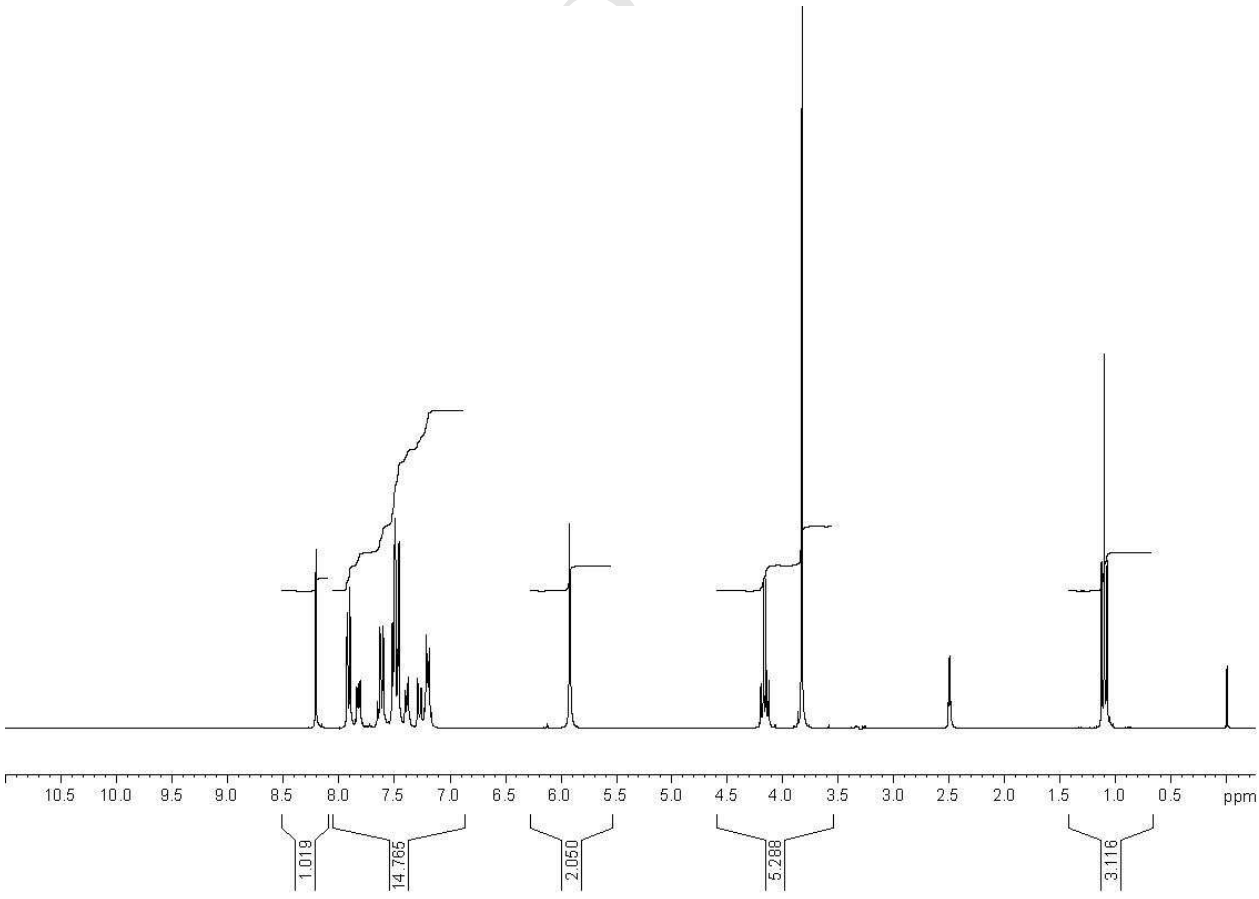

^{1}H NMR (300 MHz, DMSO) of compound 10a.

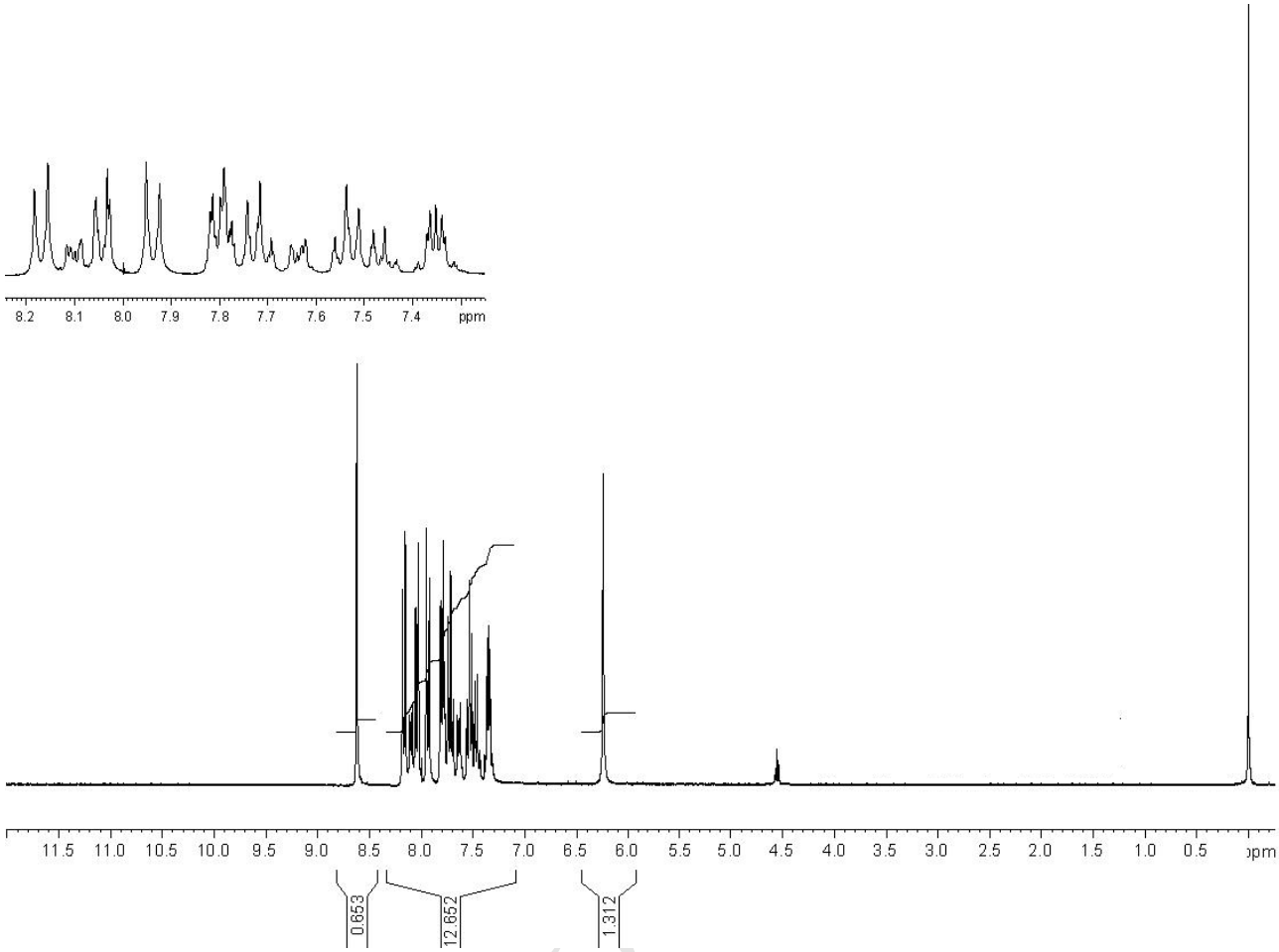

Table. S1 Raw flow cytometry data of a representative cell line, HL-60. **5e** (1577), **5l** (1575), **5p** (1578), **6a** (1579), **6b** (1576); Gates: M5 (Pre-G1), M6 (G1), M7 (S), M8 (G2/M), M10 (Polyploidy cells).

#1		#2		#3	
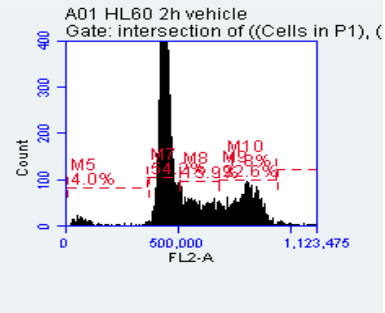		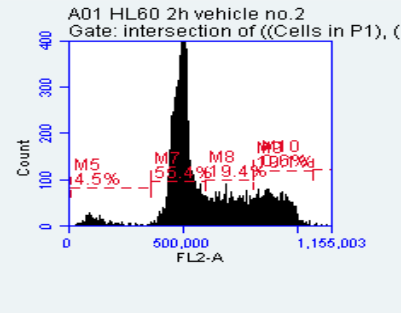		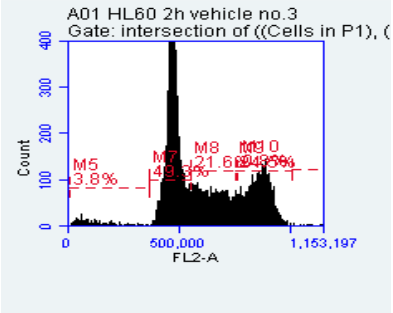	
Plot 4: A01 HL60 2h vehicle: Gated on intersection of ((Cells in P1), (Singlets in (Cells in all)))	% of This Plot	Plot 4: A01 HL60 2h vehicle no.2: Gated on intersection of ((Cells in P1), (Singlets in (Cells in all)))	% of This Plot	Plot 4: A01 HL60 2h vehicle no.3: Gated on intersection of ((Cells in P1), (Singlets in (Cells in all)))	% of This Plot
This Plot	100.00%	This Plot	100.00%	This Plot	100.00%
M5 (0.0 / 368,760.0)	4.01%	M5 (0.0 / 357,583.0)	4.45%	M5 (0.0 / 363,147.0)	3.82%
M7 (365,536.0 / 510,627.0)	54.22%	M7 (357,501.0 / 598,126.0)	55.44%	M7 (362,827.0 / 556,486.0)	49.29%
M8 (508,479.0 / 688,797.0)	15.92%	M8 (599,335.0 / 811,252.0)	19.37%	M8 (553,312.0 / 764,141.0)	21.60%
M9 (688,798.0 / 949,604.0)	22.63%	M9 (811,089.0 / 1,079,378.0)	19.06%	M9 (760,833.0 / 1,013,875.0)	24.52%
M10 (942,917.0 / 1,156,912.0)	1.83%	M10 (1,072,504.0 / 1,285,544.0)	0.56%	M10 (1,010,064.0 / 1,285,544.0)	0.77%
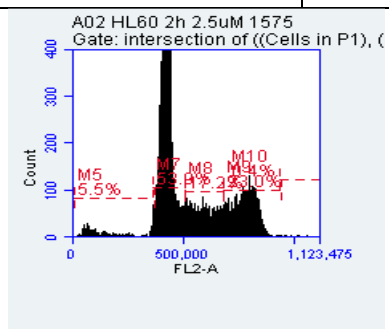		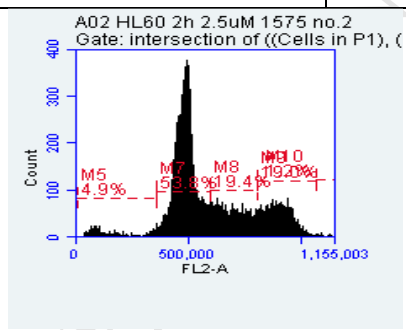		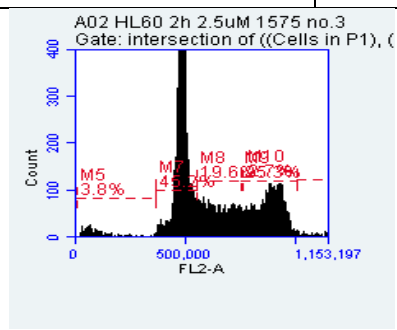	
Plot 4: A02 HL60 2h 2.5uM 1575: Gated on intersection of ((Cells in P1), (Singlets in (Cells in all)))	% of This Plot	Plot 4: A02 HL60 2h 2.5uM 1575 no.2: Gated on intersection of ((Cells in P1), (Singlets in (Cells in all)))	% of This Plot	Plot 4: A02 HL60 2h 2.5uM 1575 no.3: Gated on intersection of ((Cells in P1), (Singlets in (Cells in all)))	% of This Plot
This Plot	100.00%	This Plot	100.00%	This Plot	100.00%
M5 (0.0 / 368,760.0)	5.46%	M5 (0.0 / 357,583.0)	4.94%	M5 (0.0 / 363,147.0)	3.76%
M7 (365,536.0 / 510,627.0)	53.85%	M7 (357,501.0 / 598,126.0)	53.80%	M7 (362,827.0 / 556,486.0)	45.19%
M8 (508,479.0 / 688,797.0)	17.20%	M8 (599,335.0 / 811,252.0)	19.36%	M8 (553,312.0 / 764,141.0)	19.58%
M9 (688,798.0 / 949,604.0)	23.00%	M9 (811,089.0 / 1,079,378.0)	18.96%	M9 (760,833.0 / 1,013,875.0)	25.29%
M10 (942,917.0 / 1,156,912.0)	0.43%	M10 (1,072,504.0 / 1,285,544.0)	1.17%	M10 (1,010,064.0 / 1,285,544.0)	2.66%
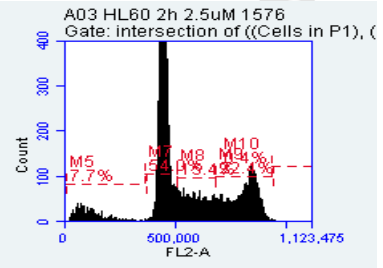		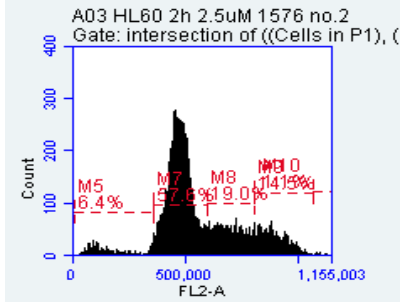		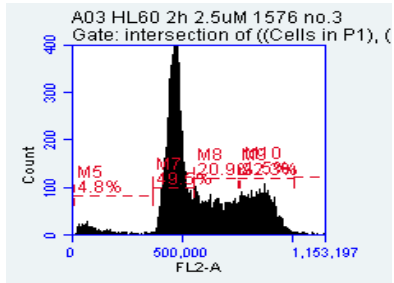	
Plot 4: A03 HL60 2h 2.5uM 1576: Gated on intersection of ((Cells in P1), (Singlets in (Cells in all)))	% of This Plot	Plot 4: A03 HL60 2h 2.5uM 1576: Gated on intersection of ((Cells in P1), (Singlets in (Cells in all)))	% of This Plot	Plot 4: A03 HL60 2h 2.5uM 1576 no.3: Gated on intersection of ((Cells in P1), (Singlets in (Cells in all)))	% of This Plot
This Plot	100.00%	This Plot	100.00%	This Plot	100.00%

M5 (0.0 / 368,760.0)	7.65%	M5 (0.0 / 357,583.0)	6.35%	M5 (0.0 / 363,147.0)	4.79%
M7 (365,536.0 / 510,627.0)	53.99%	M7 (357,501.0 / 598,126.0)	57.59%	M7 (362,827.0 / 556,486.0)	49.55%
M8 (508,479.0 / 688,797.0)	15.41%	M8 (599,335.0 / 811,252.0)	19.04%	M8 (553,312.0 / 764,141.0)	20.90%
M9 (688,798.0 / 949,604.0)	22.38%	M9 (811,089.0 / 1,079,378.0)	14.48%	M9 (760,833.0 / 1,013,875.0)	22.31%
M10 (942,917.0 / 1,156,912.0)	0.35%	M10 (1,072,504.0 / 1,285,544.0)	1.13%	M10 (1,010,064.0 / 1,285,544.0)	1.51%
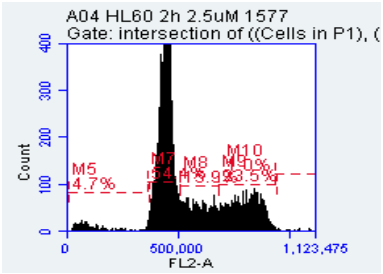		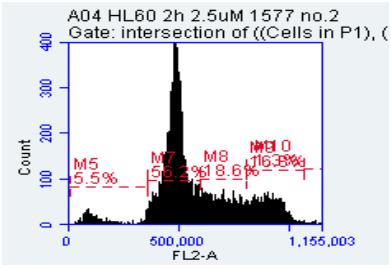		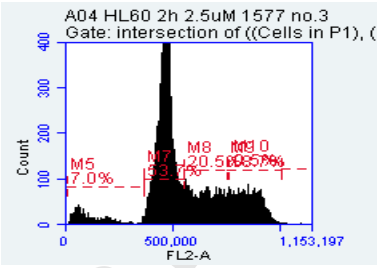	
Plot 4: A04 HL60 2h 2.5uM 1577: Gated on intersection of ((Cells in P1), (Singlets in (Cells in all)))	% of This Plot	Plot 4: A04 HL60 2h 2.5uM 1577 no.2: Gated on intersection of ((Cells in P1), (Singlets in (Cells in all)))	% of This Plot	Plot 4: A04 HL60 2h 2.5uM 1577 no.3: Gated on intersection of ((Cells in P1), (Singlets in (Cells in all)))	% of This Plot
This Plot	100.00%	This Plot	100.00%	This Plot	100.00%
M5 (0.0 / 368,760.0)	4.68%	M5 (0.0 / 357,583.0)	5.45%	M5 (0.0 / 363,147.0)	7.02%
M7 (365,536.0 / 510,627.0)	54.38%	M7 (357,501.0 / 598,126.0)	56.17%	M7 (362,827.0 / 556,486.0)	53.68%
M8 (508,479.0 / 688,797.0)	15.91%	M8 (599,335.0 / 811,252.0)	18.59%	M8 (553,312.0 / 764,141.0)	20.46%
M9 (688,798.0 / 949,604.0)	23.51%	M9 (811,089.0 / 1,079,378.0)	16.84%	M9 (760,833.0 / 1,013,875.0)	18.69%
M10 (942,917.0 / 1,156,912.0)	1.00%	M10 (1,072,504.0 / 1,285,544.0)	1.27%	M10 (1,010,064.0 / 1,285,544.0)	0.51%
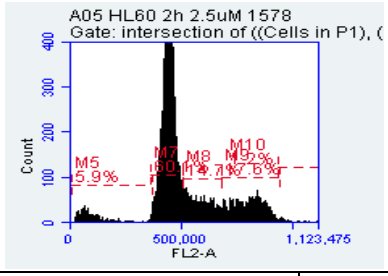		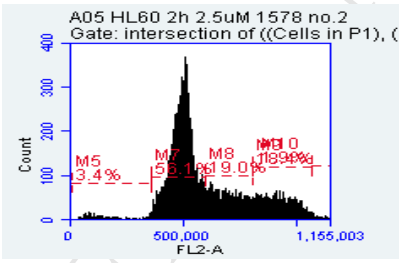		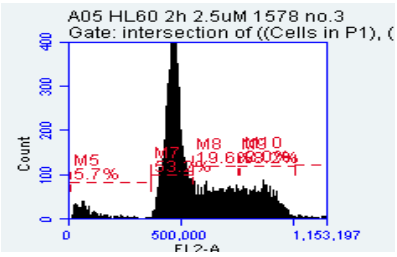	
Plot 4: A05 HL60 2h 2.5uM 1578: Gated on intersection of ((Cells in P1), (Singlets in (Cells in all)))	% of This Plot	Plot 4: A05 HL60 2h 2.5uM 1578 no.2: Gated on intersection of ((Cells in P1), (Singlets in (Cells in all)))	% of This Plot	Plot 4: A05 HL60 2h 2.5uM 1578 no.3: Gated on intersection of ((Cells in P1), (Singlets in (Cells in all)))	% of This Plot
This Plot	100.00%	This Plot	100.00%	This Plot	100.00%
M5 (0.0 / 368,760.0)	5.90%	M5 (0.0 / 357,583.0)	3.37%	M5 (0.0 / 363,147.0)	5.71%
M7 (365,536.0 / 510,627.0)	60.08%	M7 (357,501.0 / 598,126.0)	56.06%	M7 (362,827.0 / 556,486.0)	53.20%
M8 (508,479.0 / 688,797.0)	14.66%	M8 (599,335.0 / 811,252.0)	18.99%	M8 (553,312.0 / 764,141.0)	19.59%
M9 (688,798.0 / 949,604.0)	17.59%	M9 (811,089.0 / 1,079,378.0)	18.37%	M9 (760,833.0 / 1,013,875.0)	18.22%
M10 (942,917.0 / 1,156,912.0)	1.22%	M10 (1,072,504.0 / 1,285,544.0)	1.87%	M10 (1,010,064.0 / 1,285,544.0)	2.01%
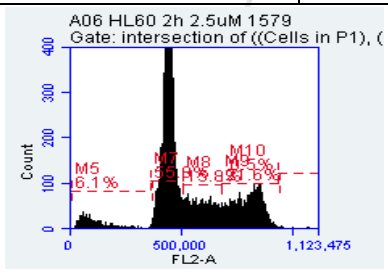		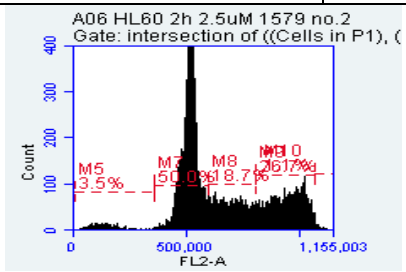		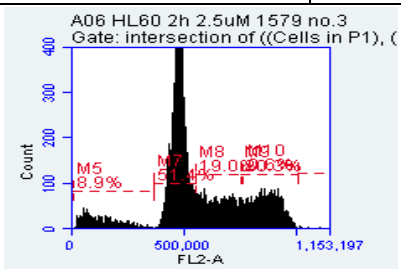	
Plot 4: A06 HL60 2h 2.5uM 1579: Gated on intersection of ((Cells in P1), (Singlets in (Cells in all)))	% of This Plot	Plot 4: A06 HL60 2h 2.5uM 1579 no.2: Gated on intersection of ((Cells in P1), (Singlets in (Cells in all)))	% of This Plot	Plot 4: A06 HL60 2h 2.5uM 1579 no.3: Gated on intersection of ((Cells in P1), (Singlets in (Cells in all)))	% of This Plot
This Plot	100.00%	This Plot	100.00%	This Plot	100.00%
M5 (0.0 / 368,760.0)	6.10%	M5 (0.0 / 357,583.0)	3.53%	M5 (0.0 / 363,147.0)	8.87%
M7 (365,536.0 / 510,627.0)	55.76%	M7 (357,501.0 / 598,126.0)	49.97%	M7 (362,827.0 / 556,486.0)	51.42%

M8 (508,479.0 / 688,797.0)	15.79%	M8 (599,335.0 / 811,252.0)	18.67%	M8 (553,312.0 / 764,141.0)	18.97%
M9 (688,798.0 / 949,604.0)	21.65%	M9 (811,089.0 / 1,079,378.0)	26.71%	M9 (760,833.0 / 1,013,875.0)	20.32%
M10 (942,917.0 / 1,156,912.0)	0.53%	M10 (1,072,504.0 / 1,285,544.0)	1.11%	M10 (1,010,064.0 / 1,285,544.0)	0.58%

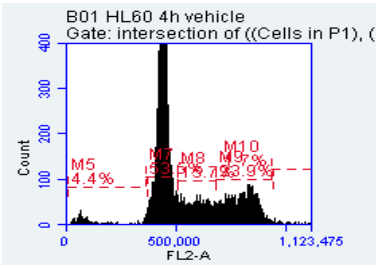

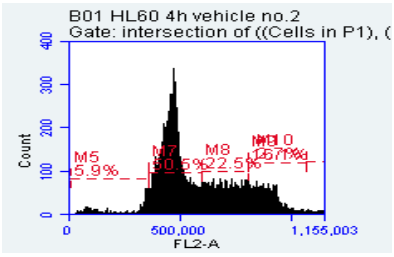

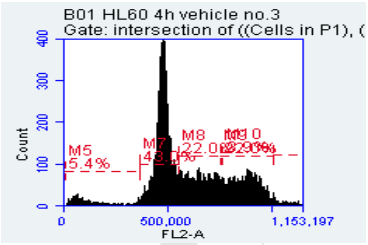

Plot 4: B01 HL60 4h vehicle: Gated on intersection of ((Cells in P1), (Singlets in (Cells in all)))	% of This Plot	Plot 4: B01 HL60 4h vehicle no.2: Gated on intersection of ((Cells in P1), (Singlets in (Cells in all)))	% of This Plot	Plot 4: B01 HL60 4h vehicle no.3: Gated on intersection of ((Cells in P1), (Singlets in (Cells in all)))	% of This Plot
This Plot	100.00%	This Plot	100.00%	This Plot	100.00%
M5 (0.0 / 368,760.0)	4.42%	M5 (0.0 / 357,583.0)	5.93%	M5 (0.0 / 363,147.0)	5.41%
M7 (365,536.0 / 510,627.0)	53.46%	M7 (357,501.0 / 598,126.0)	50.48%	M7 (362,827.0 / 556,486.0)	43.03%
M8 (508,479.0 / 688,797.0)	15.68%	M8 (599,335.0 / 811,252.0)	22.46%	M8 (553,312.0 / 764,141.0)	22.02%
M9 (688,798.0 / 949,604.0)	23.89%	M9 (811,089.0 / 1,079,378.0)	16.15%	M9 (760,833.0 / 1,013,875.0)	22.04%
M10 (942,917.0 / 1,156,912.0)	1.73%	M10 (1,072,504.0 / 1,285,544.0)	2.74%	M10 (1,010,064.0 / 1,285,544.0)	3.92%

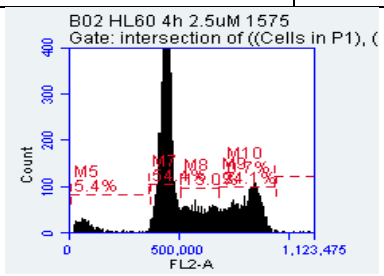

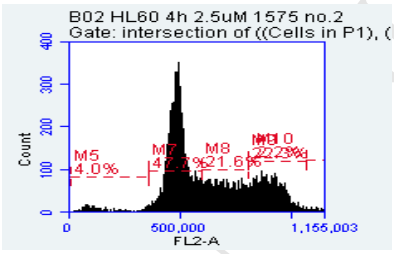

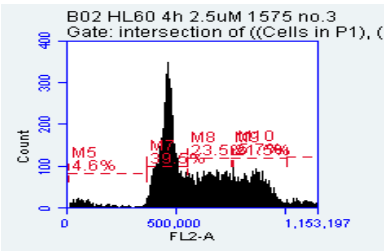

Plot 4: B02 HL60 4h 2.5uM 1575: Gated on intersection of ((Cells in P1), (Singlets in (Cells in all)))	% of This Plot	Plot 4: B02 HL60 4h 2.5uM 1575 no.2: Gated on intersection of ((Cells in P1), (Singlets in (Cells in all)))	% of This Plot	Plot 4: B02 HL60 4h 2.5uM 1575 no.3: Gated on intersection of ((Cells in P1), (Singlets in (Cells in all)))	% of This Plot
This Plot	100.00%	This Plot	100.00%	This Plot	100.00%
M5 (0.0 / 368,760.0)	5.35%	M5 (0.0 / 357,583.0)	3.96%	M5 (0.0 / 363,147.0)	4.64%
M7 (365,536.0 / 510,627.0)	54.37%	M7 (357,501.0 / 598,126.0)	47.72%	M7 (362,827.0 / 556,486.0)	39.48%
M8 (508,479.0 / 688,797.0)	15.01%	M8 (599,335.0 / 811,252.0)	21.59%	M8 (553,312.0 / 764,141.0)	23.47%
M9 (688,798.0 / 949,604.0)	24.07%	M9 (811,089.0 / 1,079,378.0)	22.25%	M9 (760,833.0 / 1,013,875.0)	21.47%
M10 (942,917.0 / 1,156,912.0)	0.70%	M10 (1,072,504.0 / 1,285,544.0)	2.22%	M10 (1,010,064.0 / 1,285,544.0)	5.75%

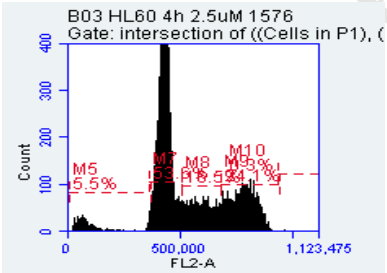

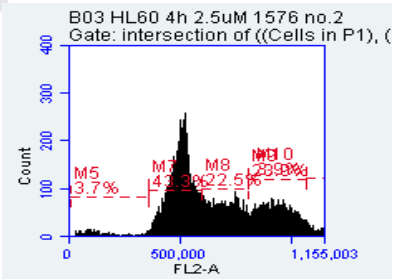

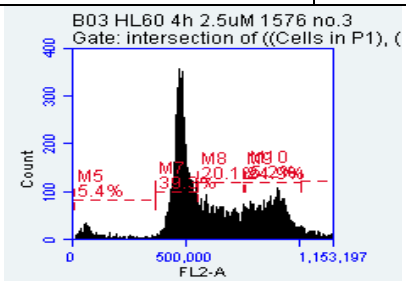

Plot 4: B03 HL60 4h 2.5uM 1576: Gated on intersection of ((Cells in P1), (Singlets in (Cells in all)))	% of This Plot	Plot 4: B03 HL60 4h 2.5uM 1576 no.2: Gated on intersection of ((Cells in P1), (Singlets in (Cells in all)))	% of This Plot	Plot 4: B03 HL60 4h 2.5uM 1576 no.3: Gated on intersection of ((Cells in P1), (Singlets in (Cells in all)))	% of This Plot
This Plot	100.00%	This Plot	100.00%	This Plot	100.00%
M5 (0.0 / 368,760.0)	5.46%	M5 (0.0 / 357,583.0)	3.74%	M5 (0.0 / 363,147.0)	5.44%
M7 (365,536.0 / 510,627.0)	53.65%	M7 (357,501.0 / 598,126.0)	43.34%	M7 (362,827.0 / 556,486.0)	39.26%
M8 (508,479.0 / 688,797.0)	16.54%	M8 (599,335.0 / 811,252.0)	22.45%	M8 (553,312.0 / 764,141.0)	20.06%
M9 (688,798.0 / 949,604.0)	24.06%	M9 (811,089.0 / 1,079,378.0)	23.90%	M9 (760,833.0 / 1,013,875.0)	24.93%
M10 (942,917.0 / 1,156,912.0)	0.29%	M10 (1,072,504.0 / 1,285,544.0)	3.92%	M10 (1,010,064.0 / 1,285,544.0)	5.16%

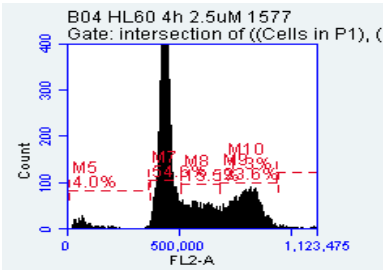

Plot 4: B04 HL60 4h 2.5uM 1577: Gated on intersection of ((Cells in P1), (Singlets in (Cells in all)))	% of This Plot
This Plot	100.00%
M5 (0.0 / 368,760.0)	4.04%
M7 (365,536.0 / 510,627.0)	54.62%
M8 (508,479.0 / 688,797.0)	15.45%
M9 (688,798.0 / 949,604.0)	23.63%
M10 (942,917.0 / 1,156,912.0)	1.34%

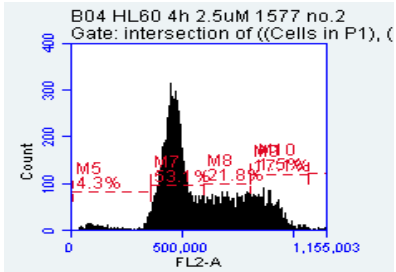

Plot 4: B04 HL60 4h 2.5uM 1577 no.2: Gated on intersection of ((Cells in P1), (Singlets in (Cells in all)))	% of This Plot
This Plot	100.00%
M5 (0.0 / 357,583.0)	4.28%
M7 (357,501.0 / 598,126.0)	53.07%
M8 (599,335.0 / 811,252.0)	21.81%
M9 (811,089.0 / 1,079,378.0)	17.12%
M10 (1,072,504.0 / 1,285,544.0)	1.49%

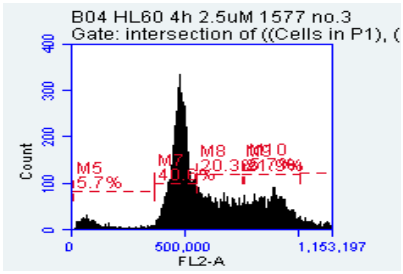

Plot 4: B04 HL60 4h 2.5uM 1577 no.3: Gated on intersection of ((Cells in P1), (Singlets in (Cells in all)))	% of This Plot
This Plot	100.00%
M5 (0.0 / 363,147.0)	5.68%
M7 (362,827.0 / 556,486.0)	40.60%
M8 (553,312.0 / 764,141.0)	20.28%
M9 (760,833.0 / 1,013,875.0)	21.91%
M10 (1,010,064.0 / 1,285,544.0)	5.69%

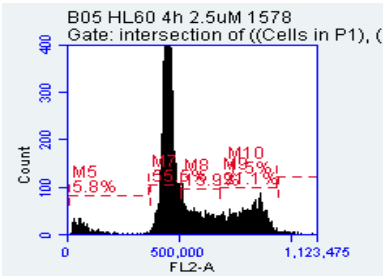

Plot 4: B05 HL60 4h 2.5uM 1578: Gated on intersection of ((Cells in P1), (Singlets in (Cells in all)))	% of This Plot
This Plot	100.00%
M5 (0.0 / 368,760.0)	5.78%
M7 (365,536.0 / 510,627.0)	55.48%
M8 (508,479.0 / 688,797.0)	15.86%
M9 (688,798.0 / 949,604.0)	21.10%
M10 (942,917.0 / 1,156,912.0)	1.45%

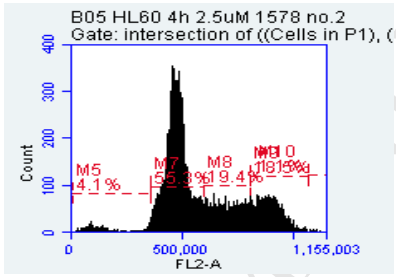

Plot 4: B05 HL60 4h 2.5uM 1578 no.2: Gated on intersection of ((Cells in P1), (Singlets in (Cells in all)))	% of This Plot
This Plot	100.00%
M5 (0.0 / 357,583.0)	4.14%
M7 (357,501.0 / 598,126.0)	55.33%
M8 (599,335.0 / 811,252.0)	19.45%
M9 (811,089.0 / 1,079,378.0)	18.51%
M10 (1,072,504.0 / 1,285,544.0)	1.06%

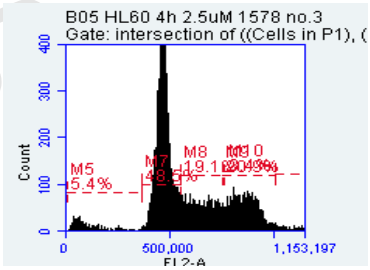

Plot 4: B05 HL60 4h 2.5uM 1578 no.3: Gated on intersection of ((Cells in P1), (Singlets in (Cells in all)))	% of This Plot
This Plot	100.00%
M5 (0.0 / 363,147.0)	5.36%
M7 (362,827.0 / 556,486.0)	48.53%
M8 (553,312.0 / 764,141.0)	19.13%
M9 (760,833.0 / 1,013,875.0)	20.88%
M10 (1,010,064.0 / 1,285,544.0)	3.36%

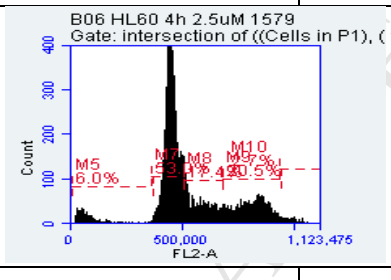

Plot 4: B06 HL60 4h 2.5uM 1579: Gated on intersection of ((Cells in P1), (Singlets in (Cells in all)))	% of This Plot
This Plot	100.00%
M5 (0.0 / 368,760.0)	5.96%
M7 (365,536.0 / 510,627.0)	53.00%
M8 (508,479.0 / 688,797.0)	17.40%
M9 (688,798.0 / 949,604.0)	20.51%
M10 (942,917.0 / 1,156,912.0)	2.68%

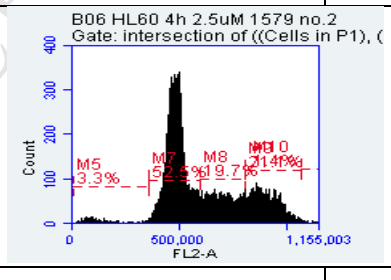

Plot 4: B06 HL60 4h 2.5uM 1579 no.2: Gated on intersection of ((Cells in P1), (Singlets in (Cells in all)))	% of This Plot
This Plot	100.00%
M5 (0.0 / 357,583.0)	3.31%
M7 (357,501.0 / 598,126.0)	52.53%
M8 (599,335.0 / 811,252.0)	19.73%
M9 (811,089.0 / 1,079,378.0)	21.11%
M10 (1,072,504.0 / 1,285,544.0)	1.43%

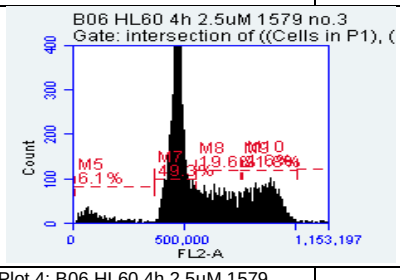

Plot 4: B06 HL60 4h 2.5uM 1579 no.3: Gated on intersection of ((Cells in P1), (Singlets in (Cells in all)))	% of This Plot
This Plot	100.00%
M5 (0.0 / 363,147.0)	6.12%
M7 (362,827.0 / 556,486.0)	49.28%
M8 (553,312.0 / 764,141.0)	19.63%
M9 (760,833.0 / 1,013,875.0)	21.83%
M10 (1,010,064.0 / 1,285,544.0)	1.61%

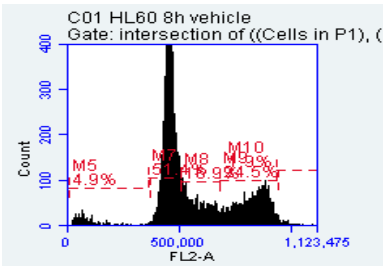

Plot 4: C01 HL60 8h vehicle: Gated on intersection of ((Cells in P1), (Singlets in (Cells in all)))	% of This Plot
This Plot	100.00%
M5 (0.0 / 368,760.0)	4.94%
M7 (365,536.0 / 510,627.0)	51.39%
M8 (508,479.0 / 688,797.0)	16.87%
M9 (688,798.0 / 949,604.0)	24.52%
M10 (942,917.0 / 1,156,912.0)	1.85%

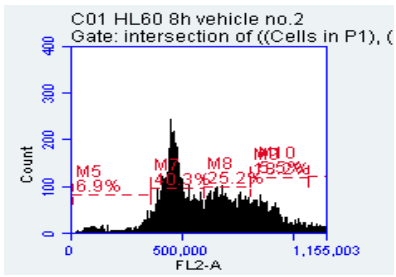

Plot 4: C01 HL60 8h vehicle no.2: Gated on intersection of ((Cells in P1), (Singlets in (Cells in all)))	% of This Plot
This Plot	100.00%
M5 (0.0 / 357,583.0)	6.91%
M7 (357,501.0 / 598,126.0)	40.30%
M8 (599,335.0 / 811,252.0)	25.23%
M9 (811,089.0 / 1,079,378.0)	18.18%
M10 (1,072,504.0 / 1,285,544.0)	5.52%

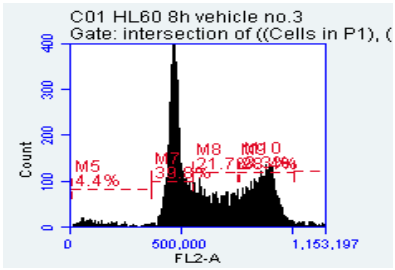

Plot 4: C01 HL60 8h vehicle no.3: Gated on intersection of ((Cells in P1), (Singlets in (Cells in all)))	% of This Plot
This Plot	100.00%
M5 (0.0 / 363,147.0)	4.45%
M7 (362,827.0 / 556,486.0)	39.80%
M8 (553,312.0 / 764,141.0)	21.74%
M9 (760,833.0 / 1,013,875.0)	28.36%
M10 (1,010,064.0 / 1,285,544.0)	3.27%

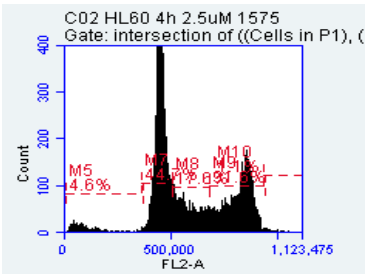

Plot 4: C02 HL60 4h 2.5uM 1575: Gated on intersection of ((Cells in P1), (Singlets in (Cells in all)))	% of This Plot
This Plot	100.00%
M5 (0.0 / 368,760.0)	4.59%
M7 (365,536.0 / 510,627.0)	44.70%
M8 (508,479.0 / 688,797.0)	17.64%
M9 (688,798.0 / 949,604.0)	31.62%
M10 (942,917.0 / 1,156,912.0)	1.05%

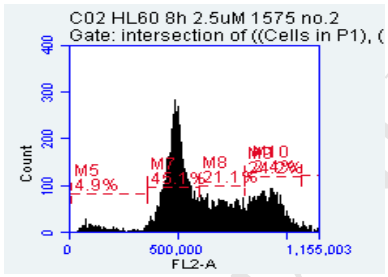

Plot 4: C02 HL60 8h 2.5uM 1575 no.2: Gated on intersection of ((Cells in P1), (Singlets in (Cells in all)))	% of This Plot
This Plot	100.00%
M5 (0.0 / 357,583.0)	4.89%
M7 (357,501.0 / 598,126.0)	45.15%
M8 (599,335.0 / 811,252.0)	21.08%
M9 (811,089.0 / 1,079,378.0)	24.25%
M10 (1,072,504.0 / 1,285,544.0)	2.39%

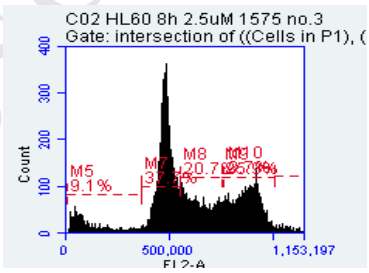

Plot 4: C02 HL60 8h 2.5uM 1575 no.3: Gated on intersection of ((Cells in P1), (Singlets in (Cells in all)))	% of This Plot
This Plot	100.00%
M5 (0.0 / 363,147.0)	9.07%
M7 (362,827.0 / 556,486.0)	37.71%
M8 (553,312.0 / 764,141.0)	20.70%
M9 (760,833.0 / 1,013,875.0)	25.87%
M10 (1,010,064.0 / 1,285,544.0)	3.70%

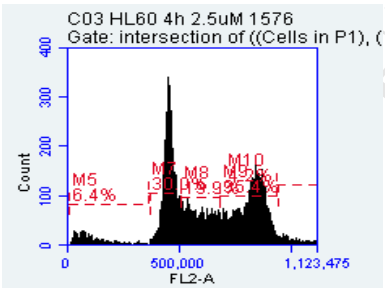

Plot 4: C03 HL60 4h 2.5uM 1576: Gated on intersection of ((Cells in P1), (Singlets in (Cells in all)))	% of This Plot
This Plot	100.00%
M5 (0.0 / 368,760.0)	6.39%
M7 (365,536.0 / 510,627.0)	30.01%
M8 (508,479.0 / 688,797.0)	19.90%
M9 (688,798.0 / 949,604.0)	35.36%
M10 (942,917.0 / 1,156,912.0)	4.22%

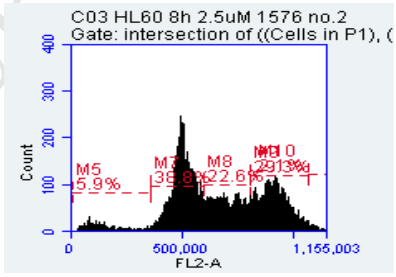

Plot 4: C03 HL60 8h 2.5uM 1576 no.2: Gated on intersection of ((Cells in P1), (Singlets in (Cells in all)))	% of This Plot
This Plot	100.00%
M5 (0.0 / 357,583.0)	5.91%
M7 (357,501.0 / 598,126.0)	38.77%
M8 (599,335.0 / 811,252.0)	22.59%
M9 (811,089.0 / 1,079,378.0)	29.34%
M10 (1,072,504.0 / 1,285,544.0)	2.06%

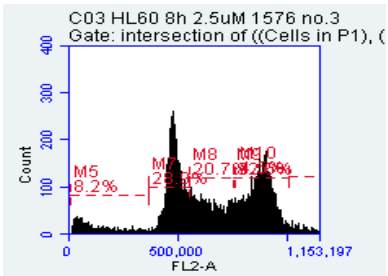

Plot 4: C03 HL60 8h 2.5uM 1576 no.3: Gated on intersection of ((Cells in P1), (Singlets in (Cells in all)))	% of This Plot
This Plot	100.00%
M5 (0.0 / 363,147.0)	8.20%
M7 (362,827.0 / 556,486.0)	28.92%
M8 (553,312.0 / 764,141.0)	20.67%
M9 (760,833.0 / 1,013,875.0)	32.56%
M10 (1,010,064.0 / 1,285,544.0)	4.54%

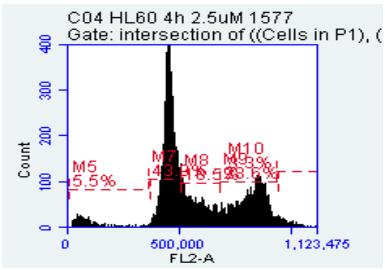

Plot 4: C04 HL60 4h 2.5uM 1577: Gated on intersection of ((Cells in P1), (Singlets in (Cells in all)))	% of This Plot
This Plot	100.00%
M5 (0.0 / 368,760.0)	5.52%
M7 (365,536.0 / 510,627.0)	43.86%
M8 (508,479.0 / 688,797.0)	18.49%
M9 (688,798.0 / 949,604.0)	28.63%
M10 (942,917.0 / 1,156,912.0)	3.30%

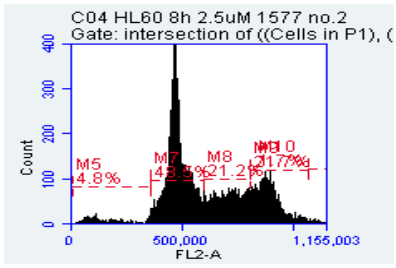

Plot 4: C04 HL60 8h 2.5uM 1577 no.2: Gated on intersection of ((Cells in P1), (Singlets in (Cells in all)))	% of This Plot
This Plot	100.00%
M5 (0.0 / 357,583.0)	4.83%
M7 (357,501.0 / 598,126.0)	48.52%
M8 (599,335.0 / 811,252.0)	21.19%
M9 (811,089.0 / 1,079,378.0)	21.71%
M10 (1,072,504.0 / 1,285,544.0)	1.70%

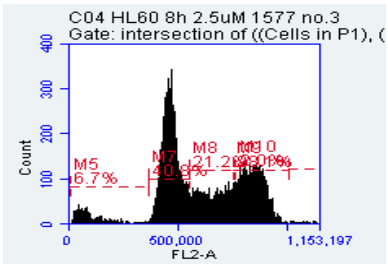

Plot 4: C04 HL60 8h 2.5uM 1577 no.3: Gated on intersection of ((Cells in P1), (Singlets in (Cells in all)))	% of This Plot
This Plot	100.00%
M5 (0.0 / 363,147.0)	6.72%
M7 (362,827.0 / 556,486.0)	40.75%
M8 (553,312.0 / 764,141.0)	21.23%
M9 (760,833.0 / 1,013,875.0)	28.09%
M10 (1,010,064.0 / 1,285,544.0)	1.95%

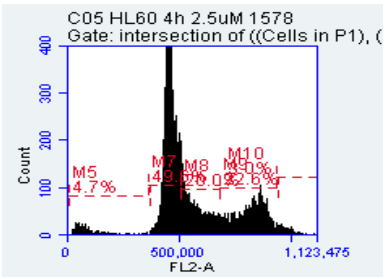

Plot 4: C05 HL60 4h 2.5uM 1578: Gated on intersection of ((Cells in P1), (Singlets in (Cells in all)))	% of This Plot
This Plot	100.00%
M5 (0.0 / 368,760.0)	4.67%
M7 (365,536.0 / 510,627.0)	49.58%
M8 (508,479.0 / 688,797.0)	20.03%
M9 (688,798.0 / 949,604.0)	22.65%
M10 (942,917.0 / 1,156,912.0)	3.01%

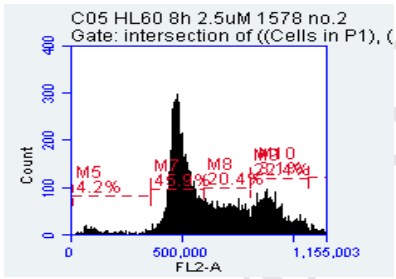

Plot 4: C05 HL60 8h 2.5uM 1578 no.2: Gated on intersection of ((Cells in P1), (Singlets in (Cells in all)))	% of This Plot
This Plot	100.00%
M5 (0.0 / 357,583.0)	4.24%
M7 (357,501.0 / 598,126.0)	45.93%
M8 (599,335.0 / 811,252.0)	20.38%
M9 (811,089.0 / 1,079,378.0)	22.45%
M10 (1,072,504.0 / 1,285,544.0)	3.09%

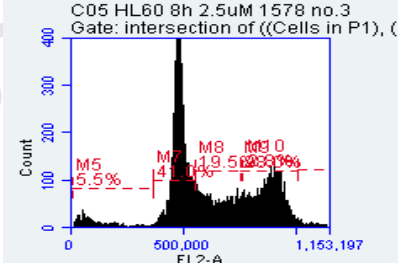

Plot 4: C05 HL60 8h 2.5uM 1578 no.3: Gated on intersection of ((Cells in P1), (Singlets in (Cells in all)))	% of This Plot
This Plot	100.00%
M5 (0.0 / 363,147.0)	5.48%
M7 (362,827.0 / 556,486.0)	41.03%
M8 (553,312.0 / 764,141.0)	19.47%
M9 (760,833.0 / 1,013,875.0)	27.98%
M10 (1,010,064.0 / 1,285,544.0)	2.81%

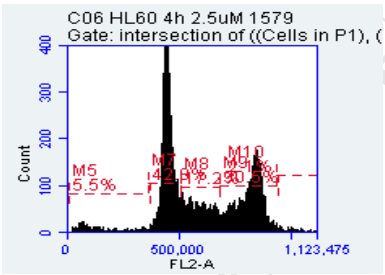

Plot 4: C06 HL60 4h 2.5uM 1579: Gated on intersection of ((Cells in P1), (Singlets in (Cells in all)))	% of This Plot
This Plot	100.00%
M5 (0.0 / 368,760.0)	5.55%
M7 (365,536.0 / 510,627.0)	42.79%
M8 (508,479.0 / 688,797.0)	17.24%
M9 (688,798.0 / 949,604.0)	30.48%
M10 (942,917.0 / 1,156,912.0)	2.15%

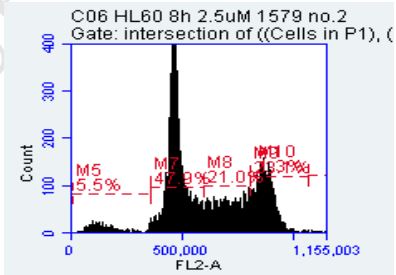

Plot 4: C06 HL60 8h 2.5uM 1579 no.2: Gated on intersection of ((Cells in P1), (Singlets in (Cells in all)))	% of This Plot
This Plot	100.00%
M5 (0.0 / 357,583.0)	5.46%
M7 (357,501.0 / 598,126.0)	47.89%
M8 (599,335.0 / 811,252.0)	20.98%
M9 (811,089.0 / 1,079,378.0)	23.06%
M10 (1,072,504.0 / 1,285,544.0)	1.34%

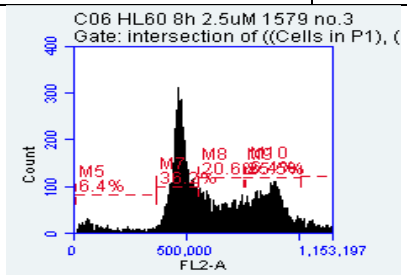

Plot 4: C06 HL60 8h 2.5uM 1579 no.3: Gated on intersection of ((Cells in P1), (Singlets in (Cells in all)))	% of This Plot
This Plot	100.00%
M5 (0.0 / 363,147.0)	6.40%
M7 (362,827.0 / 556,486.0)	36.21%
M8 (553,312.0 / 764,141.0)	20.65%
M9 (760,833.0 / 1,013,875.0)	25.51%
M10 (1,010,064.0 / 1,285,544.0)	6.36%

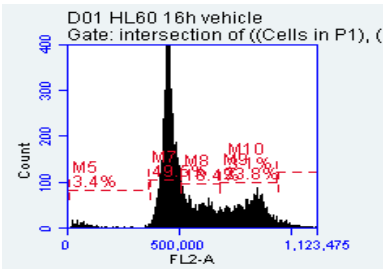

Plot 4: D01 HL60 16h vehicle: Gated on intersection of ((Cells in P1), (Singlets in (Cells in all)))	% of This Plot
This Plot	100.00%
M5 (0.0 / 368,760.0)	3.35%
M7 (365,536.0 / 510,627.0)	49.55%
M8 (508,479.0 / 688,797.0)	18.43%
M9 (688,798.0 / 949,604.0)	23.75%
M10 (942,917.0 / 1,156,912.0)	3.08%

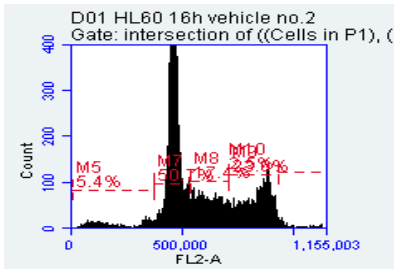

Plot 4: D01 HL60 16h vehicle no.2: Gated on intersection of ((Cells in P1), (Singlets in (Cells in all)))	% of This Plot
This Plot	100.00%
M5 (0.0 / 371,525.0)	5.41%
M7 (371,251.0 / 537,848.0)	50.72%
M8 (537,460.0 / 714,389.0)	17.39%
M9 (714,267.0 / 941,877.0)	23.02%
M10 (941,470.0 / 1,285,544.0)	2.51%

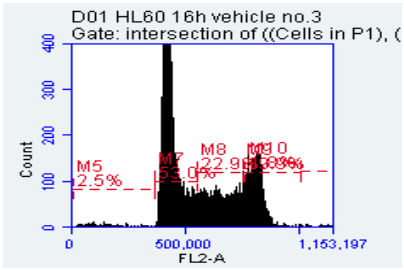

Plot 4: D01 HL60 16h vehicle no.3: Gated on intersection of ((Cells in P1), (Singlets in (Cells in all)))	% of This Plot
This Plot	100.00%
M5 (0.0 / 363,147.0)	2.51%
M7 (362,827.0 / 556,486.0)	53.01%
M8 (553,312.0 / 764,141.0)	22.88%
M9 (760,833.0 / 1,013,875.0)	19.89%
M10 (1,010,064.0 / 1,285,544.0)	1.75%

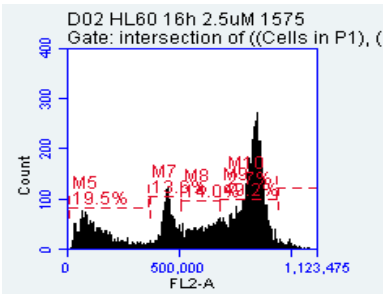

Plot 4: D02 HL60 16h 2.5uM 1575: Gated on intersection of ((Cells in P1), (Singlets in (Cells in all)))	% of This Plot
This Plot	100.00%
M5 (0.0 / 368,760.0)	19.47%
M7 (365,536.0 / 510,627.0)	13.65%
M8 (508,479.0 / 688,797.0)	14.00%
M9 (688,798.0 / 949,604.0)	49.24%
M10 (942,917.0 / 1,156,912.0)	2.66%

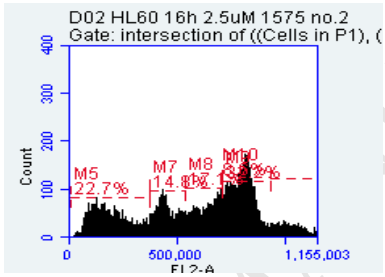

Plot 4: D02 HL60 16h 2.5uM 1575 no.2: Gated on intersection of ((Cells in P1), (Singlets in (Cells in all)))	% of This Plot
This Plot	100.00%
M5 (0.0 / 371,525.0)	22.73%
M7 (371,251.0 / 537,848.0)	14.83%
M8 (537,460.0 / 714,389.0)	17.08%
M9 (714,267.0 / 941,877.0)	32.22%
M10 (941,470.0 / 1,285,544.0)	8.64%

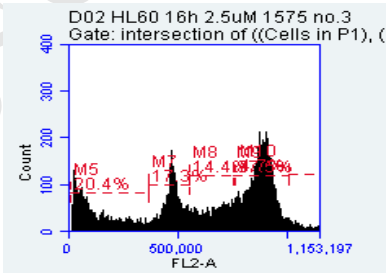

Plot 4: D02 HL60 16h 2.5uM 1575 no.3: Gated on intersection of ((Cells in P1), (Singlets in (Cells in all)))	% of This Plot
This Plot	100.00%
M5 (0.0 / 363,147.0)	20.37%
M7 (362,827.0 / 556,486.0)	17.29%
M8 (553,312.0 / 764,141.0)	14.43%
M9 (760,833.0 / 1,013,875.0)	37.50%
M10 (1,010,064.0 / 1,285,544.0)	4.69%

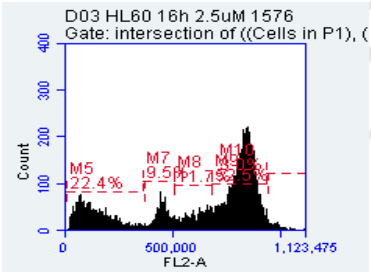

Plot 4: D03 HL60 16h 2.5uM 1576: Gated on intersection of ((Cells in P1), (Singlets in (Cells in all)))	% of This Plot
This Plot	100.00%
M5 (0.0 / 368,760.0)	22.44%
M7 (365,536.0 / 510,627.0)	9.53%
M8 (508,479.0 / 688,797.0)	11.75%
M9 (688,798.0 / 949,604.0)	52.53%
M10 (942,917.0 / 1,156,912.0)	2.98%

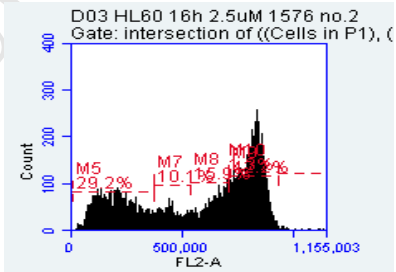

Plot 4: D03 HL60 16h 2.5uM 1576 no.2: Gated on intersection of ((Cells in P1), (Singlets in (Cells in all)))	% of This Plot
This Plot	100.00%
M5 (0.0 / 371,525.0)	29.17%
M7 (371,251.0 / 537,848.0)	10.05%
M8 (537,460.0 / 714,389.0)	15.87%
M9 (714,267.0 / 941,877.0)	42.21%
M10 (941,470.0 / 1,285,544.0)	1.31%

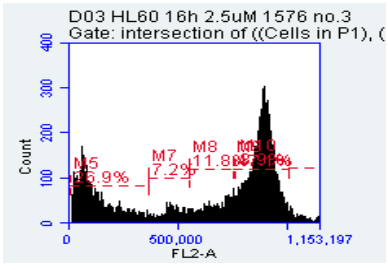

Plot 4: D03 HL60 16h 2.5uM 1576 no.3: Gated on intersection of ((Cells in P1), (Singlets in (Cells in all)))	% of This Plot
This Plot	100.00%
M5 (0.0 / 363,147.0)	26.94%
M7 (362,827.0 / 556,486.0)	7.17%
M8 (553,312.0 / 764,141.0)	11.78%
M9 (760,833.0 / 1,013,875.0)	47.11%
M10 (1,010,064.0 / 1,285,544.0)	3.94%

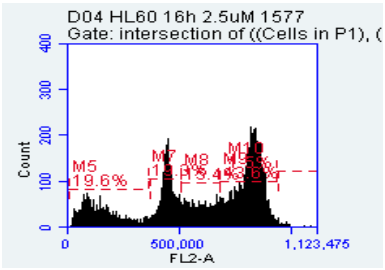

Plot 4: D04 HL60 16h 2.5uM 1577: Gated on intersection of ((Cells in P1), (Singlets in (Cells in all)))	% of This Plot
This Plot	100.00%
M5 (0.0 / 368,760.0)	19.59%
M7 (365,536.0 / 510,627.0)	19.34%
M8 (508,479.0 / 688,797.0)	15.36%
M9 (688,798.0 / 949,604.0)	43.62%
M10 (942,917.0 / 1,156,912.0)	1.50%

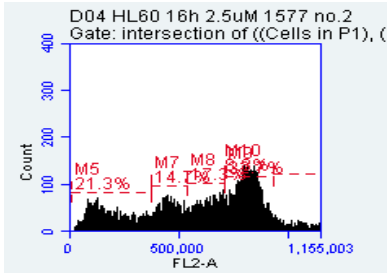

Plot 4: D04 HL60 16h 2.5uM 1577 no.2: Gated on intersection of ((Cells in P1), (Singlets in (Cells in all)))	% of This Plot
This Plot	100.00%
M5 (0.0 / 371,525.0)	21.33%
M7 (371,251.0 / 537,848.0)	14.67%
M8 (537,460.0 / 714,389.0)	17.35%
M9 (714,267.0 / 941,877.0)	32.74%
M10 (941,470.0 / 1,285,544.0)	8.81%

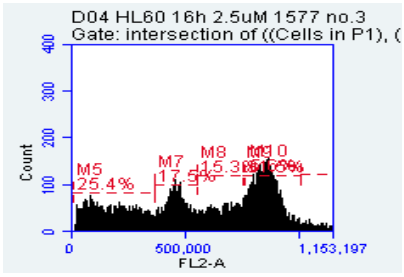

Plot 4: D04 HL60 16h 2.5uM 1577 no.3: Gated on intersection of ((Cells in P1), (Singlets in (Cells in all)))	% of This Plot
This Plot	100.00%
M5 (0.0 / 363,147.0)	25.40%
M7 (362,827.0 / 556,486.0)	17.45%
M8 (553,312.0 / 764,141.0)	15.32%
M9 (760,833.0 / 1,013,875.0)	31.46%
M10 (1,010,064.0 / 1,285,544.0)	5.57%

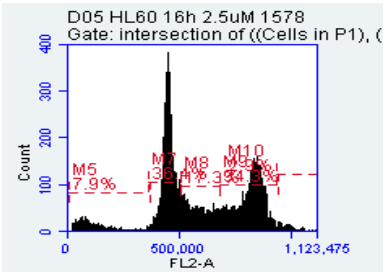

Plot 4: D05 HL60 16h 2.5uM 1578: Gated on intersection of ((Cells in P1), (Singlets in (Cells in all)))	% of This Plot
This Plot	100.00%
M5 (0.0 / 368,760.0)	7.85%
M7 (365,536.0 / 510,627.0)	36.44%
M8 (508,479.0 / 688,797.0)	17.33%
M9 (688,798.0 / 949,604.0)	34.33%
M10 (942,917.0 / 1,156,912.0)	2.94%

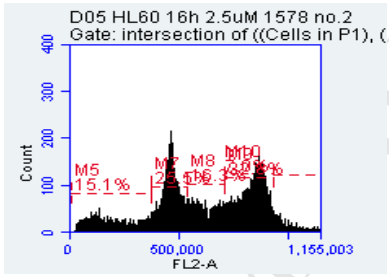

Plot 4: D05 HL60 16h 2.5uM 1578 no.2: Gated on intersection of ((Cells in P1), (Singlets in (Cells in all)))	% of This Plot
This Plot	100.00%
M5 (0.0 / 371,525.0)	15.06%
M7 (371,251.0 / 537,848.0)	25.52%
M8 (537,460.0 / 714,389.0)	16.33%
M9 (714,267.0 / 941,877.0)	32.84%
M10 (941,470.0 / 1,285,544.0)	7.02%

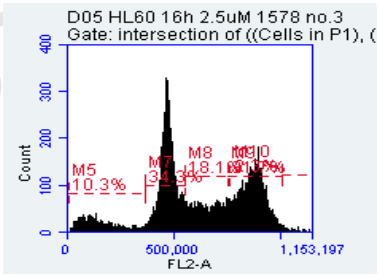

Plot 4: D05 HL60 16h 2.5uM 1578 no.3: Gated on intersection of ((Cells in P1), (Singlets in (Cells in all)))	% of This Plot
This Plot	100.00%
M5 (0.0 / 363,147.0)	10.27%
M7 (362,827.0 / 556,486.0)	34.27%
M8 (553,312.0 / 764,141.0)	18.06%
M9 (760,833.0 / 1,013,875.0)	31.73%
M10 (1,010,064.0 / 1,285,544.0)	2.29%

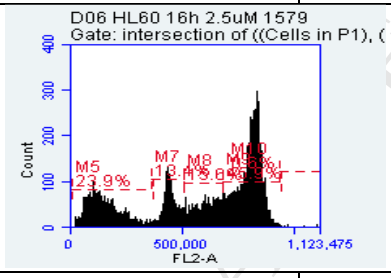

Plot 4: D06 HL60 16h 2.5uM 1579: Gated on intersection of ((Cells in P1), (Singlets in (Cells in all)))	% of This Plot
This Plot	100.00%
M5 (0.0 / 368,760.0)	23.92%
M7 (365,536.0 / 510,627.0)	13.35%
M8 (508,479.0 / 688,797.0)	15.55%
M9 (688,798.0 / 949,604.0)	45.85%
M10 (942,917.0 / 1,156,912.0)	0.58%

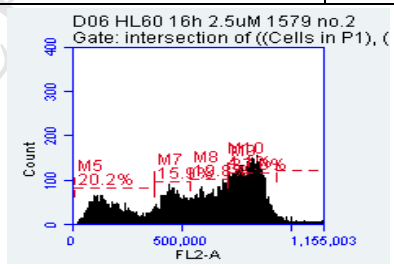

Plot 4: D06 HL60 16h 2.5uM 1579 no.2: Gated on intersection of ((Cells in P1), (Singlets in (Cells in all)))	% of This Plot
This Plot	100.00%
M5 (0.0 / 371,525.0)	20.16%
M7 (371,251.0 / 537,848.0)	15.94%
M8 (537,460.0 / 714,389.0)	19.82%
M9 (714,267.0 / 941,877.0)	36.97%
M10 (941,470.0 / 1,285,544.0)	4.11%

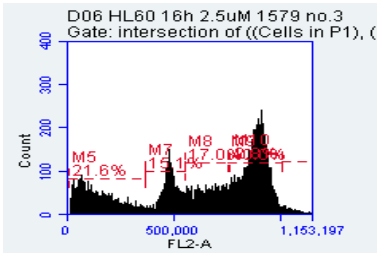

Plot 4: D06 HL60 16h 2.5uM 1579 no.3: Gated on intersection of ((Cells in P1), (Singlets in (Cells in all)))	% of This Plot
This Plot	100.00%
M5 (0.0 / 363,147.0)	21.57%
M7 (362,827.0 / 556,486.0)	15.06%
M8 (553,312.0 / 764,141.0)	17.00%
M9 (760,833.0 / 1,013,875.0)	39.96%
M10 (1,010,064.0 / 1,285,544.0)	2.84%

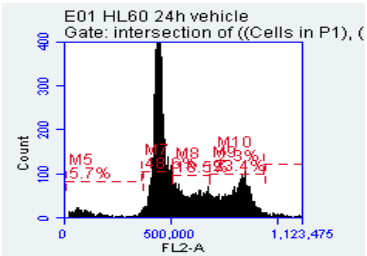

Plot 4: E01 HL60 24h vehicle: Gated on intersection of ((Cells in P1), (Singlets in (Cells in all)))	% of This Plot
This Plot	100.00%
M5 (0.0 / 368,760.0)	5.74%
M7 (365,536.0 / 510,627.0)	48.62%
M8 (508,479.0 / 688,797.0)	18.50%
M9 (688,798.0 / 949,604.0)	23.38%
M10 (942,917.0 / 1,156,912.0)	2.26%

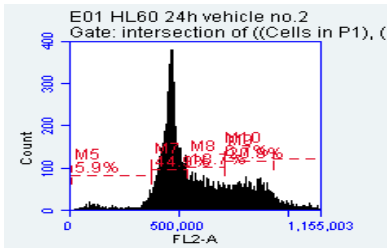

Plot 4: E01 HL60 24h vehicle no.2: Gated on intersection of ((Cells in P1), (Singlets in (Cells in all)))	% of This Plot
This Plot	100.00%
M5 (0.0 / 371,525.0)	5.91%
M7 (371,251.0 / 537,848.0)	44.87%
M8 (537,460.0 / 714,389.0)	18.71%
M9 (714,267.0 / 941,877.0)	20.89%
M10 (941,470.0 / 1,285,544.0)	6.73%

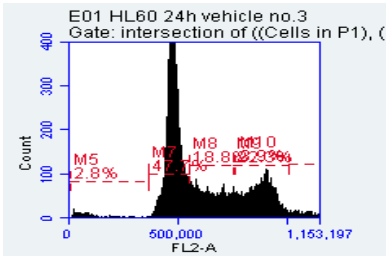

Plot 4: E01 HL60 24h vehicle no.3: Gated on intersection of ((Cells in P1), (Singlets in (Cells in all)))	% of This Plot
This Plot	100.00%
M5 (0.0 / 363,147.0)	2.82%
M7 (362,827.0 / 556,486.0)	47.69%
M8 (553,312.0 / 764,141.0)	18.82%
M9 (760,833.0 / 1,013,875.0)	22.31%
M10 (1,010,064.0 / 1,285,544.0)	3.95%

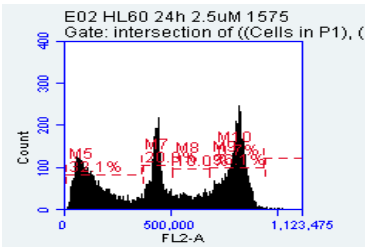

Plot 4: E02 HL60 24h 2.5uM 1575: Gated on intersection of ((Cells in P1), (Singlets in (Cells in all)))	% of This Plot
This Plot	100.00%
M5 (0.0 / 368,760.0)	32.08%
M7 (365,536.0 / 510,627.0)	20.75%
M8 (508,479.0 / 688,797.0)	9.97%
M9 (688,798.0 / 949,604.0)	36.07%
M10 (942,917.0 / 1,156,912.0)	0.69%

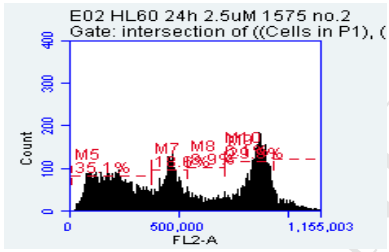

Plot 4: E02 HL60 24h 2.5uM 1575 no.2: Gated on intersection of ((Cells in P1), (Singlets in (Cells in all)))	% of This Plot
This Plot	100.00%
M5 (0.0 / 371,525.0)	35.13%
M7 (371,251.0 / 537,848.0)	18.64%
M8 (537,460.0 / 714,389.0)	8.87%
M9 (714,267.0 / 941,877.0)	29.87%
M10 (941,470.0 / 1,285,544.0)	6.10%

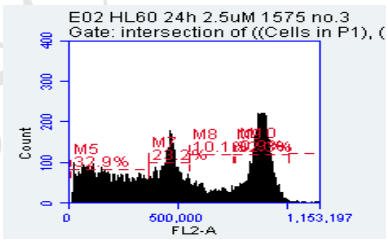

Plot 4: E02 HL60 24h 2.5uM 1575 no.3: Gated on intersection of ((Cells in P1), (Singlets in (Cells in all)))	% of This Plot
This Plot	100.00%
M5 (0.0 / 363,147.0)	32.86%
M7 (362,827.0 / 556,486.0)	23.15%
M8 (553,312.0 / 764,141.0)	10.14%
M9 (760,833.0 / 1,013,875.0)	32.34%
M10 (1,010,064.0 / 1,285,544.0)	0.93%

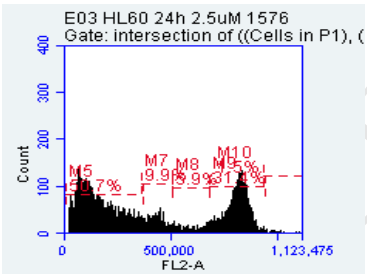

Plot 4: E03 HL60 24h 2.5uM 1576: Gated on intersection of ((Cells in P1), (Singlets in (Cells in all)))	% of This Plot
This Plot	100.00%
M5 (0.0 / 368,760.0)	50.69%
M7 (365,536.0 / 510,627.0)	9.91%
M8 (508,479.0 / 688,797.0)	5.91%
M9 (688,798.0 / 949,604.0)	31.39%
M10 (942,917.0 / 1,156,912.0)	1.46%

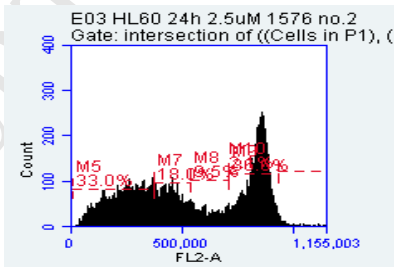

Plot 4: E03 HL60 24h 2.5uM 1576 no.2: Gated on intersection of ((Cells in P1), (Singlets in (Cells in all)))	% of This Plot
This Plot	100.00%
M5 (0.0 / 371,525.0)	32.99%
M7 (371,251.0 / 537,848.0)	17.96%
M8 (537,460.0 / 714,389.0)	9.51%
M9 (714,267.0 / 941,877.0)	36.64%
M10 (941,470.0 / 1,285,544.0)	2.14%

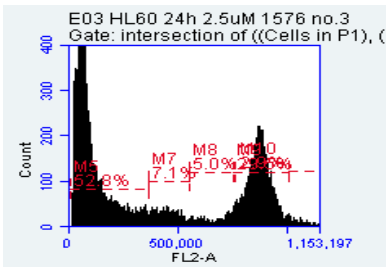

Plot 4: E03 HL60 24h 2.5uM 1576 no.3: Gated on intersection of ((Cells in P1), (Singlets in (Cells in all)))	% of This Plot
This Plot	100.00%
M5 (0.0 / 363,147.0)	52.79%
M7 (362,827.0 / 556,486.0)	7.08%
M8 (553,312.0 / 764,141.0)	4.97%
M9 (760,833.0 / 1,013,875.0)	29.50%
M10 (1,010,064.0 / 1,285,544.0)	2.94%

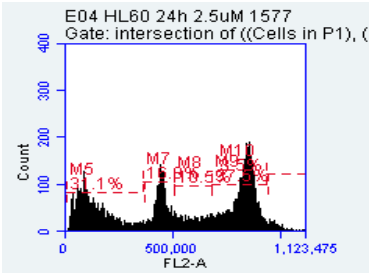

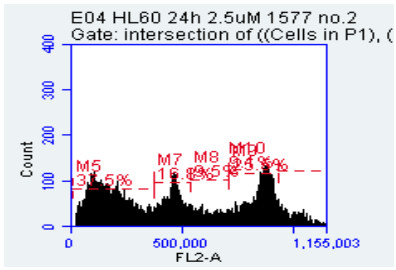

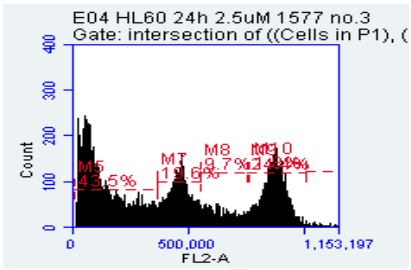

Plot 4: E04 HL60 24h 2.5uM 1577: Gated on intersection of ((Cells in P1), (Singlets in (Cells in all)))	% of This Plot
This Plot	100.00%
M5 (0.0 / 368,760.0)	31.07%
M7 (365,536.0 / 510,627.0)	16.79%
M8 (508,479.0 / 688,797.0)	10.46%
M9 (688,798.0 / 949,604.0)	37.52%
M10 (942,917.0 / 1,156,912.0)	3.48%

Plot 4: E04 HL60 24h 2.5uM 1577 no.2: Gated on intersection of ((Cells in P1), (Singlets in (Cells in all)))	% of This Plot
This Plot	100.00%
M5 (0.0 / 371,525.0)	37.46%
M7 (371,251.0 / 537,848.0)	16.80%
M8 (537,460.0 / 714,389.0)	9.48%
M9 (714,267.0 / 941,877.0)	25.48%
M10 (941,470.0 / 1,285,544.0)	9.09%

Plot 4: E04 HL60 24h 2.5uM 1577 no.3: Gated on intersection of ((Cells in P1), (Singlets in (Cells in all)))	% of This Plot
This Plot	100.00%
M5 (0.0 / 363,147.0)	43.47%
M7 (362,827.0 / 556,486.0)	19.61%
M8 (553,312.0 / 764,141.0)	9.68%
M9 (760,833.0 / 1,013,875.0)	24.36%
M10 (1,010,064.0 / 1,285,544.0)	1.79%

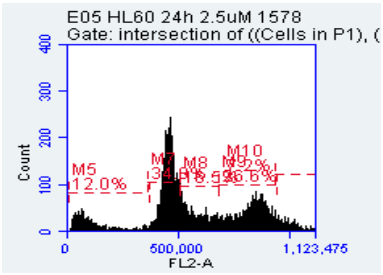

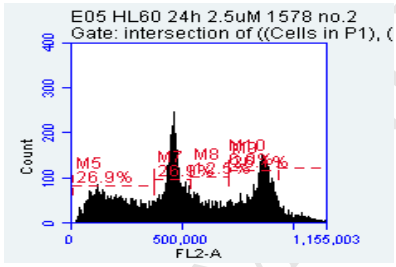

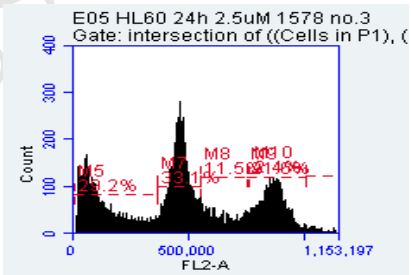

Plot 4: E05 HL60 24h 2.5uM 1578: Gated on intersection of ((Cells in P1), (Singlets in (Cells in all)))	% of This Plot
This Plot	100.00%
M5 (0.0 / 368,760.0)	12.00%
M7 (365,536.0 / 510,627.0)	34.82%
M8 (508,479.0 / 688,797.0)	16.54%
M9 (688,798.0 / 949,604.0)	26.60%
M10 (942,917.0 / 1,156,912.0)	7.21%

Plot 4: E05 HL60 24h 2.5uM 1578 no.2: Gated on intersection of ((Cells in P1), (Singlets in (Cells in all)))	% of This Plot
This Plot	100.00%
M5 (0.0 / 371,525.0)	26.90%
M7 (371,251.0 / 537,848.0)	26.86%
M8 (537,460.0 / 714,389.0)	12.46%
M9 (714,267.0 / 941,877.0)	26.08%
M10 (941,470.0 / 1,285,544.0)	6.01%

Plot 4: E04 HL60 24h 2.5uM 1577 no.3: Gated on intersection of ((Cells in P1), (Singlets in (Cells in all)))	% of This Plot
This Plot	100.00%
M5 (0.0 / 363,147.0)	43.47%
M7 (362,827.0 / 556,486.0)	19.61%
M8 (553,312.0 / 764,141.0)	9.68%
M9 (760,833.0 / 1,013,875.0)	24.36%
M10 (1,010,064.0 / 1,285,544.0)	1.79%

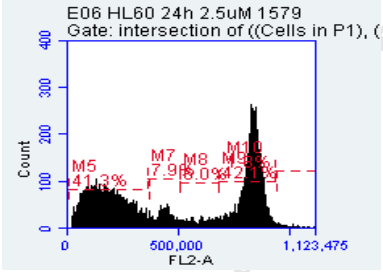

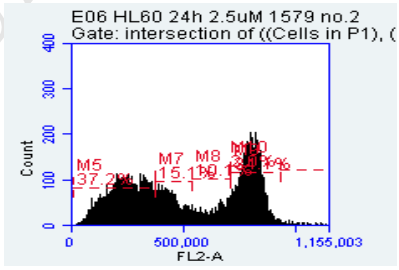

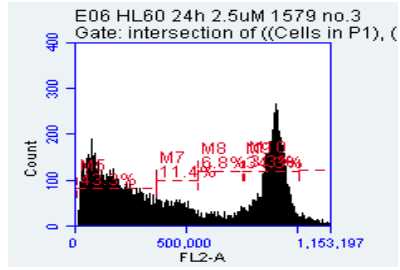

Plot 4: E06 HL60 24h 2.5uM 1579: Gated on intersection of ((Cells in P1), (Singlets in (Cells in all)))	% of This Plot
This Plot	100.00%
M5 (0.0 / 368,760.0)	41.34%
M7 (365,536.0 / 510,627.0)	7.91%
M8 (508,479.0 / 688,797.0)	5.98%
M9 (688,798.0 / 949,604.0)	42.06%
M10 (942,917.0 / 1,156,912.0)	1.81%

Plot 4: E06 HL60 24h 2.5uM 1579 no.2: Gated on intersection of ((Cells in P1), (Singlets in (Cells in all)))	% of This Plot
This Plot	100.00%
M5 (0.0 / 371,525.0)	37.17%
M7 (371,251.0 / 537,848.0)	15.05%
M8 (537,460.0 / 714,389.0)	10.06%
M9 (714,267.0 / 941,877.0)	34.12%
M10 (941,470.0 / 1,285,544.0)	1.96%

Plot 4: E04 HL60 24h 2.5uM 1577 no.3: Gated on intersection of ((Cells in P1), (Singlets in (Cells in all)))	% of This Plot
This Plot	100.00%
M5 (0.0 / 363,147.0)	43.47%
M7 (362,827.0 / 556,486.0)	19.61%
M8 (553,312.0 / 764,141.0)	9.68%
M9 (760,833.0 / 1,013,875.0)	24.36%
M10 (1,010,064.0 / 1,285,544.0)	1.79%

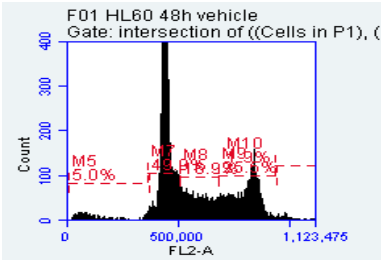

Plot 4: F01 HL60 48h vehicle: Gated on intersection of ((Cells in P1), (Singlets in (Cells in all)))	% of This Plot
This Plot	100.00%
M5 (0.0 / 368,760.0)	4.95%
M7 (365,536.0 / 510,627.0)	49.95%
M8 (508,479.0 / 688,797.0)	16.88%
M9 (688,798.0 / 949,604.0)	25.55%
M10 (942,917.0 / 1,156,912.0)	1.91%

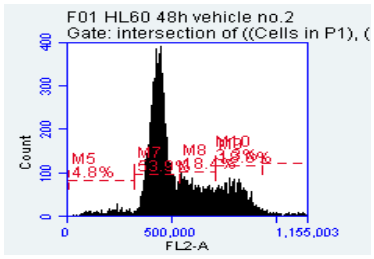

Plot 4: F01 HL60 48h vehicle no.2: Gated on intersection of ((Cells in P1), (Singlets in (Cells in all)))	% of This Plot
This Plot	100.00%
M5 (0.0 / 323,126.0)	4.77%
M7 (323,126.0 / 537,848.0)	53.86%
M8 (537,460.0 / 714,389.0)	18.37%
M9 (714,267.0 / 941,877.0)	18.62%
M10 (941,470.0 / 1,285,544.0)	3.33%

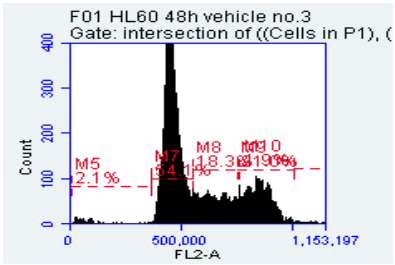

Plot 4: F01 HL60 48h vehicle no.3: Gated on intersection of ((Cells in P1), (Singlets in (Cells in all)))	% of This Plot
This Plot	100.00%
M5 (0.0 / 363,147.0)	2.10%
M7 (362,827.0 / 556,486.0)	54.06%
M8 (553,312.0 / 764,141.0)	18.29%
M9 (760,833.0 / 1,013,875.0)	21.02%
M10 (1,010,064.0 / 1,285,544.0)	1.90%

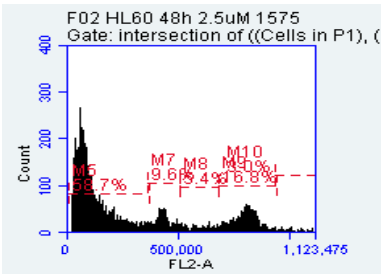

Plot 4: F02 HL60 48h 2.5uM 1575: Gated on intersection of ((Cells in P1), (Singlets in (Cells in all)))	% of This Plot
This Plot	100.00%
M5 (0.0 / 368,760.0)	58.68%
M7 (365,536.0 / 510,627.0)	9.62%
M8 (508,479.0 / 688,797.0)	5.39%
M9 (688,798.0 / 949,604.0)	16.77%
M10 (942,917.0 / 1,156,912.0)	2.97%

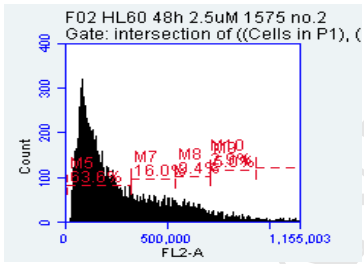

Plot 4: F02 HL60 48h 2.5uM 1575 no.2: Gated on intersection of ((Cells in P1), (Singlets in (Cells in all)))	% of This Plot
This Plot	100.00%
M5 (0.0 / 323,126.0)	63.59%
M7 (323,126.0 / 537,848.0)	15.99%
M8 (537,460.0 / 714,389.0)	9.35%
M9 (714,267.0 / 941,877.0)	5.00%
M10 (941,470.0 / 1,285,544.0)	2.92%

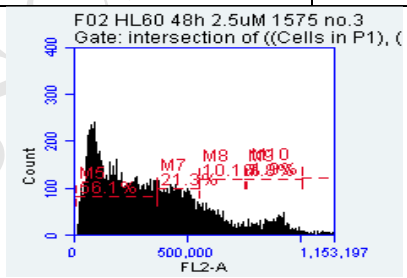

Plot 4: F02 HL60 48h 2.5uM 1575 no.3: Gated on intersection of ((Cells in P1), (Singlets in (Cells in all)))	% of This Plot
This Plot	100.00%
M5 (0.0 / 363,147.0)	56.05%
M7 (362,827.0 / 556,486.0)	21.32%
M8 (553,312.0 / 764,141.0)	10.06%
M9 (760,833.0 / 1,013,875.0)	7.78%
M10 (1,010,064.0 / 1,285,544.0)	1.93%

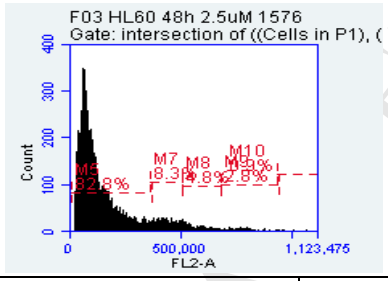

Plot 4: F03 HL60 48h 2.5uM 1576: Gated on intersection of ((Cells in P1), (Singlets in (Cells in all)))	% of This Plot
This Plot	100.00%
M5 (0.0 / 368,760.0)	82.83%
M7 (365,536.0 / 510,627.0)	8.31%
M8 (508,479.0 / 688,797.0)	4.81%
M9 (688,798.0 / 949,604.0)	2.85%
M10 (942,917.0 / 1,156,912.0)	0.87%

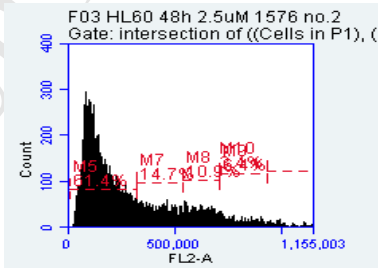

Plot 4: F03 HL60 48h 2.5uM 1576 no.2: Gated on intersection of ((Cells in P1), (Singlets in (Cells in all)))	% of This Plot
This Plot	100.00%
M5 (0.0 / 323,126.0)	61.43%
M7 (323,126.0 / 537,848.0)	14.71%
M8 (537,460.0 / 714,389.0)	10.85%
M9 (714,267.0 / 941,877.0)	6.36%
M10 (941,470.0 / 1,285,544.0)	3.37%

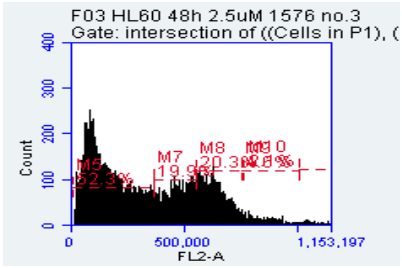

Plot 4: F03 HL60 48h 2.5uM 1576 no.3: Gated on intersection of ((Cells in P1), (Singlets in (Cells in all)))	% of This Plot
This Plot	100.00%
M5 (0.0 / 363,147.0)	52.29%
M7 (362,827.0 / 556,486.0)	19.95%
M8 (553,312.0 / 764,141.0)	20.30%
M9 (760,833.0 / 1,013,875.0)	4.55%
M10 (1,010,064.0 / 1,285,544.0)	2.08%

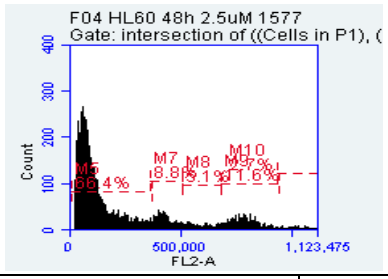

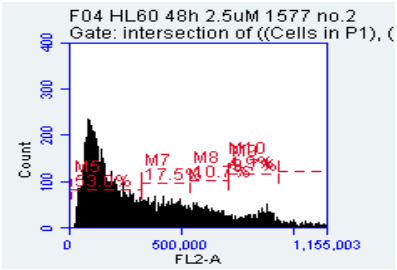

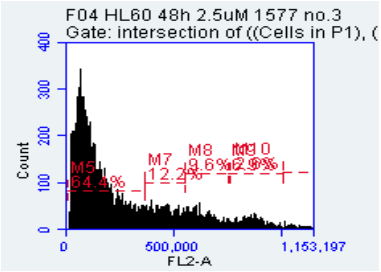

Plot 4: F04 HL60 48h 2.5uM 1577: Gated on intersection of ((Cells in P1), (Singlets in (Cells in all)))	% of This Plot
This Plot	100.00%
M5 (0.0 / 368,760.0)	66.38%
M7 (365,536.0 / 510,627.0)	8.82%
M8 (508,479.0 / 688,797.0)	5.10%
M9 (688,798.0 / 949,604.0)	11.63%
M10 (942,917.0 / 1,156,912.0)	2.66%

Plot 4: F04 HL60 48h 2.5uM 1577 no.2: Gated on intersection of ((Cells in P1), (Singlets in (Cells in all)))	% of This Plot
This Plot	100.00%
M5 (0.0 / 323,126.0)	52.99%
M7 (323,126.0 / 537,848.0)	17.46%
M8 (537,460.0 / 714,389.0)	10.72%
M9 (714,267.0 / 941,877.0)	9.67%
M10 (941,470.0 / 1,285,544.0)	4.87%

Plot 4: F04 HL60 48h 2.5uM 1577 no.3: Gated on intersection of ((Cells in P1), (Singlets in (Cells in all)))	% of This Plot
This Plot	100.00%
M5 (0.0 / 363,147.0)	64.44%
M7 (362,827.0 / 556,486.0)	12.22%
M8 (553,312.0 / 764,141.0)	9.63%
M9 (760,833.0 / 1,013,875.0)	6.95%
M10 (1,010,064.0 / 1,285,544.0)	2.61%

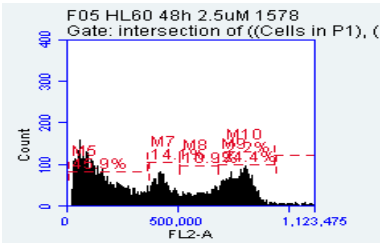

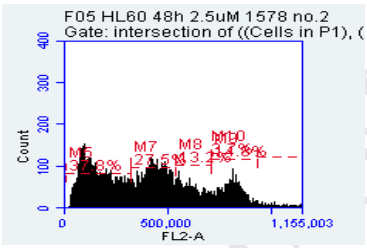

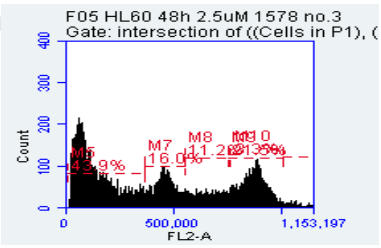

Plot 4: F05 HL60 48h 2.5uM 1578: Gated on intersection of ((Cells in P1), (Singlets in (Cells in all)))	% of This Plot
This Plot	100.00%
M5 (0.0 / 368,760.0)	45.88%
M7 (365,536.0 / 510,627.0)	14.14%
M8 (508,479.0 / 688,797.0)	10.85%
M9 (688,798.0 / 949,604.0)	24.36%
M10 (942,917.0 / 1,156,912.0)	2.15%

Plot 4: F05 HL60 48h 2.5uM 1578 no.2: Gated on intersection of ((Cells in P1), (Singlets in (Cells in all)))	% of This Plot
This Plot	100.00%
M5 (0.0 / 323,126.0)	37.80%
M7 (323,126.0 / 537,848.0)	27.50%
M8 (537,460.0 / 714,389.0)	13.23%
M9 (714,267.0 / 941,877.0)	14.77%
M10 (941,470.0 / 1,285,544.0)	3.74%

Plot 4: F05 HL60 48h 2.5uM 1578 no.3: Gated on intersection of ((Cells in P1), (Singlets in (Cells in all)))	% of This Plot
This Plot	100.00%
M5 (0.0 / 363,147.0)	43.94%
M7 (362,827.0 / 556,486.0)	15.96%
M8 (553,312.0 / 764,141.0)	11.22%
M9 (760,833.0 / 1,013,875.0)	21.51%
M10 (1,010,064.0 / 1,285,544.0)	3.34%

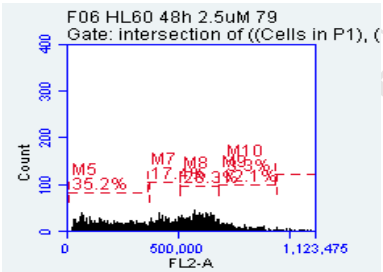

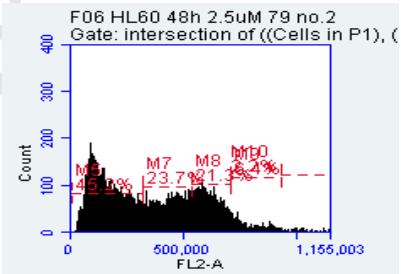

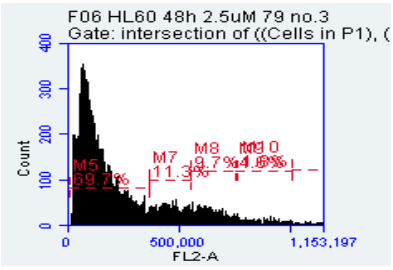

Plot 4: F06 HL60 48h 2.5uM 79: Gated on intersection of ((Cells in P1), (Singlets in (Cells in all)))	% of This Plot
This Plot	100.00%
M5 (0.0 / 368,760.0)	35.21%
M7 (365,536.0 / 510,627.0)	17.35%
M8 (508,479.0 / 688,797.0)	28.34%
M9 (688,798.0 / 949,604.0)	12.10%
M10 (942,917.0 / 1,156,912.0)	3.30%

Plot 4: F06 HL60 48h 2.5uM 79 no.2: Gated on intersection of ((Cells in P1), (Singlets in (Cells in all)))	% of This Plot
This Plot	100.00%
M5 (0.0 / 323,126.0)	45.22%
M7 (323,126.0 / 537,848.0)	23.66%
M8 (537,460.0 / 714,389.0)	21.33%
M9 (714,267.0 / 941,877.0)	6.44%
M10 (941,470.0 / 1,285,544.0)	2.22%

Plot 4: F06 HL60 48h 2.5uM 79 no.3: Gated on intersection of ((Cells in P1), (Singlets in (Cells in all)))	% of This Plot
This Plot	100.00%
M5 (0.0 / 363,147.0)	69.70%
M7 (362,827.0 / 556,486.0)	11.35%
M8 (553,312.0 / 764,141.0)	9.74%
M9 (760,833.0 / 1,013,875.0)	4.56%
M10 (1,010,064.0 / 1,285,544.0)	1.84%

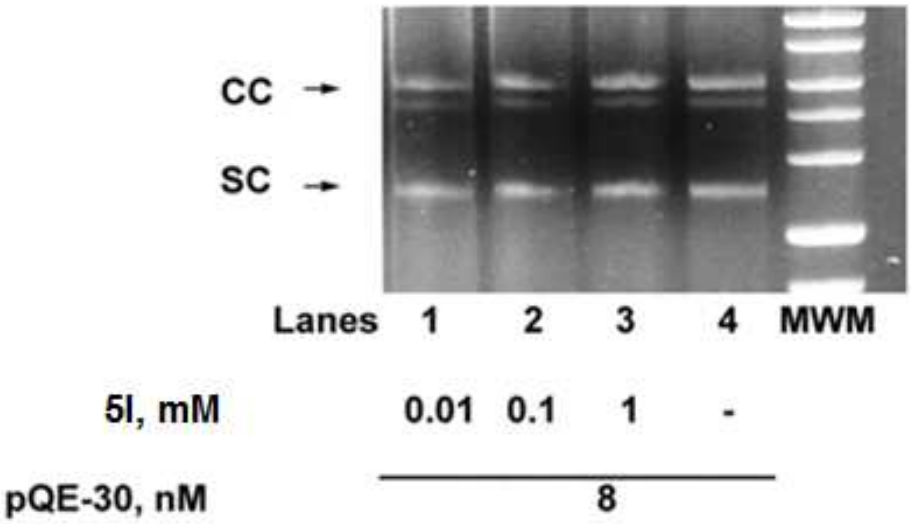

Figure S1. Increasing amounts of the inhibitor **5l** were incubated with plasmid DNA (pQE-30) at reltive ratios (M/M) of inhibitor to plasmid of 1250/1 (lane 1), 12500 (lane 2) and 125000 (lane 3). Lane 4, control reaction in the absence of inhibitor. MWM, molecuar weight markers. CC, closed circular; SC, supercoiled.